

GENERATION OF APTAMER AGAINST *SALMONELLA* SEROVAR  
ENTERITIDIS AND DEVELOPMENT OF APTAMER-BASED CAPILLARY  
BIOSENSOR

A THESIS SUBMITTED TO  
THE GRADUATE SCHOOL OF NATURAL AND APPLIED SCIENCES OF  
MIDDLE EAST TECHNICAL UNIVERSITY

BY

CEREN BAYRAÇ

IN PARTIAL FULFILLMENT OF THE REQUIREMENTS  
FOR  
THE DEGREE OF DOCTOR OF PHILOSOPHY  
IN  
BIOTECHNOLOGY

SEPTEMBER 2014



Approval of the thesis:

**GENERATION OF APTAMER AGAINST *SALMONELLA* SEROVAR  
ENTERITIDIS AND DEVELOPMENT OF APTAMER-BASED CAPILLARY  
BIOSENSOR**

submitted by **CEREN BAYRAÇ** in partial fulfillment of the requirements for  
the degree of **Doctor of Philosophy in Biotechnology Department, Middle East  
Technical University** by,

Prof. Dr. Canan Özgen  
Dean, Graduate School of **Natural and Applied Sciences**

\_\_\_\_\_

Prof. Dr. Filiz Bengü Dilek  
Head of Department, **Biotechnology**

\_\_\_\_\_

Prof. Dr. Hüseyin Avni Öktem  
Supervisor, **Biology Dept., METU**

\_\_\_\_\_

Prof. Dr. Füsün İnci Eyidoğan  
Co-Supervisor, **Educational Institution, Başkent University**

\_\_\_\_\_

**Examining Committee Members:**

Prof. Dr. Meral Yücel  
Biology Dept., METU

\_\_\_\_\_

Prof. Dr. Hüseyin Avni Öktem  
Biology Dept., METU

\_\_\_\_\_

Prof. Dr. Cumhuri Çökmüş  
Biology Dept., Ankara University

\_\_\_\_\_

Assoc. Prof. Dr. A. Elif Erson Bensan  
Biology Dept., METU

\_\_\_\_\_

Assist. Prof. Dr. Yeşim Soyer  
Food Engineering Dept., METU

\_\_\_\_\_

Date: 05.09.2014

**I hereby declare that all information in this document has been obtained and presented in accordance with academic rules and ethical conduct. I also declare that, as required by these rules and conduct, I have fully cited and referenced all material and results that are not original to this work.**

Name, Last name :

Signature :

## ABSTRACT

### GENERATION OF APTAMER AGAINST *SALMONELLA* SEROVAR ENTERITIDIS AND DEVELOPMENT OF APTAMER-BASED CAPILLARY BIOSENSOR

Bayraç, Ceren

Ph.D., Department of Biotechnology

Supervisor : Prof. Dr. Hüseyin Avni Öktem

Co-supervisor: Prof. Dr. Füsün İnci Eyidoğan

September 2014, 176 pages

Food poisoning became one of the most important diseases that threaten to human health. Among all the food-borne pathogens, *Salmonella* is the most common cause of food-borne infectious disease in the world. Among over 2500 serovars, *Salmonella enterica* serovar Enteritidis is a common foodborne pathogen associated with human diseases. Limited and time consuming diagnostic techniques such as culturing method or polymerase chain reaction lead to increase in the demands of new detection methods.

Therefore, in this study we used Cell-SELEX to find DNA aptamers that bind and recognize *S. Enteritidis* as a sensing element and applied them to construct aptamer based sandwich type detection platform. Selection was finished at round 12 of SELEX and three sequences were determined as candidate aptamers for further

studies. Among them, crn-1 and crn-2 showed high specificity and affinity against *S. Enteritidis* with  $K_d$  of  $0.971 \times 10^{-6}$  M and  $0.309 \times 10^{-6}$  M, respectively.

The construction of aptamer based sandwich type platform was optimized with the use of *S. aureus* aptamer (SA-31). The optimum parameters were found as 10  $\mu$ M capturing aptamer, 10  $\mu$ M signaling aptamer, washing at 10  $\mu$ L/sec injection speed and 5% of BSA as surface blocker. Aptamers for *S. Enteritidis* were then applied to platform with these optimum parameters. The detection limits of crn-1 and crn-2 based platforms were  $10^3$  CFU/mL. The response of detection platforms were evaluated for samples at 4°C and 37°C. It was observed that crn-1 based platform gave responses only at 4°C, while crn-2 based platform responded at 4°C and 37°C.

Keywords: DNA Aptamer, Cell-SELEX, *S. Enteritidis*, Sandwich Platform

## ÖZ

### **SALMONELLA ENTERITIDIS'E KARŞI APTAMER SEÇİMİ VE APTAMER TABANLI KAPİLER BİYOSENSÖRÜN GELİŞTİRİLMESİ**

Bayraç, Ceren

Doktora, Biyoteknoloji Bölümü

Tez Yöneticisi : Prof. Dr. Hüseyin Avni Öktem

Ortak Tez Yöneticisi : Prof. Dr. Füsün İnci Eyidoğan

Eylül 2014, 176 sayfa

Gıda zehirlenmeleri insan sağlığını tehdit eden önemli hastalıklar arasında yerini almaktadır. Belirlenen bütün patojenler arasında *Salmonella* dünyada en yaygın görülen gıda kaynaklı enfeksiyon hastalıklarının sebebi olmaktadır. 2500 fazla serotip içinde *Salmonella enterica* serovar Enteritidis insan hastalıkları ile bağlantılı yaygın bir gıda patojenidir. Hücre kültürü ve polimeraz zincir reaksiyonu gibi sınırlı ve zaman alıcı tanı sistemleri yeni tanı sistemlerine duyulan ihtiyacı arttırmaktadır. Bu yüzden bu çalışmada *S. Enteritidis*' e bağlanıp tanıyabilen DNA aptamerlerini bulmak amacıyla Cell-SELEX adı verilen yöntem kullanılmış ve bunları aptamer tabanlı sandviç çeşidinde tanıma platform geliştirmek için uygulanmıştır. Seçilim işlemi 12. SELEX turunda bitirilmiş ve 3 dizi daha sonraki çalışmalar için aday aptamer seçilmiştir. Bunların arasında, crn-1 ve crn2 *S. Enteritidis* e karşı yüksek özgünlük ve  $0.971 \times 10^{-6}$  M ve  $0.309 \times 10^{-6}$  M  $K_d$  değerleri ile yüksek afinite gösterdi. Aptamer tabanlı sandviç platform oluşturulması *S. aureus* aptameri (SA-31) ile optimize edildi. Optimum parametreler 10  $\mu$ M yakalayıcı aptamer, 10  $\mu$ M sinyal aptamer, 10  $\mu$ L/sec enjeksiyon hızıyla yıkama ve % 5'lik BSA ile yüzey bloklama olarak bulundu. *S. Enteritidis* aptamerleri daha sonra bu optimum parametrelerle

platform uygulandı. crn-1 ve crn-2 tabanlı platformların tanı limiti  $10^3$  CFU/mL bulundu. Tanı platformlarının 4°C ve 37°C'deki örneklere karşı yanıtları değerlendirildi. Crn-1 tabanlı platform sadece 4 °C'de yanıt verirken crn-2 tabanlı platformun 4°C ve 37°C'de yanıt verdiği görüldü.

Anahtar kelimeler: DNA Aptamer, Hücre-SELEX, *S. Enteritidis*, Sandviç Platformu

## ACKNOWLEDGEMENTS

I am greatly indebted to my supervisor Prof. Dr. Hüseyin Avni Öktem for his guidance, encouragements, valuable comments and endless supports. I would also like to express my gratitude to Prof. Dr. Meral Yücel for her encouragement, valuable supports and precious remarks. I am proud of being a member of their laboratory.

I would like to express gratitude to my co-supervisor Prof. Dr. Füsün İnci Eyidođan for insight, helps, valuable suggestions and comments during the study.

I would like to thank to all my thesis juri members, Prof. Dr. Cumhuri Çökmüş, Assoc. Prof. Dr. A. Elif Erson Bensen and Assist. Prof. Dr. Yeşim Soyer for their suggestions and critics.

I am also thankful to Doç. Dr. Remziye Yılmaz for her valuable suggestions, helps and guidance.

I would like to thank Prof. Dr. Mehmet Akan (Faculty of Veterinary Medicine Department at Ankara University) and Doç. Dr. Selçuk Kılıç (T.C. Halk Sađlığı Kurumu) for the supply of *S. Enteritidis* and *S. aureus*, respectively.

I want to thank Musa Kavas, Gülsüm Kalemtaş, M. Cengiz Balođlu, M. Tufan Öz, Taner Tuncer, Oya Ercan Akça, Ceyhun Kayıhan, A. Hamit Battal, Ayten Erođlu, Melih Onay, Dr. Çađla Sönmez, Dilek Çam and Işkın Köse one by one for their splendid technical and moral supports, valuable comments and sincere friendships.

I really appreciate Sena Cansız, Fatma Çınar Gül, A. Çınar Öner and Lütfiye Yıldız Özer for their endless love, patience, encouragements and being one of the important parts of my life. I believe you are with me throughout my life.

My special thanks go to MERLAB MBB members, especially to Fatma ınar Gl, Dilek Kıncal and Fatma Kahveciođlu Vatanlar for their encouragements and sincere friendships.

I would like to thank METU, Central Laboratory, Molecular Biology and Biotechnology R&D Center for providing me many facilities.

My special thanks and gratitude go to my husband A. Tahir Bayra and my son Burak Bayra for being precious part of my life, for their endless love and supports. I am thankful to my husband for encouragement, endless patience, valuable suggestions and scientific guidance in the study.

I owe my sincere gratitude to my family, Ali Karakaş, Sibel Karakaş, Volkan Karakaş, Hilal Baran Karakaş and my niece Irmak Karakaş for their endless love, thrust, encouragement and support at all stages of my life.

It is my duty to express my gratitude to TUBITAK for the support that I have received as scholarships during my graduate education.

This study was supported by The Scientific and Technological Research Council of Turkey (TUBITAK) (111M284) and several TUBITAK-TEYDEB projects granted to Nanobiz Ltd. Ankara Turkey.

## TABLE OF CONTENTS

ABSTRACT .....	v
ÖZ .....	vii
ACKNOWLEDGEMENTS .....	ix
TABLE OF CONTENTS .....	xi
LIST OF TABLES .....	xv
LIST OF ABBREVIATIONS .....	xvii
CHAPTERS	
1. INTRODUCTION .....	1
1.1 Biodetection Technology .....	1
1.2 Biosensor .....	1
1.3 Bioreceptors as Sensing Element .....	2
1.3.1 Enzymes.....	3
1.3.2 Peptides.....	4
1.3.3 Carbohydrates .....	4
1.3.4 Cells .....	5
1.3.5 Antibodies.....	5
1.3.6 Nucleic Acids.....	6
1.4 Aptamers .....	7
1.4.1 Aptamer vs Antibodies .....	8
1.4.2 Limitations of Aptamers and Solutions .....	10
1.5 SELEX.....	11

1.5.1 SELEX Variants.....	15
1.6 Aptasensors and Their Applications.....	17
1.6.1 Aptasensors in Clinical Diagnosis .....	18
1.6.2 Aptasensors for Food Safety .....	19
1.6.3 Aptasensors for Environmental Control .....	20
1.7 Classification of Aptamer-based Biosensors.....	21
1.7.1 Optical Aptasensors .....	21
1.7.2 Electrochemical Aptasensors .....	22
1.7.3 Mass-sensitive Aptasensors .....	23
1.8 <i>Salmonella</i> and Its Detection Methods.....	24
1.8.1 Conventional Detection Methods .....	25
1.8.2 Rapid Detection Methods .....	28
1.8.3 Biosensors for <i>Salmonella</i> Detection.....	30
1.9 Aim of the Study.....	32
2. MATERIALS AND METHODS .....	33
2.1 Materials .....	33
2.1.1 DNA Library, Primers and Aptamers .....	33
2.1.2 Target and Control Cells.....	33
2.1.3 Reagents.....	33
2.1.4 Supporting Material for Platform.....	34
2.1.5 Equipments .....	34
2.2 Methods .....	35
2.2.1 Cell-SELEX .....	37
2.2.1.1 Design of Primers and DNA Library .....	38
2.2.1.2 Synthesis and Purification of DNA library .....	38

2.2.1.3 Optimization of Annealing Temperature of Library and Primer Concentration in PCR Reaction .....	39
2.2.1.4 Preparation of Target Bacterial Cell .....	39
2.2.1.5 Incubation of DNA Library with Target Cell .....	40
2.2.1.6 Recovery of Bound Sequences.....	40
2.2.1.7 PCR Optimization and Single-Stranded DNA Preparation .....	41
2.2.1.8 Negative SELEX.....	44
2.2.2 Progress Control of SELEX.....	44
2.2.2.1 Fluorescent Aptamer Binding Assay .....	44
2.2.2.2 Melting Curve Analysis of DNA Pools .....	45
2.2.3 Sequence Analyses .....	45
2.2.4 Characterization and Binding Studies of Selected Aptamer.....	46
2.2.4.1 Confocal Imaging of Bacteria with Aptamer .....	46
2.2.4.2 Enzyme-Linked Aptamer Assay (ELAA).....	46
2.2.4.3 Isolation of Cell Membrane Proteins of Bacteria using Carbonate Extraction Method and Bioanalyzer Protein Assay .....	47
2.2.4.4 Isothermal Titration Calorimeter Analysis .....	48
2.2.5 Construction of Aptamer-Based Sandwich Platform for Bacterial Detection .....	48
2.2.5.1 Surface Coating.....	49
2.2.5.2 Optimization Studies for Platform Construction.....	50
2.2.5.3 Detection Platform with Quantum Dot and HRP.....	51
2.2.5.4 Signal Amplification .....	52
3. RESULTS AND DISCUSSION .....	55
3.1 Cell-SELEX.....	55
3.1.1 Design of DNA Library and Primers .....	55

3.1.2 Synthesis Results of DNA Library .....	57
3.1.3 PCR Optimization for T <sub>m</sub> and Primer Concentration .....	60
3.1.4 Preparation of Target Bacterial Cell .....	62
3.1.5 SELEX Rounds .....	65
3.1.6 Progress Control of SELEX.....	68
3.1.6.1 Fluorescent Aptamer Binding Assay.....	69
3.1.7 Sequence Analyses.....	75
3.1.8 Characterization and Binding Studies of Selected Aptamer .....	80
3.1.8.1 Confocal Imaging of Bacteria with Aptamer .....	81
3.1.8.2 Enzyme-Linked Aptamer Assay (ELAA) .....	89
3.2 Construction of Aptamer-Based Sandwich Platform for Bacterial Detection	121
3.2.1 Optimization Studies.....	125
3.2.2 Signal Amplification.....	136
3.2.3 Detection Platforms for <i>S. Enteritidis</i> .....	141
3.2.4 Effects of Capturing Temperature of <i>S. Enteritidis</i> on the Response of Detection Platform .....	151
4. CONCLUSION .....	153
REFERENCES.....	157
APPENDICES	
A. BUFFERS AND SOLUTIONS.....	171
CURRICULUM VITAE .....	175

## LIST OF TABLES

### TABLES

<b>Table 1.1</b> Comparisons of aptamers versus antibodies. ....	9
<b>Table 1.2</b> SELEX variants and their applications. ....	16
<b>Table 1.3</b> Examples of aptasensors for cancer diagnosis. ....	19
<b>Table 1.4</b> Commercially available ELISA-based <i>Salmonella</i> Detection Kits.....	28
<b>Table 1.5</b> Commercially available PCR-based <i>Salmonella</i> Detection Kits. ....	30
<b>Table 1.6</b> Aptamer-based biosensors reported in literature.....	32
<b>Table 2.1</b> Selection parameters of aptamer used in whole cell SELEX.....	41
<b>Table 2.2</b> Optimization parameters for the construction of aptamer-based capillary sandwich platform.....	51
<b>Table 3.1</b> Properties of DNA library and primers. ....	56
<b>Table 3.2</b> Optimized cycle numbers of SELEX rounds. ....	66
<b>Table 3.3</b> Melting temperatures of DNA library and pools at each round. ....	75
<b>Table 3.4</b> Sequence results of pools eluted at rounds 5, 7 and 12.....	76
<b>Table 3.5</b> Sequence results of candidate aptamers selected for <i>S. Enteritidis</i> .....	78

**Table 3.6** Mean concentrations of total proteins, main protein sizes and their percentages..... 106

**Table 3.7** Thermodynamic parameters of binding reaction between SA-31 and *S. aureus* membrane fractions (in 10 mM of PBS at pH 7) at different temperatures with one site binding model. .... 113

**Table 3.8** Thermodynamic parameters of binding reaction between crn-1/crn-2 and *S. Enteritidis* membrane fractions (in 10 mM of PBS at pH 7) at different temperatures with one site binding model..... 121

## LIST OF FIGURES

### FIGURES

<b>Figure 1.1</b> Biosensor operating principle: main subsystems.....	2
<b>Figure 1.2</b> Components of biosensors; bioreceptors and transducers. ....	3
<b>Figure 1.3</b> Application areas of aptamers.....	8
<b>Figure 1.4</b> General scheme of SELEX process .....	13
<b>Figure 1.5</b> Selection stages of DNA and RNA aptamers.....	14
<b>Figure 1.6</b> Applications of aptasensors .....	17
<b>Figure 1.7</b> Representative scheme of <i>Salmonella</i> culture method reported by FDA.....	27
<b>Figure 1.8</b> Detex Pathogen Detection Technologies.....	31
<b>Figure 2.1</b> Flowchart showing all steps of the procedure. ....	36
<b>Figure 2.2</b> Representative figure of SELEX. ....	37
<b>Figure 2.3</b> Preparation of ssDNA from dsDNA.....	43
<b>Figure 2.4</b> Construction scheme of Aptamer-Based Sandwich Platform for Bacterial Detection. ....	49
<b>Figure 3.1</b> Phosphoramidite chemistry .....	58

<b>Figure 3.2</b> HPLC purification result of DNA library. ....	59
<b>Figure 3.3</b> Agarose gel image of seven PCR products whose annealing steps were performed at seven different annealing temperatures (60.1, 61.9, 63.0, 64.3, 66.9, 68.4 and 69.9°C).....	61
<b>Figure 3.4</b> Agarose gel image of four PCR products which were amplified with four different stock primers concentrations (3, 5, 8 and 10 $\mu$ M).....	62
<b>Figure 3.5</b> Growth curve of <i>S. Enteritidis</i> at 37°C in TSB.....	64
<b>Figure 3.6</b> Exponential growth phase of <i>S. Enteritidis</i> 's growth curve at 37°C in TSB medium (n=3).....	64
<b>Figure 3.7</b> PCR cycle optimization results of pools eluted at A) round 1, B) round 2, C) round 3, D) round 4, E) round 5, F) round 6.....	67
<b>Figure 3.8</b> PCR cycle optimization results of pools eluted at A) round 7, B) round 8, C) round 9, D) round 10, E) round 11, F) round 12.....	68
<b>Figure 3.9</b> Standard curve of fluorescence labeled forward primer (P1-FAM) constructed with the concentrations at $\mu$ M or pmole unit versus relative fluorescence unit (RFU).. ....	70
<b>Figure 3.10</b> Percentages of elution yield for each round of SELEX. For each round triple replicates of pools were read with fluorospectrometer.....	71
<b>Figure 3.11</b> DNA melting temperature analyses of pools by Diversity Standard of Random Oligonucleotides assay in RT-PCR A) Melting peaks of all SELEX pools and DNA library, B) Melting curves of all SELEX pools and DNA library. ....	74

<b>Figure 3.12</b> Read length histogram of total sequences: the graph of read length versus their number. ....	76
<b>Figure 3.13</b> Guide tree of sequence data obtained from SELEX round of 12 via ArchaeopteryxA. ....	77
<b>Figure 3.14</b> Diagram of minimum free energy secondary structures of crn-1 at 4 °C, 25°C and 37°C drawn by Nupack software .....	79
<b>Figure 3.15</b> Diagram of minimum free energy secondary structures of crn-2 at 4 °C, 25°C and 37°C drawn by Nupack software. ....	79
<b>Figure 3.16</b> Diagram of minimum free energy secondary structures of crn-3 at 4 °C, 25°C and 37°C drawn by Nupack software. ....	80
<b>Figure 3.17</b> Laser scanning confocal microscope images of <i>S. aureus</i> and <i>E. coli</i> labelled with <i>S. aureus</i> aptamer SA-31(after one washing step) at 488 nm excitation wavelength by plan-neofluar 40X objective. (A) Fluorescence image (B) Optical image (C) Merge of two images of <i>S. aureus</i> , (D) Fluorescence image (E) Optical image (F) Merge of two images of <i>E. coli</i> . ....	82
<b>Figure 3.18</b> Laser scanning confocal microscope images of three cells bound with <i>S. aureus</i> aptamer SA-31 at 488 nm excitation wavelength by plan-neofluar 40X objective. (A) Fluorescence image (B) Optical image (C) Merge of two images of <i>S. aureus</i> , (D) Fluorescence image (E) Optical image (F) Merge of two images of <i>E. coli</i> , (G) Fluorescence image (H) Optical image (I) Merge of two images of <i>S. Enteritidis</i> . ....	84

**Figure 3.19** Laser scanning confocal microscope images of three cells bound with *S. Enteritidis* aptamer crn-1 at 488 nm excitation wavelength by plan-neofluar 40X objective. (A) Fluorescence image (B) Optical image (C) Merge of two images of *S. Enteritidis*, (D) Fluorescence image (E) Optical image (F) Merge of two images of *E. coli*, (G) Fluorescence image (H) Optical image (I) Merge of two images of *S. aureus*. ..... 86

**Figure 3.20** Laser scanning confocal microscope images of three cells bound with *S. Enteritidis* aptamer crn-2 at 488 nm excitation wavelength by plan-neofluar 40X objective. (A) Fluorescence image (B) Optical image (C) Merge of two images of *S. Enteritidis*, (D) Fluorescence image (E) Optical image (F) Merge of two images of *E. coli*, (G) Fluorescence image (H) Optical image (I) Merge of two images of *S. aureus* ..... 87

**Figure 3.21** Laser scanning confocal microscope images of three cells bound with *S. Enteritidis* aptamer crn-3 at 488 nm excitation wavelength by plan-neofluar 40X objective. (A) Fluorescence image (B) Optical image (C) Merge of two images of *S. Enteritidis*, (D) Fluorescence image (E) Optical image (F) Merge of two images of *E. coli*, (G) Fluorescence image (H) Optical image (I) Merge of two images of *S. aureus* ..... 88

**Figure 3.22** Schematic drawing of aptamer-based ELISA-like assay. .... 89

**Figure 3.23** Oxidation reaction of TMB as a substrate of HRP. A. TMB. B. Oxidation product. .... 90

**Figure 3.24** Turbidity measurements of bacterial cells at different amounts after washing steps. A) *S. aureus* at  $10^7$  CFU/mL, B) *S. aureus* at  $10^6$  CFU/mL, C) *S. aureus* at  $10^5$  CFU/mL, D) *S. aureus* at  $10^4$  CFU/mL, E) washing buffer without cell used as control. .... 91

**Figure 3.25** Absorbance readings of different concentrations of SA-31 at constant cell amount ( $10^6$  CFU/mL of *S. aureus*). A) 1  $\mu$ M, B) 5  $\mu$ M, C) 10  $\mu$ M, D) 20  $\mu$ M, E) Control 1, F) Control 2, G) Control 3. .... 92

**Figure 3.26** Absorbance readings of different cell amounts at constant SA-31 concentration (10  $\mu$ M). A)  $10^3$  CFU/mL of *S. aureus*, B)  $10^4$  CFU/mL of *S. aureus*, C)  $10^5$  CFU/mL of *S. aureus*, D)  $10^6$  CFU/mL of *S. aureus*, E)  $10^7$  CFU/mL of *S. aureus*, F) Control 1, G) Control 2, H) Control 3, I) Control 4 and J) Control 5. .... 95

**Figure 3.27** Turbidity measurements of bacterial cells at different amounts after washing steps. A) *S. Enteritidis* at  $10^7$  CFU/mL, B) *S. Enteritidis* at  $10^6$  CFU/mL, C) *S. Enteritidis* at  $10^5$  CFU/mL, D) *S. Enteritidis* at  $10^4$  CFU/mL, E) *S. Enteritidis* at  $10^3$  CFU/mL, F) washing buffer without cell used as control.. .... 97

**Figure 3.28** Absorbance readings of different concentrations of crn-1, crn-2 and crn-3 at constant cell amount ( $10^6$  CFU/mL of *S. Enteritidis*). A) 1  $\mu$ M, B) 5  $\mu$ M, C) 10  $\mu$ M, D) 20  $\mu$ M, E) Control 1, F) Control 2, G) Control 3. .... 99

**Figure 3.29** Absorbance readings of different *S. Enteritidis* amount at constant crn-2 concentration (10  $\mu$ M). A)  $10^3$  CFU/mL of *S. Enteritidis*, B)  $10^4$  CFU/mL of *S. Enteritidis*, C)  $10^5$  CFU/mL of *S. Enteritidis*, D)  $10^6$  CFU/mL of *S. Enteritidis*, E)  $10^7$  CFU/mL of *S. Enteritidis*, F) Control 1, G) Control 2, H) Control 3, I) Control 4 and J) Control 5. .... 103

**Figure 3.30** Gel-like images of membrane fractions extracted from *S. Enteritidis*, *S. aureus*, *E. coli*. .... 105

**Figure 3.31** Electropherograms of membrane proteins extracted from *S. Enteritidis*, *S. aureus* and *E. coli* by carbonate extraction method ..... 107

<b>Figure 3.32</b> Binding experiment of <i>S. aureus</i> aptamer SA-31 and <i>S. aureus</i> membrane fractions via ITC at 4°C; Raw ITC data (upper graph), Thermalgram of titrating SA31 with membrane fraction (lower graph).....	110
<b>Figure 3.33</b> Binding experiment of <i>S. aureus</i> aptamer SA-31 and <i>S. aureus</i> membrane fraction via ITC at 25°C; A) Raw ITC data, B) Thermalgram of titrating SA-31 with membrane fraction. ....	111
<b>Figure 3.34</b> Binding experiment of <i>S. aureus</i> aptamer SA-31 and <i>S. aureus</i> membrane fraction via ITC at 37°C; A) Raw ITC data, B) Thermalgram of titrating SA-31 with membrane fraction. ....	113
<b>Figure 3.35</b> Heat of dilution experiment: Titration of membrane fractions of <i>S. aureus</i> into PBS solution. A) Raw ITC data, B) Thermalgram of titrating buffer solution with membrane fraction.....	114
<b>Figure 3.36</b> Possible minimum free energy structures of <i>S. aureus</i> aptamer (SA-31) at 4°C, 25°C and 37°C drawn by Nupack software. ....	115
<b>Figure 3.37</b> Binding experiment of crn-1 and <i>S. Enteritidis</i> membrane fraction via ITC at 4°C; A) Raw ITC data, B) Thermalgram of titrating crn-1 with membrane fraction. ....	116
<b>Figure 3.38</b> Binding experiment of crn-1 and <i>S. Enteritidis</i> membrane fraction via ITC at 37°C; A) Raw ITC data, B) Thermalgram of titrating crn-1 with membrane fraction. ....	118
<b>Figure 3.39</b> Binding experiment of crn-2 and <i>S. Enteritidis</i> membrane fraction via ITC at 4°C; A) Raw ITC data, B) Thermalgram of titrating crn-2 with membrane fraction. ....	119

<b>Figure 3.40</b> Binding experiment of <i>crn-2</i> and <i>S. Enteritidis</i> membrane fraction via ITC at 37°C; A) Raw ITC data, B) Thermalgram of titrating <i>crn-2</i> with membrane fraction. ....	120
<b>Figure 3.41</b> Representative figure of aptamer-based sandwich platform.....	122
<b>Figure 3.42</b> Capillary images of <i>S. aureus</i> detection platforms with 5 μM of SA-31 under UV light; A) Sandwich system, B) Unspecific binding control (Control 1) C) Specificity control with <i>S. Enteritidis</i> (Control 2), D) Specificity control with <i>E. coli</i> (Control 3), E) Sel-dimer control (Control 4). ....	127
<b>Figure 3.43</b> Capillary images of <i>S. aureus</i> detection platforms with 10 μ of SA-31 under UV light; A) Sandwich system, B) Unspecific binding control (Control 1) C) Specificity control with <i>S. Enteritidis</i> (Control 2), D) Specificity control with <i>E. coli</i> (Control 3), E) Sel-dimer control (Control 4). ....	129
<b>Figure 3.44</b> Capillary images of <i>S. aureus</i> detection platforms blocked with PEG under UV light; A) Sandwich system, B) Unspecific binding control (Control 1) C) Specificity control with <i>S. Enteritidis</i> (Control 2), D) Specificity control with <i>E. coli</i> (Control 3). ....	132
<b>Figure 3.45</b> Capillary images of <i>S. aureus</i> detection platforms blocked with 2% of BSA under UV light; A) Sandwich system, B) Unspecific binding control (Control 1) C) Specificity control with <i>S. Enteritidis</i> (Control 2), D) Specificity control with <i>E. coli</i> (Control 3). ....	133
<b>Figure 3.46</b> Capillary images of <i>S. aureus</i> detection platforms blocked with 5% of BSA under UV light; A) Sandwich system, B) Unspecific binding control (Control 1) C) Specificity control with <i>S. Enteritidis</i> (Control 2), D) Specificity control with <i>E. coli</i> (Control 3). ....	134

**Figure 3.47** Capillary images of *S. aureus* detection platforms with HRP-strep signaling strategy; A) Sandwich system, B) Unspecific binding control (Control 1) C) Specificity control with *S. Enteritidis* (Control 2), D) Specificity control with *E. coli* (Control 3)..... 135

**Figure 3.48** Capillary images of *S. aureus* detection platforms constructed with strep-HRP and ultra-TMB; A) Sandwich system, B) Unspecific binding control (Control 1) C) Specificity control with *S. Enteritidis* (Control 2), D) Specificity control with *E. coli* (Control 3), E) Sel-dimer control (Control 4). ..... 138

**Figure 3.49** Representative figure of streptavidin Poly-HRP conjugates. .... 140

**Figure 3.50** Capillary images of *S. aureus* detection platforms constructed with SA-PolyHRP40 and ultra-TMB; A) Sandwich system, B) Unspecific binding control (Control 1) C) Specificity control with *S. Enteritidis* (Control 2), D) Specificity control with *E. coli* (Control 3). ..... 141

**Figure 3.51** Capillary images of crn-1 based *S. Enteritidis* detection platforms with QD signaling strategy; A) Sandwich system with crn-1, B) Unspecific binding control (Control 1) C) Specificity control with *S. aureus* (Control 2), D) Specificity control with *E. coli* (Control 3) ..... 143

**Figure 3.52** Capillary images of crn-2 based *S. Enteritidis* detection platforms with QD signaling strategy; A) Sandwich system with crn-2, B) Unspecific binding control (Control 1) C) Specificity control with *S. aureus* (Control 2), D) Specificity control with *E. coli* (Control 3) ..... 144

**Figure 3.53** Capillary images of crn-1 based *S. Enteritidis* detection platforms with HRP signaling strategy; A) Sandwich system with crn-1, B) Unspecific binding control (Control 1) C) Specificity control with *S. aureus* (Control 2), D) Specificity control with *E. coli* (Control 3). ..... 145

**Figure 3.54** Capillary images of crn-2 based *S. Enteritidis* detection platforms with HRP signaling strategy; A) Sandwich system with crn-2, B) Unspecific binding control (Control 1) C) Specificity control with *S. aureus* (Control 2), D) Specificity control with *E. coli* (Control 3). ..... 146

**Figure 3.55** Capillary images of crn-1 (left images) and crn-2 (right images) based *S. Enteritidis* detection platforms with QD signaling strategy for the determination of LOD; A) Sandwich system with  $10^6$  CFU/mL of cell, B) Sandwich system with  $10^5$  CFU/mL of cell, C) Sandwich system with  $10^4$  CFU/mL of cell, D) Sandwich system with  $10^3$  CFU/mL of cell, E) Sandwich system with  $10^2$  CFU/mL of cell, F) Unspecific binding control. .... 149

**Figure 3.56** Capillary images of crn-1 (left images) and crn-2 (right images) based *S. Enteritidis* detection platforms with HRP signaling strategy for the determination of LOD; A) Sandwich system with  $10^6$  CFU/mL of cell, B) Sandwich system with  $10^5$  CFU/mL of cell, C) Sandwich system with  $10^4$  CFU/mL of cell, D) Sandwich system with  $10^3$  CFU/mL of cell, E) Sandwich system with  $10^2$  CFU/mL of cell, F) Unspecific binding control. .... 150

**Figure 3.57** Capillary images of detection platforms constructed with crn-1 and crn-2 for the detection of *S. Enteritidis* at 4°C and 37°C. .... 151

## LIST OF ABBREVIATIONS

<b>BSA</b>	Bovine Serum Albumin
<b>ELAA</b>	Enzyme-linked Aptamer Assay
<b>ELISA</b>	Enzyme-linked Immunoabsorbent Assay
<b>DNA</b>	Deoxyribonucleic Acid
<b>dsDNA</b>	Double-Stranded Deoxyribonucleic Acid
<b>HRP</b>	Horseradish Peroxidase
<b>ITC</b>	Isothermal Titration Calorimeter
<b>PEG</b>	Polyethylene glycol
<b>PBS</b>	Phosphates Buffered Saline
<b>PCR</b>	Polymerase Chain Reaction
<b>QDs</b>	Quantum Dots
<b>SDS</b>	Sodium Dodecyl Sulfate
<b>SELEX</b>	Systematic Evolution of Ligands by Exponential Enrichment
<b>SSC</b>	Saline-Sodium Citrate
<b>ssDNA</b>	Single Stranded Deoxyribonucleic Acid
<b>TMB</b>	3, 3', 5, 5'-tetramethylbenzidine
<b>TSA</b>	Tryptic Soy Agar
<b>TSB</b>	Tryptic Soy Broth

## CHAPTER 1

### INTRODUCTION

#### 1.1 Biodetection Technology

Biological molecules and biological processes have vital roles in many disciplines such as biology, chemistry, biochemistry, medicine, food safety, environmental control and biotechnology. The needs for detection, identification and measurement of molecules have forced scientist to develop new techniques.

The concept of biosensor rose with the need of measuring some analytes in blood by an oxygen electrode in 1962 (Clark & Lyons, 1962). Professor Leland C Clark Jnr was the inventor of the first biosensing platform which measures the glucose concentration in blood with the use of an enzyme, glucose oxidase (Clark & Lyons, 1962). Since the invention of the first electrochemical sensor, the research area throughout the world has been focused on the development of many biosensors for a variety of analytes.

#### 1.2 Biosensor

The definitions of biosensors have been defined in many studies which are mainly gathered under the two main words “receptor” and “transducer”. According to International Union of Pure and Applied Chemistry (IUPAC) definition; “A biosensor is a self-contained integrated device which is capable of providing specific quantitative or semi-quantitative analytical information using a biological recognition element (biochemical receptor) which is in direct spatial contact with a transducer element” (Thevenot *et al.*, 1999). As the definition states, biosensors are constructed mainly with two elements; receptor from biological molecules and transducer. Therefore, the categorization of biosensors is made according to the types of these two main elements.

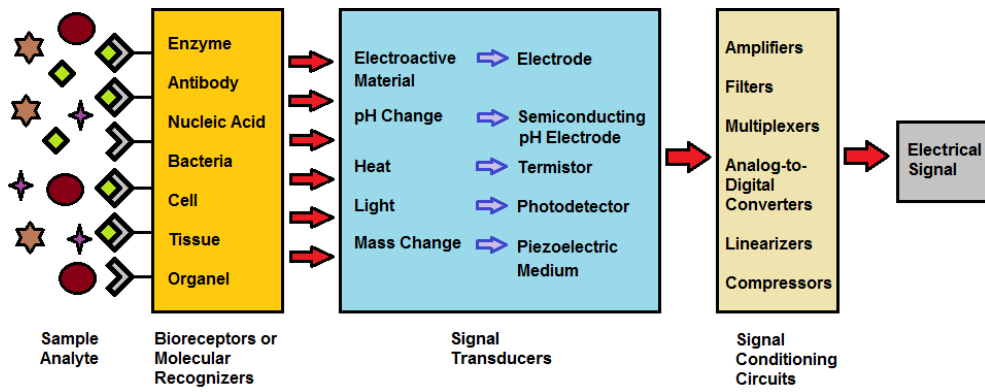


**Figure 1.1** Biosensor operating principle: main subsystems (Vargas-Bernal et al., 2012).

### 1.3 Bioreceptors as Sensing Element

Being one of the two main components of biosensor, bioreceptors, play important role in the effectiveness and success of biosensors. In order to perform recognition ideally bioreceptors should show high specificity against their targets. Also, they should give immediate response upon binding to target and detect target at low amount with high sensitivity. Natural recognition elements which have been used for the construction of biosensors are enzyme, antibodies, peptides, carbohydrates and nucleic acids (Figure1.2).

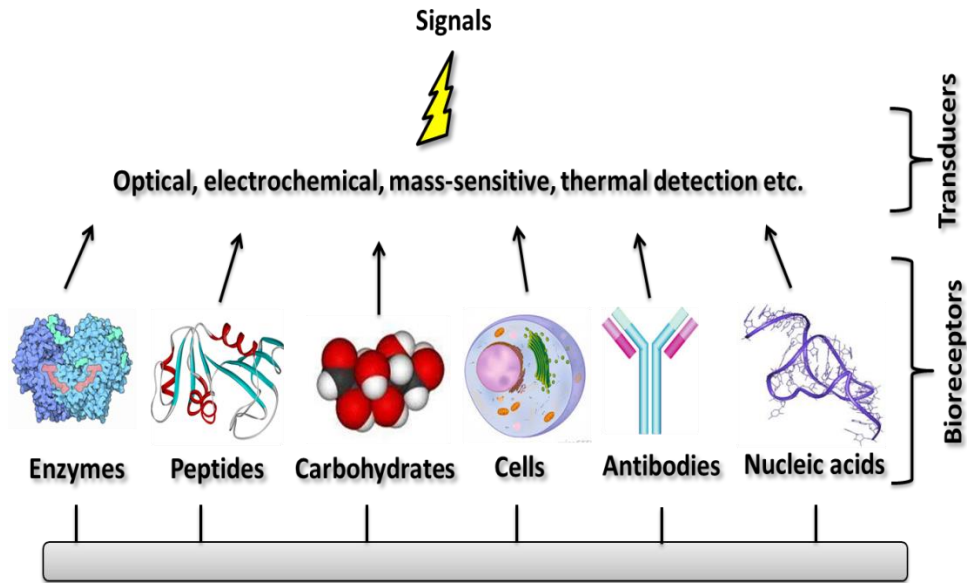


**Figure 1.2** Components of biosensors; bioreceptors and transducers.

### 1.3.1 Enzymes

Enzymes are most widely used bioreceptors in biosensor applications. They are biocatalyst that bind to their substrate with high specificity and affinity and perform catalytic reaction to produce specific products. Because of their specific binding and catalytic property, enzymes have been widespread used as sensing element in biosensors from the invention of first biosensor constructed with glucose oxidase (Clark and Lyons, 1962). Different enzymes with different transducers have been used in biosensor development in the application areas of health care, food safety and environmental monitoring. The mostly used biosensor constructed with enzyme is the one monitoring blood glucose levels, whose working principles are the enzymatic reaction between glucose oxidase immobilized to support material and blood sample from human. Other example to the enzyme biosensor in health care is biosensor detecting pH, urea and metal ions in biological samples simultaneously. It was developed with the use of combination of two enzymes, urease and acetylcholinesterase on probe (Tsai and Doong, 2005). In the field of environmental

control, pesticide biosensor was reported using acetylcholinesterase enzyme immobilized to paper support for the detection of organophosphates and carbamates (Kavruk *et al.*, 2013).

### **1.3.2 Peptides**

Beside being targets, peptides have been used as sensing elements for the detection of certain analytes in biosensing systems. As compared with proteins and antibodies, peptides are small molecules which make them attractive to be used in recognition layer for the improvement of sensitivity and stability (Nagy *et al.*, 2014). Moreover, peptides have been chemically synthesized and easily modified without altering its function and stability. A peptide based biosensor was studied for the evaluation of a specific kinase activity in certain diseases like cancer (Lipchik *et al.*, 2012). The activation and inhibition of spleen tyrosine kinase with the change in external stimulus were detected by specific peptide having similar structure with kinase substrate (Lipchik *et al.*, 2012).

In addition to be used directly in biosensor construction, they have been conjugated to nanoparticles and thus, provide required distance between donor and acceptor in effective FRET studies (Nagy *et al.*, 2014).

### **1.3.3 Carbohydrates**

Carbohydrates play two roles for the construction of biosensors. The first one is the formation of support material and the other one is acting as sensing agent in biodetection systems. Like other recognition elements, carbohydrates have improved the specificity and selectivity of biosensors. They have also provided stability and rigidity to biosensors (Jelinek and Kolusheva, 2004). In literature, there have been many studies to develop affinity based carbohydrates biosensors with different transducers. Colorimetric assays have been performed with the use of carbohydrates immobilized on matrix for the detection of microorganism and their released toxins.

For example, Pan and Charych developed recognition and colorimetric detection system against cholera toxin using carbohydrates incorporated liposomes (Pan and Charych, 1997).

#### **1.3.4 Cells**

Biosensors constructed with cells as sensing elements are special devices that detect changes in the intracellular and extracellular environment conditions and certain physiological parameters. Incorporating living cell into receptor provides the conversion of changes in environment into quantitative signals. There have been some advantages of using whole cell as sensing agents in biosensors over other recognition elements. For example, using whole cell poses natural environment for molecules on cell surface to function. Moreover, their amounts are controlled by living cell and they can be synthesized if required. As a result, living cells as recognition elements have provided biosensors to have high sensitivity, selectivity and stability.

Genetically modified yeast cells were studied as sensing element for the real time detection of formaldehyde (Korpan *et al.*, 1993). Another example of cell based biosensors was again genetically modified organisms to construct bioluminescent bioreporter integrated circuit, which detects blue light produced by cells upon a stimulus (Nivens *et al.*, 2004). In this study genetically engineered bioluminescent micro-organism, *Pseudomonas fluorescens*, was used as reporter integrated into circuit for the detection of salicylate (Nivens *et al.*, 2004).

#### **1.3.5 Antibodies**

Antibodies are protein molecules produced by the immune system in response to the presence of a foreign substance, called an antigen. Antibody based biosensors, immunosensors, have made the use of specific interactions between an antibody and an antigen (Luppa *et al.*, 2001). Immunosensors have been aimed mainly to the

detection of the presence of certain antibodies or antigens in body fluids, especially in serum, although there is also a significant concern in the development of immunosensors employing antibodies for the detection of different analytes in diverse media, e.g. the quantification of TNT in groundwater via the formation of antibody-TNT complexes (Bromage *et al.*, 2007). There have been many published studies and commercial products of biosensing systems against antigens with the use of antibodies. Currently widely used home pregnancy tests have antigen-antibody affinity working principle. This test detects chorionic gonadotropin (hCG) hormone secreted in urine of pregnant woman with the use of anti-hCG globulin as receptor.

### **1.3.6 Nucleic Acids**

The constructions of nucleic acid biosensors have been using the hybridization technique in which sensing DNA molecule immobilized on solid support detect complementary target sequences. Although the constructions of DNA or RNA based biosensors need first the preparation of oligonucleotides by isolating from certain cells or chemical synthesis and also require amplification and hybridization stages, they provide many advantageous in terms of physiological, chemical and biological properties over other recognition agents. They are rapid and low-cost detection platform of specific DNA sequences and unlike antibodies, they do not show cross-reactivity.

The detection of label free genetically modified target DNA sequences was reported with the use of sandwich type array platform via hybridization technique. In that study, specific promoter (35S) and terminator sequences (nos) and two genes, *bar* and *cry*, were detected simultaneously on multiplex array constructed with capture and signals DNA probes (Cansız *et al.*, 2012).

Another example is the development of DNA microarray for the detection of multiple pathogen bacteria some of which are foodborne and contaminating water pathogens. The chip was constructed with 7963 probes specifically synthesized based on genome sequences of bacteria (Hashsham *et al.*, 2004).

## 1.4 Aptamers

Until 1990, nucleic acids were considered as the source of hereditary information. They were carrying specific information, which was transferred from nucleotide sequences into protein sequences. Then, as time went by, different roles were arisen such as regulation of transcription and translation (riboswitches) resulting in changes in production of the proteins. At the beginning of 1990s, short oligonucleotides that could bind different targets via their specific structure were discovered by three different research groups spontaneously and independently (Robetson and Joyce, 1990; Tuerk, and Gold, 1990; Ellington and Szostak, 1990). Due to their three dimensional structures that made them to bind target specifically they were called aptamers (aptus meaning to fit in Latin) (Famulok, 1994).

Aptamers are single stranded DNA or RNA molecules that bind to targets with high affinity and specificity. Contrary to thought of binding due to complementarity between bases, they show their affinity to their specific targets because of their specific folding into unique structures (Proske, 2005). They are short oligonucleotides with generally  $\leq 100$ -mer long and they can form stable secondary motifs like double stranded oligonucleotides. They can fold into, for example, the G-quadruplex (Macaya *et al.*, 1993), hairpin structure (Fan *et al.*, 1996) and pseudoknot (Lorsch and Szostak, 1994) with the presence of divalent cations such as  $\text{Ca}^{2+}$  and  $\text{Mg}^{2+}$  in binding solutions (Girardot *et al.*, 2010, Radom *et al.*, 2013).

As targets for aptamer selection a wide variety of molecules have been selected since 1990. From small molecules such as ions and amino acids to large molecules such as proteins, viruses and even whole bacterial, plant or animal cells (Sefah *et al.*, 2010) have been studied in literature to generate DNA or RNA aptamers for different purposes. Since they have high affinity and specificity to their targets aptamers have been used in diagnosis and treatment of diseases, detection of pathogens, purification of specific molecules in chromatography and capture agents in biosensors, etc. (Figure 1.3).

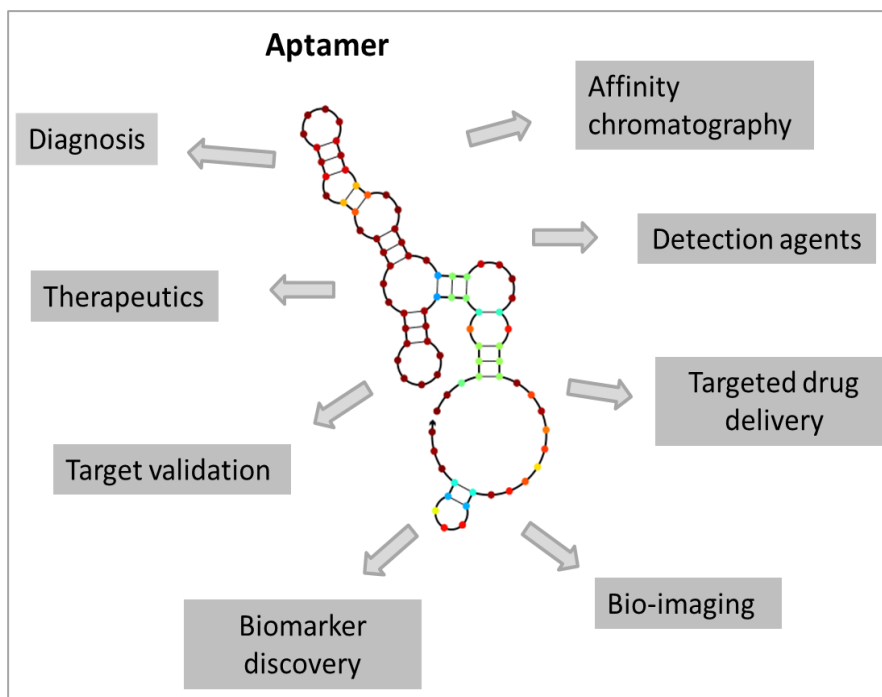


**Figure 1.3** Application areas of aptamers.

### 1.4.1 Aptamer vs Antibodies

Being specific against targets and having a variety of application areas aptamers resemble antibodies which had been the most popular molecular recognition agents until the discovery of aptamers. Although antibodies show certain advantages over their nucleic acid counterparts, aptamers are described as substitute for antibodies due to their properties summarized at Table 1.1.

**Table 1.1** Comparisons of aptamers versus antibodies.

<b>Comparison Factors</b>	<b>Aptamers</b>	<b>Antibodies</b>
<b>Production</b>	Chemically synthesized, easy, cost effective	Depends on animal cells, expensive, time consuming and laborious
<b>Stability</b>	Withstand denaturation, indefinite shelf life	Easily denatured, limited shelf life
<b>Size</b>	Small molecules	Large molecules
<b>Target Potential</b>	Applicable for any targets	Targets except toxins, non-immunogens and small molecules
<b>Modification</b>	Readily accept conjugates	Cannot accommodate conjugates
<b>Immunogenicity</b>	Low	High

The first advantage of aptamers over antibodies is the ease in their production. They are chemically synthesized with a well-known process that is highly reproducible and sequence independent. Since process does not depend on any cell culture, their production is easily scaled up with cost effective way. However, antibodies as proteins are produced biologically via growth of colonies in cell cultures. Therefore, the production of antibodies depends on predetermined physiologic conditions and can show batch to batch variations due to the changes in colonies and growth conditions (Jayasena, 1999).

Secondly, it is well known that oligonucleotides are stable at extreme conditions while the structures of proteins easily denature at high temperature and pH. Therefore, being more stable makes aptamers to yield longer shelf life as compared with antibodies and because of this property they are easily transported without the need of refrigeration (Dong *et al.*, 2014).

The comparison of aptamers and antibodies in terms of size describes one disadvantage of aptamer which can be also an advantageous in certain situations. Aptamers are small molecules and this makes them prone to kidney filtration,

resulting in shortened half-lives. However, they can bind to smaller targets that antibodies cannot reach due to their larger size preventing their access to smaller areas (Keefe *et al.*, 2010).

In contrast to antibodies, aptamers are selected against a variety of target molecules such as small molecules, toxins, peptides, proteins, viruses, bacteria, and even whole cells (Sefah *et al.*, 2010). Targets of antibodies, however, have to result in an immunological response for the production of antibodies. Toxins and antigens with low immunogenicity are not applicable to generate antibodies.

Aptamers are not recognized by the immune system as foreign, and do not evoke a negative immune response, however, antibodies are typically recognized by immune system as foreign and dangerous, evoking an undesired immune response. This risk of an immune reaction towards antibody increases with application of repeated doses (Song *et al.* 2012).

Finally, aptamers accept modifications which make aptamers to overcome certain limitations of them. For example, attachment of molecules on oligonucleotides makes them to resist nuclease degradation or renal filtration (Lakhin *et al.*, 2013). However, antibodies cannot accommodate conjugates without negative consequences such as reduced activity.

#### **1.4.2 Limitations of Aptamers and Solutions**

As mentioned above aptamers are stable molecules that can withstand high temperature and pH. However, since they are oligonucleotides, they are easily degraded when exposed to nuclease enzymes found in blood and biological media. This property limits the use of aptamers especially RNA aptamers to be used as therapeutics agents directly in blood (Lakhin *et al.*, 2013). To overcome this limitation there have been many attempts studied in literature. One of them is the use of modified nucleotides in the synthesis of starting library applied in SELEX or aptamers after selection process. The incorporation of, for example, 2'-Amino

pyrimidine nucleosides (Yan *et al.*, 2004) or 2'-fluoropyrimidine nucleosides 2' sugar position (Li *et al.*, 2011) increases the resistance of aptamers against nucleases action. Another way to prevent aptamer degradation is the synthesis of aptamers with L-nucleotides corresponding to aptamers composed of D-nucleotides selected against target. These mirror images of aptamers cannot be degraded by nucleases and thus they can stay in blood or biological fluids longer time (Lakhin *et al.*, 2013). As well as the stability of aptamers, the duration in body is also important for their applicability as therapeutic agents. Since they are small molecules with 15–100 nucleotides long, they are easily filtrated from kidney and eliminated from body. In order to increase the circulation time of aptamers in bloodstreams, they are conjugated with polyethylene glycol (Lakhin *et al.*, 2013) or cholesterol (Rusconi *et al.*, 2004).

One possible problem of aptamer can be the cross-reactivity of them towards structurally similar molecules. Although aptamers binds to their targets with high affinity and specificity, certain molecules that similar in structure to target molecules can also be recognized by aptamers as targets. This obstacle has been eliminated with the introduction of negative selection process in SELEX by using structurally similar molecules (Sefah *et al.*, 2010). After normal selection round with target molecule, eluted DNA or RNA pool is incubated with structurally similar molecule and unbound sequences are used for the next round of selection for target molecule. As a result, introduction of negative SELEX provides aptamer to become specific against target without showing cross-reactivity.

In accordance with their advantageous over antibodies and also with these solutions overcoming limitations, aptamers have been considered as substitutes for antibodies in a wide variety of applications.

## **1.5 SELEX**

A conventional *in vitro* selection method of aptamers is called SELEX which stands for **S**ystematic **E**volution of **L**igands by **E**xponential **E**nrichment. It was first described by Tuerk and Gold in the study of RNA aptamer selection against T4 DNA

polymerase (Tuerk and Gold, 1990). The word of “evolution” in the name of selection process can refer the evolution theory of Darwin. Throughout the selection process, certain sequences are enriched in pool based on their binding affinities and specific structures while others are removed from pool. Eventually at the end of the selection and partition process, pool contains outnumber specific sequences showing high affinity and specificity against target. Beside the word of “exponential enrichment” indicates the amplification of sequences via polymerase chain reaction (PCR) logarithmically after each round of SELEX.

A typical SELEX process is composed of basically four stages; DNA/RNA library design and synthesis, incubation of library with target molecule, removal of unbound sequences and elution of bound sequences and finally the amplification of eluted sequences (Figure 1.4).

The oligonucleotide library is a chemically synthesized combinatorial sequences group consisting of a random region with 20-80 nucleotides long and two constant primer binding regions (Figure 1.4). The central random region described by “N” provides the diversity of library with  $10^{13}$  to  $10^{15}$  sequence variants. It indicates A, C, G, T wobble site meaning that each N can be one of four nucleotides in chemical synthesis protocol of oligonucleotide randomly. As a result, the potential number of different sequences in library depends on random region length (number of N) and it is calculated with the N power of 4 ( $4^N$ ).

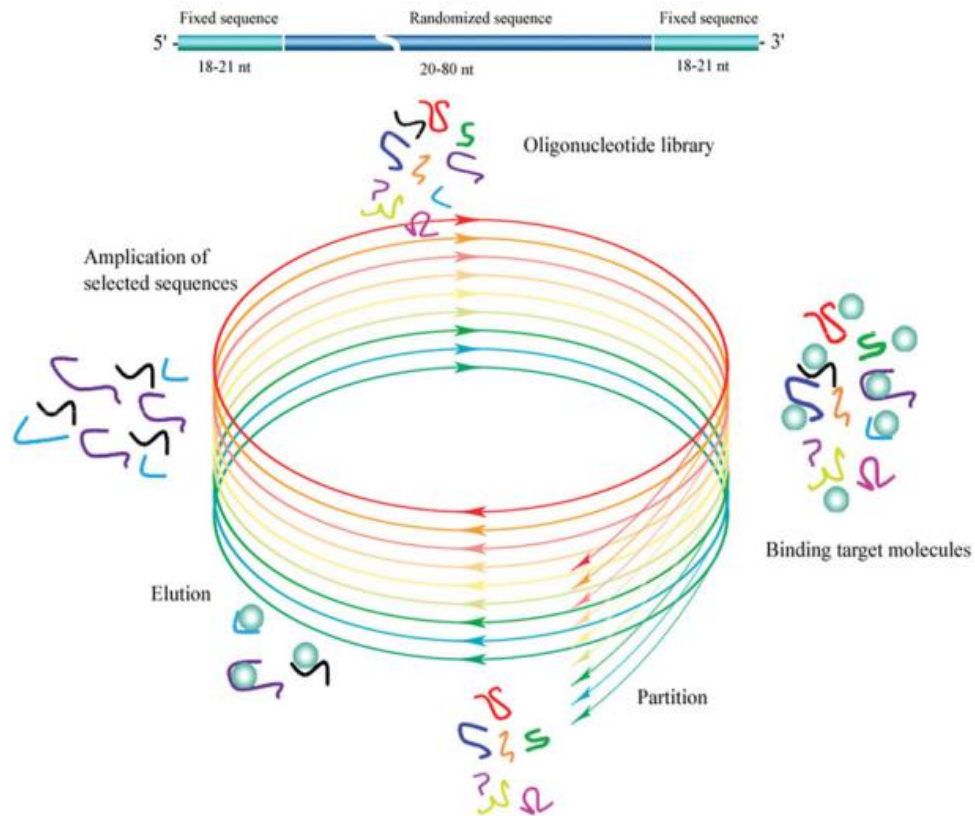


**Figure 1.4** General scheme of SELEX process (Dong *et al.*, 2014).

The second stage of SELEX is the incubation of DNA or RNA pool with target molecules under specified conditions. At this stage certain fraction of sequences have higher tendency to bind target as compared with others. At the next stage unbound sequences are removed from target bound sequences with physical separation techniques. The separation technique is based on the type of target. For example, small molecules selected as target for aptamer selection are immobilized on solid support and unbound sequences are removed by washing step. For larger molecules and whole cells, separation of unbound and bound sequences requires filtration via special membranes or precipitation by centrifugation force. After separation of unbound, bound sequences are eluted from target by applying heat or by elution



SELEX is an iterative cycles of selection process and four stages of selection are performed many rounds depending on target, library and partitioning methods. Generally, 6 to 20 rounds of SELEX have been performed in literature to select aptamer against many different targets (Dong *et al.*, 2014).

### **1.5.1 SELEX Variants**

With the changing needs and emerging new technologies certain changes have been introduced into standard SELEX process. The purposes of these changes are to rationalize oligonucleotide library, to improve aptamer selectivity, to expand target applicability, to enhance partition or selection efficiency, etc. Common SELEX variants are summarized in Table 1.2. SELEX variants are selected based on target type, starting library, specificity and affinity.

**Table 1.2** SELEX variants and their applications.

<b>SELEX Variants</b>	<b>Basic principle</b>	<b>Application</b>	<b>Example</b>
Negative SELEX	Introduction of selection step for structurally similar or related targets	Elimination of unspecific and non-target specific variants	Aptamer against BJAB lymphoblastoma cell line with negative selection applied to parental BJAB non-target cells (Meyer <i>et al.</i> , 2013)
Cell-SELEX	Use of whole cell as target in selection of aptamers	Targets at their native states on living cell	Aptamer against brain cancer cell Glioblastoma multiforme (Bayrac <i>et al.</i> , 2011)
Toggle SELEX	More than one target is toggled during the selection rounds so that selected aptamer shows affinity to all targets	Different levels of specificity against many target	Aptamer binding two structurally-related aminoglycosides (Derbyshire <i>et al.</i> , 2012)
Mirror-image SELEX	For enantiomer, target aptamer sequences are selected from D pool but L-DNA are synthesized based on D-DNA	Selection of nuclease resistant aptamer	Mirror image DNA aptamer against staphylococcal enterotoxin B (Purschke <i>et al.</i> , 2003)
Genomic SELEX (cDNA SELEX)	Oligonucleotide library is designed based on whole genome of an organism	Search for natural sequences found in genome to act as aptamers binding different molecules	RNA aptamers to find potential partners that could bind to specified RNA binding proteins in plants (Stamm <i>et al.</i> , 2012)
Tailored SELEX (primer-free SELEX)	Oligonucleotide library free of the fixed nucleotide sequences to minimize aptamer length	The requirement of short aptamers	Short aptamer sequences against migraine-associated calcitonin gene-related peptide (Vater <i>et al.</i> , 2003)
In silico SELEX	screening of aptamers by computational molecular docking or virtual screening strategy without wetlab experiment	Search for reduced sequences to quicken experimental selection process of aptamers	Aptamer against GTP via computational approach (Chushak and Stone, 2009)

## 1.6 Aptasensors and Their Applications

Biosensing elements play important roles in the development of biosensors in terms of their sensitivity and specificity. Among other recognition agents aptamers have been drawn attentions as sensing molecule for the construction of biosensors since 1990s. As compared with antibodies and peptides, they offer many advantageous that make them essential to be used in different application areas. For example, aptamers have been selected against targets in their native states and therefore, they have been used in the construction of aptasensors in food safety and environment control areas. Moreover, they have been easily modified for immobilization to different materials and for signaling purposes in detection platform without affecting their affinity. As summarized in Figure 1.6 aptamer based biosensors have been applied in different fields.

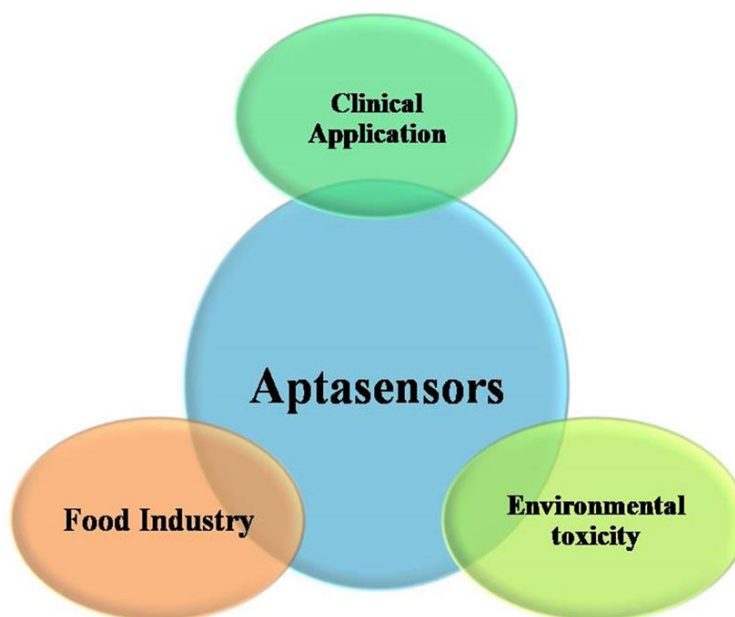


**Figure 1.6** Applications of aptasensors (Sett *et al.*, 2012).

### **1.6.1 Aptasensors in Clinical Diagnosis**

Early diagnosis of diseases in clinic studies have been playing important role in the treatment of patients effectively. Conventional techniques such as ELISA and culture dependent methods, however, prevent early diagnosis because of being dependent on special instruments and time consuming. Therefore, there have been many attempts to construct biosensing systems for diagnostic purposes with different receptor and transducers. The use of aptamers beside antibodies and other recognition elements in biosensor have improved sensitivity and efficiency of biosensors.

Aptasensors have been used for the detection of biomarkers and diagnosis of certain diseases such as cancer in clinical application area. They have been widely constructed for the detection of thrombin and immunoglobulin (Ig) E in literature. An electrochemical aptasensor was reported, for example, for the detection of thrombin with the use of thrombin aptamer-nanoparticle conjugates immobilized on graphene (Wang *et al.*, 2011). The detection of immunoglobulin (Ig) E was studied via surface plasmon resonance transduction system constructed with aptamers as receptor and signal molecules (Wang *et al.*, 2008).

In the field of cancer diagnosis, aptasensors have been recently applied for the detection of tumor markers present in blood. Some examples of aptasensors in cancer diagnosis are given in Table 1.3.

**Table 1.3** Examples of aptasensors for cancer diagnosis.

<b>Types of cancer cell</b>	<b>Types of aptamer</b>	<b>Detection type</b>	<b>Solid support</b>	<b>Reference</b>
Hela cell	DNA	Electrochemical, Label free	Graphene	Feng <i>et al.</i> , 2011
Ramos cancer cell	DNA	Label free	Gold electrode or magnetic bead	Hun <i>et al.</i> , 2011
Cell surface associated mucin1	DNA	Electrochemical	Single polypyrrole nanowire	Huang <i>et al.</i> , 2011

### 1.6.2 Aptasensors for Food Safety

The contamination of foods by chemicals, microorganisms and toxins has been the major concern in food safety and the increase in health problems resulted from consumption of contaminated foods accelerate the development of biosensors for food safety issue.

Aptamers as receptor molecule have been used in food safety control because as compared with antibodies they do not show variations in their productions from batch to batch and they are suitable for chemical modification. Moreover, they show longer stability and higher selectivity than antibodies which affect the effectiveness of biosensor.

Aptasensors have been studied for the determination of antibiotics and pesticide residues found in foods or for the detection of pathogenic bacteria and their toxins in food samples or for the detection of heavy metals.

The presence of antibiotic residues in food samples results in the transmission of antibiotic resistance to human upon consumption of contaminated foods and thus makes treatment of diseases with these antibiotics impossible. The detection of antibiotics with high sensitivity and selectivity, therefore, play important in food safety. There have been reported studies in which DNA and RNA aptamers have been selected against tetracycline (Berens *et al.*, 2001 and Xiao *et al.*, 2008) and

chloramphenicol (Mehta *et al.*, 2011 and Pilehvar *et al.*, 2012) and biosensors have been constructed with these aptamers in literature. Recently, Kim *et al.* was published the development of aptasensor for the detection of a derivative of tetracycline in milk. In this study, they used biotin modified aptamers selected against oxytetracycline as biosensing agents and indirect competitive enzyme-linked aptamer assay was constructed for the detection of antibiotics in milk with detection limit lower than limit stated in codex (Kim *et al.*, 2014).

Some examples of aptasensors have been reported for the detection of toxins in food and agricultural products. First study was conducted by Cruz-Aguado and Penner for the detection of mycotoxin in naturally contaminated wheat samples quantitatively. They used DNA aptamers to construct aptamer-based test to measure mycotoxins level in wheat samples (Cruz-Aquado and Penner, 2008). A recent study show the development of aptasensor for aflatoxin B1 detection in infant rice cereal and Chinese wildrye hay samples (Guo *et al.*, 2014). The sensitivity and selectivity of biosensor in this study is higher than other detection platform constructed for the determination of aflatoxin.

In addition to antibiotics, toxins and other small molecules such as heavy metals, detection of microorganisms in food samples have been performed with the use of aptamer-based biosensors. Specific DNA and RNA sequences have been conjugated to nanoparticles such as quantum dots. Current examples of aptasensor for pathogenic bacteria detection have been reported for *Bacillus thuringiensis* spores (Ikanovic *et al.*, 2007), *E. coli* (So *et al.*, 2008) and *Salmonella* Typhimurium (Cella *et al.*, 2010; Ozalp *et al.*, 2014).

### **1.6.3 Aptasensors for Environmental Control**

Increase in population of human and possible emergence of biological treat has raised the need of pollution control in environment. Common techniques for monitoring environment have same limitations such as being time consuming (Rogers, 2006). However, aptamers provide higher selectivity and specificity to

detection systems. Aptamer based biosensors are portable so that can be used at fields and highly stable against environmental conditions. Similar to food samples, aptasensors have been used for the detection of toxins and pathogens in water samples. Besides, organic and inorganic pollutants and drug residues have been detected by aptamer based biosensors (Sett *et al.*, 2012). An optical aptasensor was developed for detection of bisphenol A which is one of the endocrine disrupting compounds (EDCs) (Yildirim *et al.*, 2014). DNA probes complementary to bisphenol A aptamer were immobilized on fiber surface. After premixing of aptamer and bisphenol A, unbound sequences were hybridized with DNA probe on fiber and thus the amount of bisphenol A in water samples was measured indirectly by measuring signal coming from hybridized probe-unbound aptamer complex (Yildirim *et al.*, 2014).

## **1.7 Classification of Aptamer-based Biosensors**

The first use of aptamers as recognition elements in the construction of biosensors was reported for the detection of human neutrophil elastase (Davis *et al.*, 1996). Davis *et al.* was studied optical biosensor with the use of fluorescence modified aptamer for the detection of human neutrophil elastase immobilized on polystyrene beads. (Davis *et al.*, 1996). Since then, there have been many reported studies in literature for the construction of aptasensors. Biodetection platform based on aptamers have been categorized in terms of their transducer as optical, electrochemical and mass-sensitive sensors.

### **1.7.1 Optical Aptasensors**

Optical biosensors are detection platforms constructed with optical materials as solid supports and they measure the change in light absorption, fluorescence, luminescence, reflectance, Raman scattering and refractive index upon binding reaction between analytes and receptors. Enzymes, antibodies, cells and aptamers have been applied as recognition elements in the construction process. Aptamer-

based optical biosensors are constructed with labeled aptamers or with aptamers in label-free detection systems. Fluorescent-based aptasensors have been widely used because aptamers are easily modified with different fluorophores and quenchers and the detection of analytes have been performed at actual time. An example for the use of aptamer modified with both fluorescent molecule and quencher in detection platform is aptasensor for cocaine reported by Stojanovic *et al.* The basic working principle was quenching of fluorescent molecule on aptamer by the change in three dimensional structure of aptamer upon binding to cocaine (Stojanovic *et al.*, 2001). Beside quenching molecules, nanoparticles have been used as quencher in fluorescent-based aptasensors. Zhang *et al.*, reported the development of a fluorescent aptasensor for adenosine triphosphate (ATP) detection with dye-labelled aptamer single-walled carbon nanotubes (SWNTs). The detection of ATP was performed by the elimination of quenching property of carbon nanotubes when ATP binds to dye-labelled aptamer (Zhang *et al.*, 2010). In label-free detection systems of aptasensors DNA intercalation dyes and metal nanoparticles have been used recently. Wang *et al.*, developed an detection assay for ATP with the use of  $[\text{Ru}(\text{phen})_2(\text{dppz})]^{2+}$  dye. When intercalated aptamers bound to ATP, changes in the structure resulted in the productions of luminescence signals by free dye (Wang *et al.*, 2005). Although there have been many attempts to develop optical aptasensors for biological molecules, because of some limitations like complexity of biological environment they have needed to be improved in further studies (Feng *et al.*, 2014).

### **1.7.2 Electrochemical Aptasensors**

Electrochemical biosensors are the detection platforms constructed with electrode surfaces and measure the change in electrical current upon binding reaction between analytes and receptor molecule immobilized on support material. As in the other biosensor types, electrochemical biosensors have different receptor elements ranging from whole cell to nucleic acids.

The construction of sandwich type biosensing platform for the detection of thrombin with capture aptamer immobilized on gold electrode and glucose dehydrogenase

modified signal aptamer was the first electrochemical aptasensor (Ikebukuro *et al.*, 2004). Since then, many aptamer based sensing platforms have been reported for detection of biological molecules. Zhou *et al.* studied the development of quantum dot-based electrochemical aptasensor for ATP sensing. The working principle behind this electrochemical aptasensor was the decrease in current due to binding of QD to complementary strand which was dissociated from aptamer immobilized on three-dimensionally ordered macroporous (3DOM) upon binding of ATP to aptamer (Zhou *et al.*, 2010). Aptamer-based array electrodes were fabricated for the detection of Human IgE with label-free electrochemical system. In this system a gold surface was immobilized with aptamer and detection has been based on the electrochemical impedance spectroscopy method (Xu *et al.*, 2005).

The use of aptasensors for the detection of biological samples practically has some problems. Although aptamers are oligonucleotides having high affinity and selectivity against their targets, nonspecific binding of non-target molecules may occur which lead to decrease in the efficiency aptasensor for biological samples. Also, nucleic acids naturally found in biological samples may be complementary to aptamers so that prevent specific binding between aptamer and its target (Radi, 2011). Therefore, the fabrication technologies of aptasensors have needed to be improved in the future.

### **1.7.3 Mass-sensitive Aptasensors**

The mass sensitive biosensors, as the name implies, measure the changes in mass upon binding of analytes to receptor molecules immobilized to specific surfaces. Aptamer-based mass-sensitive biosensors, therefore, detect the change in size or mass of aptamer immobilized to surface.

There have been different studies for the fabrication of mass-sensitive aptasensors with the use of techniques like surface plasmon resonance (SPR) (Wang *et al.*, 2008), quartz crystal microbalance (QCM) (Min *et al.*, 2008) and surface acoustic wave device (SAW) (Schlensog *et al.*, 2004). Tombelli *et al.*, fabricated mass-sensitive

aptasensor for the detection of HIV-1 Trans-Activator of Transcription (Tat) protein with the immobilization of biotin modified RNA aptamer to streptavidin coated SPR chips (Tombelli *et al.*, 2005). The differences in binding options of RNA and DNA aptamer for interferon-gamma were reported in a quartz crystal microbalance-based study. Thiol modified aptamers were immobilized on gold electrode and binding reactions between aptamers and interferon-gamma which is a selective marker for tuberculosis was measured via quartz crystal microbalance. The results of this study indicated that RNA aptamer based detection platform is more sensitive with lower detection limit due to binding preference of RNA aptamer towards high multimeric state of IFN-gamma (Min *et al.*, 2008).

Although there have been fabrication studies of aptasensors for different biological analytes, they are inadequate as compared with antibody based biosensors. However, aptamer-based biosensors will replace other biosensors with the development of SELEX technology and immobilization techniques (Song *et al.*, 2008).

### **1.8 *Salmonella* and Its Detection Methods**

*Salmonella* is gram negative enterobacteria which have been representing the common causative agent of food poisoning over the world. It was firstly isolated from patients consuming contaminated beef in 1888 by German scientist Gaertner and since then it has been identified in certain moderate and severe infection diseases such as gastroenteritis and in more severe diseases such as typhoid fever, paratyphoid fever and fever associated with long-standing disease. Salmonellosis, infection caused by *Salmonella* is a food poisoning disease developing diarrhea, fever and abdominal cramps 8 to 72 hours after consumption of contaminated foods. Life – threatening complications and even death may occur if infection is not detected or treated early. The Center for Disease Control and Prevention (CDC) has been reported that approximately 1.4 million human have been infected by *Salmonella* in the United States annually by the consumption of contaminated poultry, egg, milk, beef, and raw foods and almost 600 of infection cases have ended up with death

(www.cdc.gov, last visited on September 2014). In addition, the World Health Organization (WHO) has accounted approximately 16 million cases of typhoid fever, 1.3 billion cases of gastroenteritis, and 3 million deaths resulted from *Salmonella* infections worldwide annually.

Recent studies have reported over 2500 serotypes of *Salmonella* all around the world. In Turkey, it was reported that the total number of serovars of *Salmonella* isolated from human and non-human sources was 129 till 2011 (91 serovars from human and 38 serovars from non-human sources) (Töreci *et al.*, 2013). Among them, *Salmonella enterica* serovar Enteritidis and *Salmonella enterica* serovar Typhimurium are the most common pathogenic bacteria causing salmonellosis. They contaminate mainly poultry, egg, milk, fruits, vegetables and spices. Early detection of *Salmonella* in food samples prevents the occurrence of diseases, spread of infection and thus improves food safety and reduces economical loses. In literature there have been many different studies for the detection of *Salmonella* in different samples. In the following section, conventional detection techniques, rapid detection techniques and recently developed biosensors for *Salmonella* detection were explained basically.

### **1.8.1 Conventional Detection Methods**

Conventional detection methods of microorganisms involve the isolation of bacteria (sampling), pre-selective growth on common media and selective enrichment on specified media. These methods require the presence of viable cells and longer period for detection of bacteria (Baron, 2011).

For *Salmonella* detection, different traditional methods have been reported by International Organization for Standardization (ISO), Food and Drug Administration (FDA) and Association of Official Analytical Chemistry (AOAC). In Figure 1.6, a standard method for culturing *Salmonella* reported by FDA is shown.

In the pre-enrichment stage, nonselective media have been used for the recovery of *Salmonella* by preventing the growth of other bacteria in media with the use of certain antibiotics (Tietjen *et al.*, 1995). Generally, buffered peptone water and lactose broth have been used for pre-selective growth of *Salmonella*. After recovery

in pre-selective media, *Salmonella* have been grown in certain selective media. Rappaport-Vassiliadis soy peptone medium and tetrathionate broth are approved media by FDA to be used in selective enrichment of *Salmonella*. Enriched *Salmonella*, then, have been subcultured in selective solid media such as Salmonella-Shigella (SS) agar, bismuth sulfite agar, Hektoen enteric (HE) medium, brilliant green agar and xylose-lisine-deoxycholate (XLD) agar. Different subspecies or serovars grow on selective media differently due to their biochemical and physical properties and these differences on colony morphology provide discrimination of *Salmonella* serovars (Mallinson *et al.*, 2000). For example, while *S. enterica* subsp. *arizonae* grow on XLD agar and form pink to red colonies, *S. enterica* serovar *typhi* grow on SS agar and form blacked centered colorless colonies.

Although the use of conventional methods provides high selectivity and specificity, easy use and lower cost for detection of *Salmonella*, faster screening techniques have been required for the detection and identification of *Salmonella* in food and environmental samples.

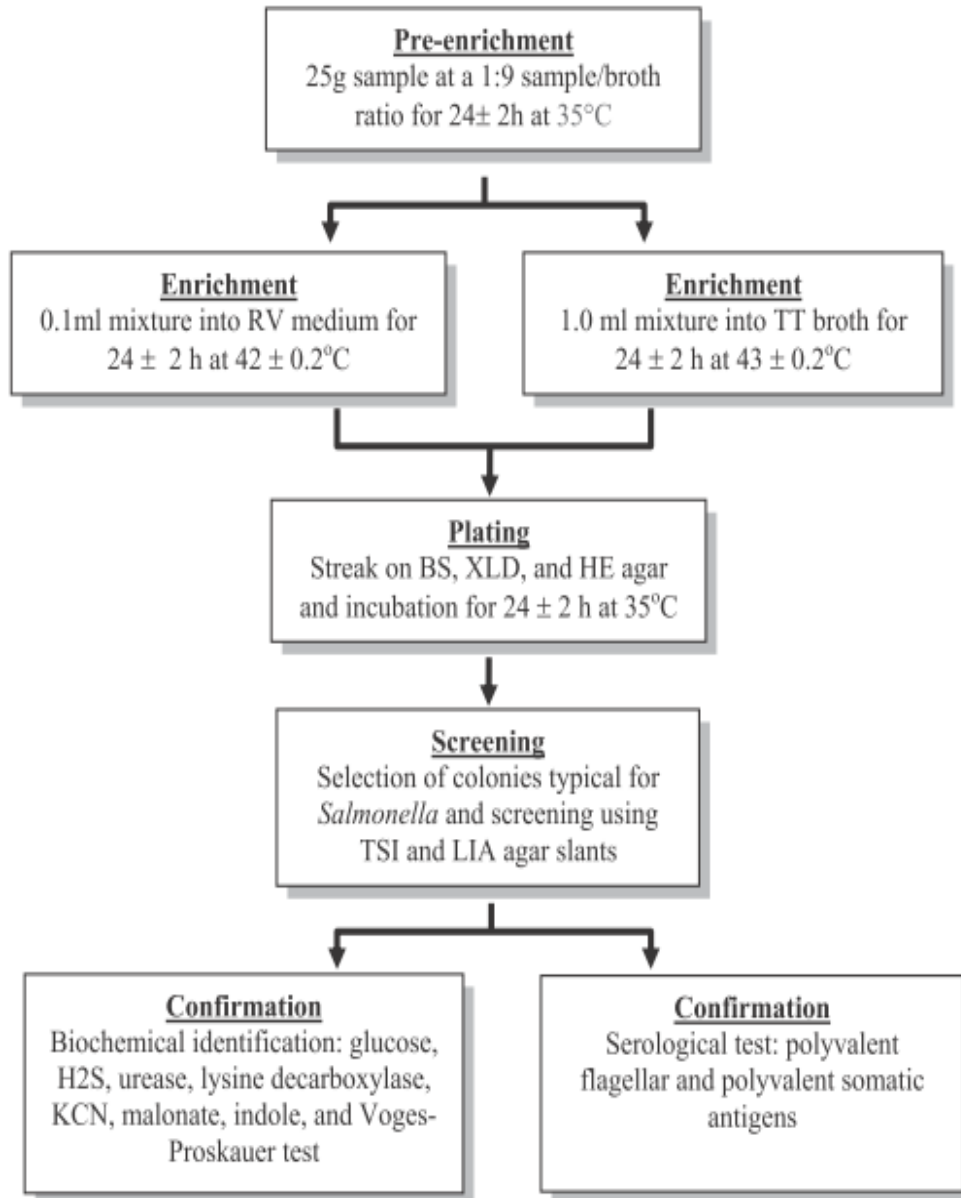


**Figure 1.7** Representative scheme of *Salmonella* culture method reported by FDA. RV, Rappaport-Vassiliadis medium; BS, bismuth sulfite agar; HE, Hektoen enteric agar; XLD, xylose lysine desoxycholate agar; TT, tetrathionate broth, TSI, Triple sugar iron agar, and LIA, Lysine iron agar (Lee *et al.*, 2015).

### 1.8.2 Rapid Detection Methods

Rapid detections of bacteria rely on modern molecular techniques which provide lower detection limit, higher sensitivity and specificity and faster detection as compared with conventional methods. Antibody based methods like ELISA and nucleic acid based techniques like PCR have been widely used for detection and identification of *Salmonella* species.

The uses of monoclonal and polyclonal antibodies for the detection of antigens of *Salmonella* species have been reported in many studies (Prusak-Sochaczewsk *et al.*, 1989; Tietjen *et al.*, 1995; Proux *et al.*, 2000; Wiuff *et al.*, 2000). The basic principle underlying detection of *Salmonella* via ELISA has been the formation of antibody – antigen complex resulting in the color change due to enzymatic reaction. Some commercially available ELISA kits for *Salmonella* detection is given at Table 1.4.

**Table 1.4** Commercially available ELISA-based *Salmonella* Detection Kits.

Assay	Manufacturer
3M™ Tecra™ Salmonella Visual Immunoassay	3M
Oxoid™	Thermo Scientific
MaxSignal®	Bioo Scientific
Salmotype	Labor Diag Leipzig
Salmonella Typhi IgG ELISA Kit	BQ Kits
IDEXX SE Ab Test	IDEXX
Salmonella IgM ELISA	Genway Biotech
MASTAZYME	MAST

Nucleic acid based detection methods rely on the amplification of specific sequences belonging to *Salmonella* via PCR. This method provides higher sensitivity and selectivity and does not require pure *Salmonella* culture.

In the literature there have been many PCR based studies for the detection of *Salmonella* (Chen et al., 2010). Certain target genes used widely for *Salmonella* detection are invasion protein gene (*invA*) (Ferretti et al., 2001; Malorny et al., 2003; Rahn et al., 1992), major fimbrial subunit encoding gene (*fimA*) (Doran et al., 1994), virulence gene (*spv*) (Lampel et al., 1996) and invasion gene transcriptional activator (*hilA*) (Guo et al., 2000; Pathmanathan et al., 2003). For example, Pathmanathan et al., reported direct PCR amplification method targeting *hilA* gene and results indicated that specific amplifications of *hilA* gene in 33 *Salmonella* strains easily discriminated *Salmonella* species from non-*Salmonella* strains (Pathmanathan et al., 2003). Moreover, Eyigor et al. studied the determination of *Salmonella* profile isolated from chickens from 2000 till 2003 by RT-PCR. In this study, *invA* gene was used for detection of *Salmonella* in a total of 1785 samples comprised of chicken intestinal samples, cloacal swabs, drag swabs, litter samples and chick dust samples collected from 15 companies in the Marmara region of Turkey. As a result, the presence of *S. Enteritidis* was highly observed in isolated samples (Eyigor et al., 2005).

In addition to commercially available ELISA-based detection kits, there have been PCR and Real-Time PCR kits for the detection of *Salmonella* strains. Most widely used commercial kits are given at Table 1.5.

**Table 1.5** Commercially available PCR-based *Salmonella* Detection Kits.

Assay	Manufacturer
foodproof® Salmonella Detection Kit	Biotecon
mericon Salmonella spp Kit	Qiagen
MicroSEQ® Salmonella spp. Detection Kit	Applied Biosystems
SureTect™ Salmonella Species PCR Assay	Thermo Scientific
BAX® System PCR assays	DuPont
iQ-Check Salmonella II Kit	BioRad

### 1.8.3 Biosensors for *Salmonella* Detection

Being high sensitive, specific, easy use and having lower response time, biosensors have taken place of conventional and rapid methods for detection of *Salmonella*. Different biosensor studies have been published with the use of enzyme, antibody and nucleic acids as receptor molecules for *Salmonella* detection and identification. Song *et al.* has developed an enzyme-based biosensor for the detection of *S. Enteritidis* with the use of nicking enzyme and carbon nanoparticles. The basic working principle of the biosensor is the emission of fluorescence by carbon nanoparticles upon the dissociation of quencher molecules from nanoparticle after binding to *Salmonella* (Song *et al.*, 2014). Pathirana *et al.* studied the construction of antibody-based biosensor with a polyvalent somatic O antibody immobilized on quartz crystal acoustic wave device (Pathirana *et al.*, 2000). Beside enzyme and antibody based biosensors, nucleic acid based biosensors have been reported for *Salmonella* detection. For example, Yan *et al.* developed a sandwich-type surface plasmon resonance biosensor. The specific probes designed for *invA* gene were used to detect target sequence on *invA* gene of *Salmonella* (Yan *et al.*, 2014).

Although there have been many attempts to construct detection platform for *Salmonella*, there are very few biosensors for the detection of *Salmonella* in the market. One of them, DETEX, is an electro-immunoassay biosensor which detects the presence of bacterial contamination in food samples by measuring reactions occurring between target bacteria and specific antibodies (Figure 1.8). The responses of this biosensor are shown against multiple pathogens such as *E.coli* O157, *Salmonella*, *Campylobacter* and *Listeria* simultaneously.

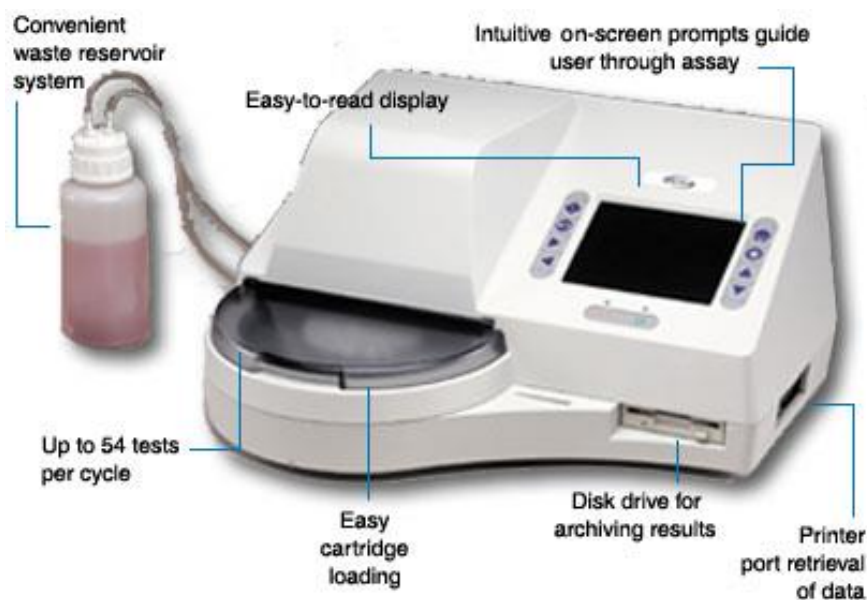


**Figure 1.8** Detex Pathogen Detection Technologies.

Aptamers have been recently reported as recognition elements in the construction of biosensor for the detection of *Salmonella* species. Published aptasensor studies are given at Table 1.6. In spite of being recent, with the rapid development in SELEX and biosensor technologies aptasensors may replace all pathogen detection techniques in future.

**Table 1.6** Aptamer-based biosensors reported in literature.

<b>Targets of biosensor</b>	<b>Types of sensor</b>	<b>Receptor element</b>	<b>Solid support</b>	<b>Reference</b>
<i>S. Enteritidis</i>	aptamer-based impedimetric sensor	DNA aptamer	Gold nanoparticles-modified screen-printed carbon electrode	Labib <i>et al.</i> , 2012
<i>E.coli O157:H7</i> and <i>S. Typhimurium</i>	label-free aptamer based sensor	DNA aptamer	Gold nanoparticles (AuNPs)	Wu <i>et al.</i> , 2012
<i>S. Enteritidis</i>	Aptamer-based FRET detection	DNA aptamer	Graphene oxide nanosheet	Wu <i>et al.</i> , 2014
<i>S. aureus</i> , <i>V. parahemolyticus</i> , and <i>S. Typhimurium</i> .	Aptamer based	DNA aptamer	Multicolor oleic acid-capped upconversion nanoparticles	Wu <i>et al.</i> , 2014
<i>S. Typhimurium</i>	Fluorescent aptasensor	DNA aptamer	Graphene oxide	Duan <i>et al.</i> , 2014

### 1.9 Aim of the Study

In this study, the two main aims are:

- generation of DNA aptamer against *Salmonella* Enteritidis via Cell-SELEX
- development of aptamer based sandwich type capillary platform for the detection of *S. Enteritidis* with the use of selected aptamer in this study.

## CHAPTER 2

### MATERIALS AND METHODS

#### 2.1 Materials

##### 2.1.1 DNA Library, Primers and Aptamers

DNA library designed for SELEX against *Salmonella* Enteritidis was synthesized with ABI 3400 DNA synthesizer at the Department of Chemistry in University of Florida. Beside DNA library all other oligonucleotides (Fluorescein modified forward primer, biotin modified reverse primer, fluorescein, biotin and thiol modified *Staphylococcus aureus* aptamers, fluorescein, biotin and thiol modified *Salmonella* Enteritidis aptamers) were purchased from Integrated DNA Technologies (Coralville, IA, USA).

##### 2.1.2 Target and Control Cells

*S. Enteritidis* was kindly provided by Prof. Dr. Mehmet Akan (Faculty of Veterinary Medicine, Ankara University). Also, *Staphylococcus aureus* was kindly supplied by Doç. Dr. Selçuk Kılıç (T.C. Halk Sağlığı Kurumu).

##### 2.1.3 Reagents

Tryptic soy agar and tryptic soy broth used as growth medium of target cell, *S. Enteritidis*, and control cells, *E. coli* and *S. aureus*, were purchased from Sigma-Aldrich (Darmstadt, Germany). All chemicals used for buffer preparation were analytical grade and purchased from Sigma-Aldrich or Merck (Darmstadt, Germany) unless otherwise specified. [N-e-Maleimidocaproyloxy] sulfosuccinimide ester

(EMCS) as cross-linker was bought from Pierce (IL, USA). For DNA purification and desalting, Illustra NAP-5 Columns and streptavidin agarose resin were purchased from GE Healthcare Bio-Sciences (Pittsburgh, USA) and Thermo Scientific (Rockford, USA), respectively. Quantum dot conjugated streptavidin was purchased from Invitrogen (Carlsbad, CA, USA). The support material was coated with poly-L-lysine solution purchased from Sigma-Aldrich (Darmstadt, Germany).

All solutions including buffers were prepared with distilled water and preparations of them were given at Appendix A.

#### **2.1.4 Supporting Material for Platform**

Glass capillaries purchased from Marienfeld GmbH & Co. (Lauda-Königshofen, Germany) were used as support materials for the construction of platform.

#### **2.1.5 Equipments**

The selection of aptamer by SELEX method required the use of shaking incubator for the growth of bacteria, thermal cycler for the amplification of pools and freeze-dryer for the lyophilization of amplified pools.

The control of selection process was performed via fluorospectrometer (Nanodrop 3300, Thermo) and Real-time PCR (LightCycler 1.5, Roche).

The sequences were determined with ion semiconductor sequencing method by IonTorrent Ion Hi-Q™.

The selected sequences were characterized with laser scanning confocal microscope (Zeiss LSM 510), absorbance microplate reader for ELISA (SPECTRAmax 340PC) and isothermal titration micro calorimeter (MicroCal VP-ITC).

## 2.2 Methods

This study was constituted in two main parts which were carried out spontaneously. In the first part, selection of aptamers against *Salmonella* Enteritidis was performed. The second part consisted of the optimization of characterization studies of aptamers with the use of *Staphylococcus aureus* aptamer taken from literature and also the optimization studies of aptamer based capillary sandwich platform again with the use of *S. aureus* aptamer. All optimized techniques and optimized detection platform, then, were applied to *S. Enteritidis* aptamer selected in this study. The basic time flow scheme of this study was represented in Figure 2.1.

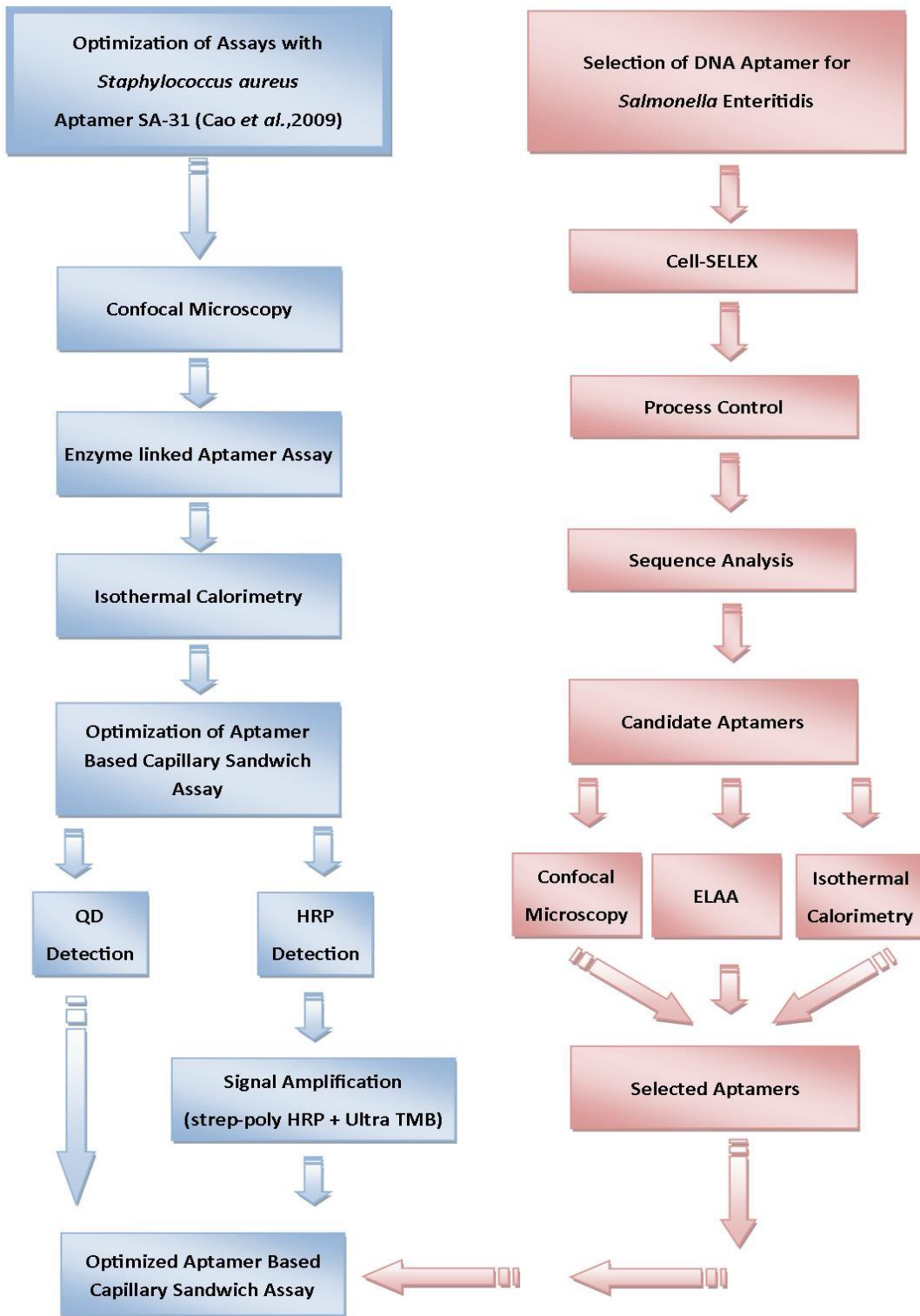


**Figure 2.1** Flowchart showing all steps of the procedure.

### 2.2.1 Cell-SELEX

In this study, whole *Salmonella* Enteritidis cells were used as target for aptamer selection. The entire process of aptamer selection (Cell-SELEX) was a complex set of experiment containing a) selection of sequences b) process control of SELEX c) sequence analysis d) characterization of candidate aptamers with binding and affinity studies. The general selection process was explained in Figure 2.2.



**Figure 2.2** Representative figure of SELEX; 1) incubation of target cells and library pool, 2) removal of unbound and elution of bound sequences, 3) PCR amplification of eluted pool, 4) converting dsDNA into ssDNA, 5) sequencing and 6) binding analysis via confocal microscope and ITC (modified from Bayrac *et al.*, 2011).

### 2.2.1.1 Design of Primers and DNA Library

Primers were designed using OligoAnalyzer 3.1 software supported by Integrated DNA Technologies (IDT) ([www.idtdna.com](http://www.idtdna.com)). Based on standard primer design considerations fluorescein modified forward primer and biotin modified reverse primer were designed as 5'-AAGGGCTGGCTGGGATGGA-3' and 5'-AGTGGGGTCCGTGGAGTGA-3', respectively. They were purchased from Integrated DNA Technologies Inc., Coralville, IA.

DNA library was designed with constant primer binding regions and a central random region of 42 nucleotides for the construction of pool containing different sequences (5'-AAGGGCTGGCTGGGATGGA-N<sub>42</sub>-TCACTCCACGGACCCCACT-3').

### 2.2.1.2 Synthesis and Purification of DNA library

DNA library for SELEX was synthesized chemically with ABI 3400 DNA synthesizer at the Chemistry Department of University of Florida. The standard phosphoramidite chemistry was used for synthesis (Figure 3.1).

For the purification of synthesized DNA library reverse-phase HPLC was used with a C<sub>18</sub> column (250 mm × 4.6 mm, 5- $\mu$ m particle size) and a gradient mobile-phase mixture of acetonitrile and aqueous 0.1 M triethyl ammonium amine. Purified library was precipitated with 3M sodium chloride solution and cold ethanol at -80°C for 10 minutes. After centrifugation at 14000 rpm for 20 min pellet was dried with speed vacuum for 5 minutes. The stock library was resuspended in sterile distilled water and stored at -20°C.

### **2.2.1.3 Optimization of Annealing Temperature of Library and Primer Concentration in PCR Reaction**

For the determination of optimum annealing temperature of PCR, DNA library was amplified at seven different temperatures (60.1, 61.9, 63.0, 64.3, 66.9, 68.4 and 69.9°C) with the use of gradient PCR technique. The reaction mixtures for 7 tubes for gradient PCR and 1 tube for negative control were prepared as follows. The each reaction mixture of 50 µL contained 5 µL of PCR buffer, 4 µL of dNTPs stock solution (2.5 mM of each dNTP), 2.5 µL of 10 mM primer mix, 0.15 µL of Takara Taq DNA Polymerase (5 units/µL), 35.85 µL of distilled water and 2.5 µL of 10nM DNA library. The amplification protocol was set as initial denaturation at 95°C for 3 min, denaturation at 95°C for 30 seconds, annealing for seven tubes at 60.1, 61.9, 63.0, 64.3, 66.9, 68.4 and 69.9°C accordingly for 30 seconds and elongation at 72°C for 30 s, followed by final extension for 3 min at 72°C.

Four different primer concentrations were prepared for estimation of optimum primer concentration in PCR. Primer mixes at concentrations of 3, 5, 8 and 10 µM were used in the preparation of reaction mix containing 5 µL of PCR buffer, 4 µL of dNTPs (2.5 mM of each dNTP), 0.15 µL of Takara Taq DNA Polymerase (5 units/µL), 35.85 µL of distilled water and 2.5 µL of 10 nM DNA library.

PCR products were analyzed on 4 % of agarose gel and specific bands belonging to desired PCR products were determined for optimum PCR conditions.

### **2.2.1.4 Preparation of Target Bacterial Cell**

Single colony of *S. Enteritidis* was inoculated to tryptic soy agar (TSA) by streak plate method and incubated at 37°C for 24 hours. From that plate a single colony was inoculated to 100 mL of tryptic soy broth (TSB) and incubated at 37°C for 18 hours at 100 rpm shaker for late stationary phase of bacterial growth. Then, 100 µL of cell

suspension was inoculated to 150 mL of TSB. Absorbances of cell suspension at 600 nm from time 0 through 6,5 hours with time interval of 30 minutes were measured in three replicates (n=3). Mean values were calculated to draw the growth curve of *S. Enteritidis* in TSB medium at 37°C and 100 rpm shaking.

Early growth phase of *S. Enteritidis* at time 180 minutes ( $OD_{600} = 0.3$ ) was selected for the preparation of cell at each round of SELEX. Predetermined volume of cell culture was pelleted by centrifugation at 1000 g for 5 min at 4°C and media was discarded without touching the pellet. Cell pellet was washed with 1 mL of washing buffer and re-centrifuged at 1000 g for 5 min again to remove washing buffer. Washed cell pellet was resuspended in 500  $\mu$ L of binding buffer to be used in SELEX rounds.

#### **2.2.1.5 Incubation of DNA Library with Target Cell**

At the first round of SELEX, 5 nmoles of DNA library in 500  $\mu$ L of binding buffer was denatured at 95°C for 5 min and instantly cooled down on ice in order to allow single stranded DNA (ssDNA) folding. After denaturation, prepared target cell suspension and DNA library were mixed thoroughly and the mixture was incubated on a shaker at 4°C for 1 hour. Incubation time of cell and library was reduced in subsequent rounds (3 minutes less per round) from 1 hour to 30 minutes.

#### **2.2.1.6 Recovery of Bound Sequences**

After incubation, target cell-DNA library complex was centrifuged at 1000 g for 5 min. The unbound sequences in upper phase were poured off and pellet was washed once with 1 mL of washing buffer and centrifuged to remove supernatant. The number of washing step was increased in subsequent rounds of SELEX. Parameters changed throughout SELEX rounds were summarized at Table 2.1.

**Table 2.1** Selection parameters of aptamer used in whole cell SELEX.

<b>SELEX Rounds</b>	<b>Target Cell Concentration (million/ml)</b>	<b>DNA Pool Concentration</b>	<b>Incubation Time (min)</b>	<b>Washing Step</b>
1st round	100	5 nmole	60	1
2nd round	75	100 pmole	57	1
3rd round	75	100 pmole	54	1
4th round	50	100 pmole	51	1
5th round	50	100 pmole	48	1
6th round	50	100 pmole	45	1
7th round	50	100 pmole	42	2
8th round	25	100 pmole	39	2
9th round	25	100 pmole	36	2
10th round	25	100 pmole	33	2
11th round	10	100 pmole	30	3
12th round	10	100 pmole	30	3

At the first round of selection cell-DNA library pellet was resuspended in 500  $\mu$ L of distilled water. DNA sequences bound to *S. Enteritidis* were recovered by heating at 95°C for 15 minutes followed by centrifugation at 10,000 g for 5 minutes. The supernatant which was named as first pool contained the sequences that bind to the target cell.

#### **2.2.1.7 PCR Optimization and Single-Stranded DNA Preparation**

After the elution of first pool three different PCR reactions were performed. At first, all eluted pool (500  $\mu$ L) was amplified within a final volume of 1000  $\mu$ L of PCR

mixture. The reaction mixture contained 100  $\mu\text{L}$  of PCR buffer, 80  $\mu\text{L}$  of dNTPs (2.5 mM of each dNTP), 50  $\mu\text{L}$  of 10 mM primer mix, 3  $\mu\text{L}$  of Takara Taq DNA Polymerase (5 units/ $\mu\text{L}$ ), 270  $\mu\text{L}$  of distilled water and 500  $\mu\text{L}$  of first pool. The reaction mixture was amplified with the following protocol: initial denaturation at 95°C for 3 min, denaturation at 95°C for 30 seconds, annealing at 63°C for 30 seconds and elongation at 72°C for 30 s with 10 cycles, followed by final extension for 3 min at 72°C. After first amplification, second PCR reaction was prepared for the optimization of cycle number of eluted pool. Seven tubes each of which contained 5  $\mu\text{L}$  of PCR buffer, 4  $\mu\text{L}$  of dNTPs (2.5 mM of each dNTP), 2.5  $\mu\text{L}$  of 10 mM primer mix, 0.15  $\mu\text{L}$  of Takara Taq DNA Polymerase (5 units/ $\mu\text{L}$ ), 33.35  $\mu\text{L}$  of distilled water and 5  $\mu\text{L}$  of 10 cycle pre-amplified pool were amplified and collected at the following cycles: 4, 6, 8, 10 and 12, and one negative control at the twelfth cycle. After optimized PCR cycle was selected the third PCR reaction was set up for the next round of selection.

In the subsequent rounds of SELEX, eluted pools were amplified first for cycle optimization and then final PCR amplifications were performed as explained above to prepare pool for next round.

At each round of SELEX amplified pools were converted to single stranded DNA (ssDNA) pools to be used at the next round as DNA library. The biotin labeled strand of amplified pool was removed with the use of column having filter in one end and syringe in the other end. The 200  $\mu\text{L}$  of streptavidin beads solution was added to syringe and plunger was pushed until all solutions were out. The syringe was removed from the column to remove plunger from syringe. Then, the syringe was put back onto column. The beads loaded on column were washed with 2 mL of PBS solution (1X). After washing step, PCR product was loaded onto syringe and

collected from column. Loading of PCR product was repeated three times, however, filtrate at the third time was not collected from column. Amplified pool bound to beads was washed with 2 mL of PBS solution (1X) to remove unbound primers on beads. Unzipping of double stranded DNA was performed by adding 500  $\mu\text{L}$  of 200

nM NaOH solution to collect fluorescein modified ssDNA. The preparation of ssDNA was summarized at Figure 2.3.

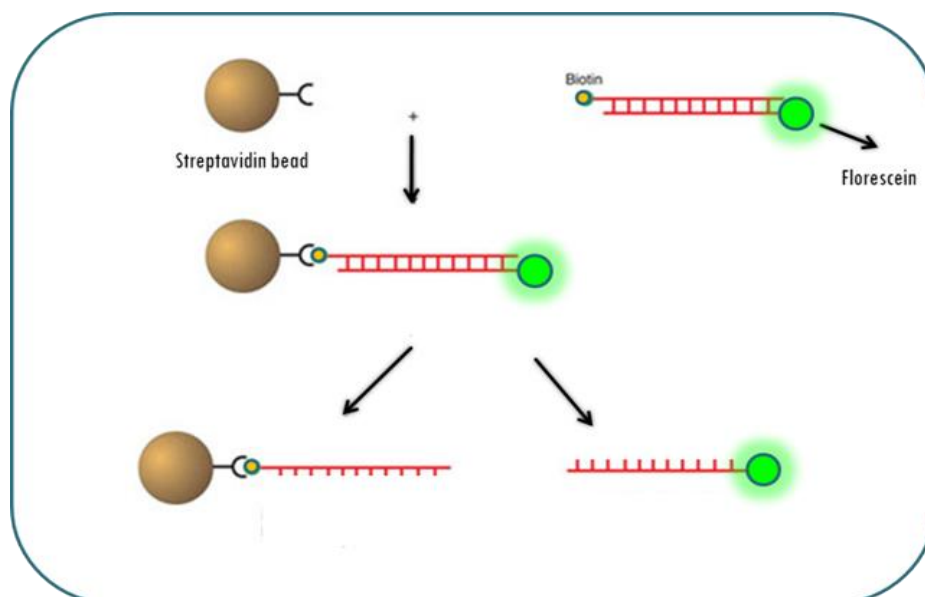


**Figure 2.3** Preparation of ssDNA from dsDNA.

After the collection of ssDNA within sodium hydroxide solution from column, alkaline solution was removed with the use of desalting column (Illustra Nap-5 Columns, Sephadex G-25 DNA Grade). Before adding filtrate desalting column was washed with 15 mL of distilled water. When the last drop of water was out, filtrate was loaded to column and waited until filtrate penetrated into the column completely. In order to collect ssDNA 1 mL of distilled water was added to column and the solution containing ssDNA pool was collected to be used in next round of SELEX.

The ssDNA pool was lyophilized and pellet was resuspended in 100  $\mu$ L of distilled water. The concentration of pool was measured spectrally at 260 nm and 100 pmoles of library were used for the next round of selection.

### **2.2.1.8 Negative SELEX**

Aim of negative selection was the elimination of unspecific and non-target cell specific variants from the specifically bound ones selected in SELEX rounds.

Negative cell, *E. coli*, was prepared as a target cell as mentioned previously. Starting from the sixth round, 50 million/mL of *E. coli* was incubated with DNA pool recovered as bound sequences to *S. Enteritidis* for 40 minutes at 4°C. In order to pellet *E. coli* with non-specific binder sequences, cell –DNA pool mixture was centrifuged at 10,000 g for 5 minutes. The supernatant contained sequences that did not bind to *E.coli*. These sequences were amplified with optimum cycle number and converted to ssDNA for the next round of SELEX.

## **2.2.2 Progress Control of SELEX**

### **2.2.2.1 Fluorescent Aptamer Binding Assay**

Fluorescence modified primer (P1-FAM) was prepared at different concentrations (0.01, 0.05, 0.1, 0.5, 1, 5 and 10 pmole). Their relative fluorescence units were read with fluorospectrometer (Nanodrop 3300 Fluorospectrometer, Thermo). Relative fluorescence units of each concentration of P1-FAM were read as quinary replicates (n=5) and mean units were plotted against concentrations at pmole and  $\mu\text{M}$  for the construction of standard curve. The pools eluted after each round were prepared at 1 pmole in binding buffer and incubated with  $10^6$  CFU/mL of *S. Enteritidis* at 4° for 30 min. The cell-DNA pool mixtures were centrifuged to remove unbound sequences and washed with washing buffer twice. The cell-DNA mixtures were exposed to heat at 95°C for 15 minutes. After centrifugation, bound portions of pools were eluted in binding buffer. Relative fluorescence units of eluted pools were measured with fluorospectrometer. The elution yield of each SELEX round was estimated by

dividing relative fluorescence units of bound ones to that of initial pool concentrations.

#### **2.2.2.2 Melting Curve Analysis of DNA Pools**

The eluted pools of each round of SELEX were amplified in Real Time PCR (Lightcycler® 1.5 carousel, Roche) with 20  $\mu\text{L}$  of PCR reaction containing 2  $\mu\text{L}$  of SYBR Green enzyme mix, 1  $\mu\text{L}$  of each primer (final concentration of each 0.5  $\mu\text{M}$  in reaction mix), 2.4  $\mu\text{L}$   $\text{MgCl}_2$  (final concentration of 4  $\mu\text{M}$  in reaction mix), 11.6  $\mu\text{L}$  of water and 2  $\mu\text{L}$  of DNA pool. As negative control water and as positive control 1nM of DNA library were added to mix instead of pool. The PCR protocol was set as 15 minutes of denaturation, followed by 35 cycles of 10 sec at 95°C, 4 sec at 63°C, 4 sec at 72°C and 1 sec at 72°C for amplification. The melting curve analysis was performed 15 sec at 95°C, 0 sec at 37°C with ramp rate of 0.05, and 0 sec at 37°C with continuous measurement. Finally, reaction was cooled at 37°C for 30 sec.

#### **2.2.3 Sequence Analyses**

Final eluted pool was sequenced with IonTorrent (Life technologies) sequencing technology by Sentegen Biotech (Ankara, Turkey). Data was analyzed with multiple sequence alignment tools; MAFFT (Multiple Alignment using Fast Fourier Transform), Clustal, MView (EMBL-EBI) and NUPACK (Nucleic Acid Package, [www.nupack.org](http://www.nupack.org)).

## **2.2.4 Characterization and Binding Studies of Selected Aptamer**

### **2.2.4.1 Confocal Imaging of Bacteria with Aptamer**

Single colony of *S. Enteritidis* was inoculated to 10 mL of TSB and incubated at 37°C shaking overnight. From bacterial solution 10 µL was inoculated to 10 mL of TSB and incubated at 37°C for 3 hours at 100 rpm shaker till absorbance of cell suspension was read as 0.3 at 600 nm. Cell solution was pelleted at 5000 rpm for 5 min and re-suspended with PBS (1X). Cell suspension having 10<sup>6</sup> CFU/mL of *S. Enteritidis* was incubated with 500 nM FITC labelled *S. Enteritidis* aptamer at room temperature for 30 min. After the removal of unbound aptamer, cells-aptamer complex was washed twice with PBS. One drop of cell-aptamer complex was dropped on glass slide and bacteria smear was fixed to slide by passing slide three times through flame of Bunsen burner. Confocal images were taken under 488 nm exciting light and visible light. Control slides were prepared as explained above with *S. aureus*, *E.coli* and aptamer selected for *S. Enteritidis*.

### **2.2.4.2 Enzyme-Linked Aptamer Assay (ELAA)**

Single colony of *S. Enteritidis* was inoculated to 10 mL of TSB and incubated at 37°C and 100 rpm shaker overnight. From that cell solution 10 µL was inoculated to 10 mL of TSB and incubated at 37°C for 3 hours for early stationary phase of bacterial growth. In order to pellet the cell, solution was centrifuged at 5000 rpm for 5 min. Cell pellet was resuspended in washing solution (1X PBS containing 5 mM MgCl<sub>2</sub> and 0.1% Tween 20) and added to wells of 96-well plate at previously determined amounts of cell. Before adding aptamer solution to wells, it was preheated at 95°C for 5 min and instantly cooled down on ice. The biotin modified aptamers were added at predetermined concentration to each well and plate was incubated at room temperature for 30 min. The cell-aptamer solutions in wells were

centrifuged at 5000 rpm for 5 min to remove unbound aptamers and washed with washing solution once. HRP modified streptavidins (diluted at 1:20.000 ratio) were added to wells and incubated at room temperature for 30 min. After washing plate to remove unbound streptavidins, 50  $\mu$ L of TMB solutions were added to wells. The absorbance readings of wells at 370 and 600 nm were recorded. Different aptamer concentrations (1, 5, 10 and 20  $\mu$ M), cell numbers ( $10^7$ ,  $10^6$ ,  $10^5$ ,  $10^4$  and  $10^3$ ) and control wells were used in this study.

#### **2.2.4.3 Isolation of Cell Membrane Proteins of Bacteria using Carbonate Extraction Method and Bioanalyzer Protein Assay**

Overnight grown 150 mL of *S. Enteritidis* culture was centrifuged at 2500 g for 8 minutes to remove media. The cell pellet was washed with 20 mL of 50 mM Tris-HCl solution (pH 7.5). After washing cell, pellet was resuspended in 20 mL of Tris-HCL solution. The cell culture was ruptured by passing cell solution through a cold French Press at 14000 psi (0.97 bars) twice. The ruptured cell solution was pelleted and supernatant was added to 50 mL of 100 mM cold sodium carbonate buffer (pH 11.0). This solution was stirred slowly for 2 hours in ice and centrifuged at 115,000 g for 30 minutes at 4°C. The pellet was resuspended in 1 mL of PBS solution (1X). The absorbance of isolated membrane proteins was read at 280 nm and concentration was calculated assuming that 1 absorbance at 280 nm was approximately equal to 1 mg/mL of protein. Isolated membrane proteins were analyzed on Bioanalyzer (Agilent 2100 Bioanalyzer) supported by Molecular Biology and Biotechnology R&D Center. Protein 80 assay was performed with protein 80 kit. The protein samples of 4 $\mu$ L were mixed with 2  $\mu$ L of sample denaturing buffer and heated at 95°C for 5 minutes. Heated protein samples were diluted with 84  $\mu$ L of distilled water and then 6  $\mu$ L of sample was loaded to protein 80 chip. Data was analyzed with The 2100 Expert Software.

#### **2.2.4.4 Isothermal Titration Calorimeter Analysis**

Titration calorimeter analysis was performed with MicroCal VP-ITC supported by METU Molecular Biology and Biotechnology R&D Center. The sample cell was washed with PBS buffer (1X) before experiment. Then sample cell and syringe were loaded with 10  $\mu$ M aptamer with volume of 1.5 mL and 50  $\mu$ M of isolated membrane protein, respectively. After 1200 seconds of initial delay, membrane proteins in syringe was injected into aptamer solution serially 25 times with each volume of 10  $\mu$ L. the duration of injection was 20 seconds and between each injection the spacing time was 300 seconds. Titration experiment was performed under constant stirring speed of 300 rpm and at 37°C.

Binding mechanisms were analyzed at three different temperatures; 4°C, 25°C and 37°C and in PBS solution at sodium chloride concentrations of 50, 137 and 200 mM. Raw data was analyzed with Origin 7.0 software (OriginLab Corporation, Northampton, MA, USA).

#### **2.2.5 Construction of Aptamer-Based Sandwich Platform for Bacterial Detection**

For the construction of aptamer-based sandwich platform we firstly carried out the surface coating of capillaries which were used as support materials. Followed by the immobilization of thiol modified aptamer on coated surface bacterial cells were captured and sandwich assay was completed with binding of aptamer carrying signal molecules to captured cells. Two signaling molecules, streptavidin conjugated quantum dots and streptavidin conjugated horseradish peroxidase were used independently. General scheme of aptamer-based sandwich platform construction was represented in Figure 2.4.

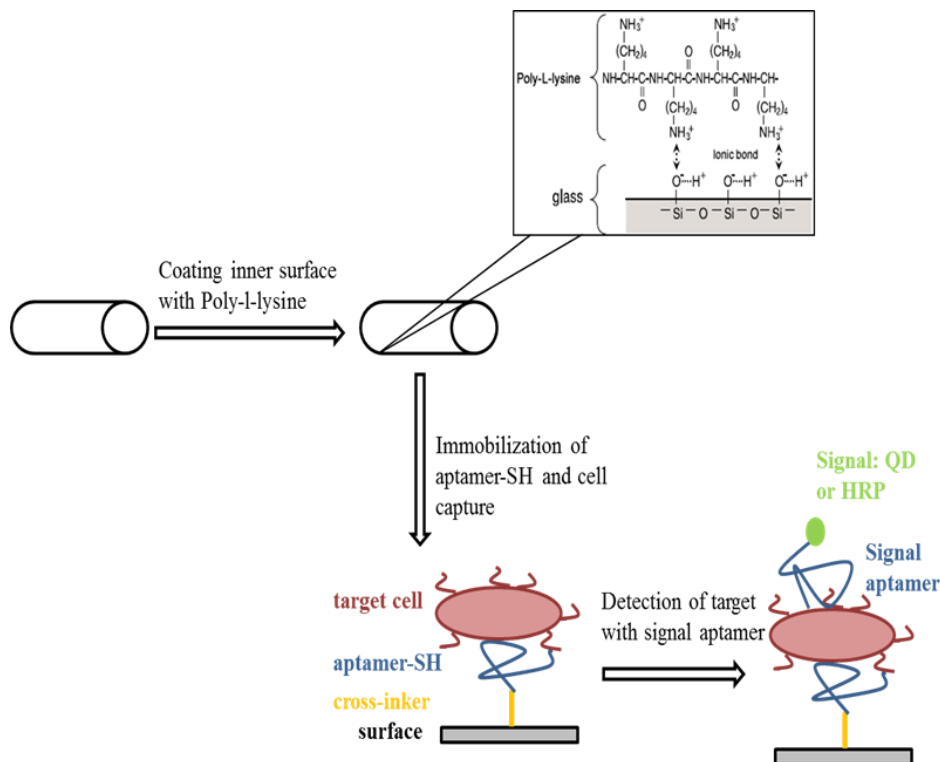


**Figure 2.4** Construction scheme of Aptamer-Based Sandwich Platform for Bacterial Detection.

### 2.2.5.1 Surface Coating

Glass capillaries were washed with distilled water first. Then, pre-washed capillaries were washed with sodium hydroxide washing solution for 2 hours followed by washing step again with distilled water. After washing, capillaries were incubated with poly-l-lysine solution for one hour at room temperature. Coated capillaries were dried by spinning at 1000 rpm for 5 minutes and stored at 4°C for at least 15 days before experiment.

Coating and washing steps were performed with syringe pump at injection speed of 10 $\mu$ L/sec.

### 2.2.5.2 Optimization Studies for Platform Construction

Coated slides were washed with washing buffer (1 X PBS, 0.05 % Tween-20) twice and submerged in washing solution during the preparation of aptamer and amine-to-sulfhydryl crosslinker solutions.

The crosslinker, N-epsilon-Maleimidocaproyl-oxysulfosuccinimide ester (Sulfo-EMCS), was prepared fresh before each experiment in 10mM PBS (pH: 7.2). Meanwhile, thiol modified aptamers were denatured at 95 °C for 5 minutes and instantly cooled down on ice.

Predetermined concentration of thiol modified aptamers, Sulfo-EMCS solution with a final concentration of 2 mM and tris(2-carboxyethyl)phosphine (TCEP) with a final concentration of 0.1 mM were prepared in PBS (1X) and the mixture was incubated at room temperature for 30 minutes to reduce disulfide bonds of thiol modified aptamers. After pre-incubation, aptamers were immobilized on poly-l-lysine coated capillaries by incubating aptamer-crosslinker solution in capillaries at room temperature for one hour. At the end of incubation, capillaries were washed with 5 X saline-sodium citrate (SSC) buffer containing 0.1% sodium dodecyl sulfate (SDS) followed by distilled water at 50  $\mu$ L/sec of injection speed. During the preparation of bacterial solution capillaries were filled with binding buffer (1X PBS, 1 % BSA, 0.1 $\mu$ g/mL and 0.05 % Tween-20).

*S. aureus*, *S. Enteritidis* and *E.coli* were grown in TSB at 37°C till early log growth phase with OD<sub>600</sub> = 0.3. Cell solutions were washed with binding buffer and predetermined amount of cells were incubated in capillaries for one hour. The incubation temperature of *S. aureus*, *S. Enteritidis* and *E.coli* in capillaries immobilized with *S. aureus* aptamer was 37 °C while it was 4 °C for *S. Enteritidis*, *S. aureus* and *E. coli* in capillaries immobilized with *S. Enteritidis* aptamers. After incubation capillaries were washed with washing buffer (1X PBS and 0.05 % Tween-20) and predetermined concentration of biotin modified aptamers (in binding buffer) were added to construct sandwich assay. After incubation at room temperature for

one hour unbound aptamers were removed with washing buffer and stored in washing buffer at room temperature.

General experimental stages of platform construction were explained above. Optimization parameters at certain stages were given at Table 2.2.

**Table 2.2** Optimization parameters for the construction of aptamer-based capillary sandwich platform.

<b>Construction stages</b>	<b>Parameters</b>	<b>Conditions</b>
Immobilization of thiol modified aptamers	Concentration of thiol modified aptamer	5 $\mu$ M or 10 $\mu$ M
	Incubation period of aptamer in capillary	1 hour or 1hour 30 min
	Washing speed	50 $\mu$ L/sec or 10 $\mu$ L/sec
Blocking of surface	Blocking agent	BSA (2 % in PBS) or BSA (5 % in PBS) or PEG
Addition of bacterial cell	Incubation temperature	Room temperature or 37 °C

### 2.2.5.3 Detection Platform with Quantum Dot and HRP

For the detection of bacteria captured in sandwich system which was constructed with thiol and biotin modified aptamers, two different signaling strategies were used in this study.

In the first one, streptavidin conjugated-quantum dot (QD) was applied to capillary constructed with sandwich system. Washing buffer in constructed capillaries were removed and then streptavidin conjugated-QD (1:100 diluted in binding buffer) was applied to capillaries. After incubation at room temperature for one hour, excess QDs were removed by washing with washing buffer. Capillaries were finally visualized under UV illuminating instrument (Vilber Lourmart Infinity 1000).

The second strategy was the use of streptavidin horseradish peroxidase (HRP) conjugate in platform. The streptavidin HRP conjugate was diluted as 1: 10000 ratio in 1% skim milk prepared in PBS (1X, pH 7.2) and applied to previously constructed capillaries. At the end of incubation (one hour at room temperature), capillaries were washed with washing buffer. The chromogenic substrate for HRP, 3,3',5,5'-tetramethylbenzidine (TMB), was added to capillaries and waited until color changes were observed clearly.

#### **2.2.5.4 Signal Amplification**

The signal amplification studies were performed with streptavidin HRP conjugated signal systems. Two strategies were applied to optimized sandwich platform.

In the first strategy, polymerized HRP was used as streptavidin-HRP conjugates. The molar ratio of HRP was increased on conjugate during manufacturing process while maintaining functionality. Streptavidin-poly-HRP contained 200 (40 X 5) enzyme molecules on it to perform reaction with substrate and therefore, signal was amplified in platform constructed with poly HRP streptavidin conjugate. Similarly, it was diluted as 1: 10000 ratio in 1% skim milk prepared in PBS (1X, pH 7.2) and applied to previously constructed capillaries. They were incubated at room temperature for one hour and then washed with washing buffer.

The second strategy was the use of Ultra-TMB instead of TMB as substrate for enzymatic reaction of HRP. The strep-poly HRP conjugates were directly added to

capillaries and incubated till clearly visible color formation took place. The signal resulted from the oxidation of ultra-TMB was higher than that of normal TMB.



## CHAPTER 3

### RESULTS AND DISCUSSION

#### 3.1 Cell-SELEX

##### 3.1.1 Design of DNA Library and Primers

DNA library was used in SELEX for the construction of a pool containing different sequences with constant primer binding regions and central random region. Its design with certain considerations was one of the critical steps in the proper selection of aptamer against target molecule. First of all, DNA library should not be too stable meaning that it must denature easily at 95°C. For the success of polymerase chain reaction at each round of SELEX, DNA library should not bind tightly to constant primer binding regions. It should not contain guanine (G) both at 5' and 3' end of its sequence because the presence of G at 5' end leads to quench the fluorescence of the fluorophore bound to forward primer. Also, G at 3' end causes the prolongation of deprotection step in DNA synthesis procedure. DNA library used in aptamer selection against *S. Enteritidis* was designed with considerations explained above. It contained random region with 42 nucleotides ( $N_{42}$ ). The potential number of different sequences based on random region length was  $4^{42}$  with formula of  $4^N$  where 4 represented four deoxyribonucleotides. By having 42 nucleotides long random region DNA library (5'-AAGGGCTGGCTGGGATGGA- $N_{42}$ -TCACTCCACGGACCCCACT-3') in this study provided diverse DNA pool for the selection of aptamer.

The design of primers was as important as DNA library design for SELEX procedure. Both forward and reverse primer should have 18-20 bases and approximately same annealing temperature (55-65°C) with  $\pm 1^\circ\text{C}$  difference. They should not build self-dimers with  $|\Delta G| > 5^\circ\text{C}$  meaning that they should not bind to

itself with more than 3 bonds. Also, they should not build hetero-dimers with  $|AG| > 5^\circ\text{C}$  meaning that they should not bind to other primer with more than 3 bonds. They should not form hairpin structures with melting temperature above  $10^\circ\text{C}$ . The GC content is important parameter determining the stability of DNA therefore; both primers should have 50 % or more GC content to have stable DNA library. For the design of best primers it should contain A at the both ends and have annealing temperature at  $60^\circ\text{C}$  to prevent non-specific amplification in PCR. Based on standard primer design considerations explained above fluorescein modified forward primer (P1) and biotin modified reverse primer (P2) were designed as **5'-FAM-AAGGGCTGGCTGGGATGGA-3'** and **5'-Bio-AGTGGGGTCCGTGGAGTGA-3'**, respectively. The presence of FAM modification was used for process control throughout SELEX rounds by fluorescence spectrophotometer analysis of bound and unbound pools to target cell. The presence of biotin modification was used for ssDNA preparation after PCR at each round of SELEX. The dsDNA was bound to streptavidin beads through biotin modified strand and FAM modified strand was eluted by alkaline denaturation for the next round of selection. The properties of DNA library and primers were given at Table 3.1.

**Table 3.1** Properties of DNA library and primers.

	<b>Length (base)</b>	<b>GC Content (%)</b>	<b>Melting Temperature (T<sub>m</sub>) (°C)</b>	<b>Molecular Weight (g/mole)</b>
<b>DNA Library</b>	80	56.3	64.4 - 82.1	24665.5
<b>Forward Primer</b>	19	63.2	61.8	6511.4
<b>Reverse Primer</b>	19	63.2	60.8	6358.3

### 3.1.2 Synthesis Results of DNA Library

After designing the DNA library, it was synthesized with standard phosphoramidite chemistry. In chemical synthesis, protected nucleotides and controlled pore glass (cpg) beads were used as building block and solid support, respectively. It began with the 3' nucleotide and proceeds through a series of cycles composed of four steps that were repeated until the 5' nucleotide was attached. These steps were deprotection, coupling, capping, and stabilization. Basically, at the first step protective group on the 5' carbon of sugar backbone of nucleotide was removed by trichloroacetic acid (TCA) so that the hydroxyl group appeared for the addition of next nucleotide. At coupling step, a weak acid, tetrazole, attacked nucleoside to form tetrazolyl phosphoramidite intermediate which then reacted with the hydroxyl group of the nucleoside attached to the cpg bead. As a result, the 5' to 3' linkage was formed at this step. Then, the elimination of failure of coupling reaction took place with the use of acetylating reagent composed of acetic anhydride and N-methyl imidazole. This reagent reacted only with free hydroxyl groups to irreversibly cap the oligonucleotides in which coupling failed. At the last synthesis step, the phosphate linkage between bases was stabilized by adding iodine and water. After synthesis of DNA at given sequence the cpg beads were removed from 3' ends (Caruthers, 1983; Caruthers, 1985; Caruthers, 1987). The representation of phosphoramidite chemistry was shown in Figure 3.1 schematically.

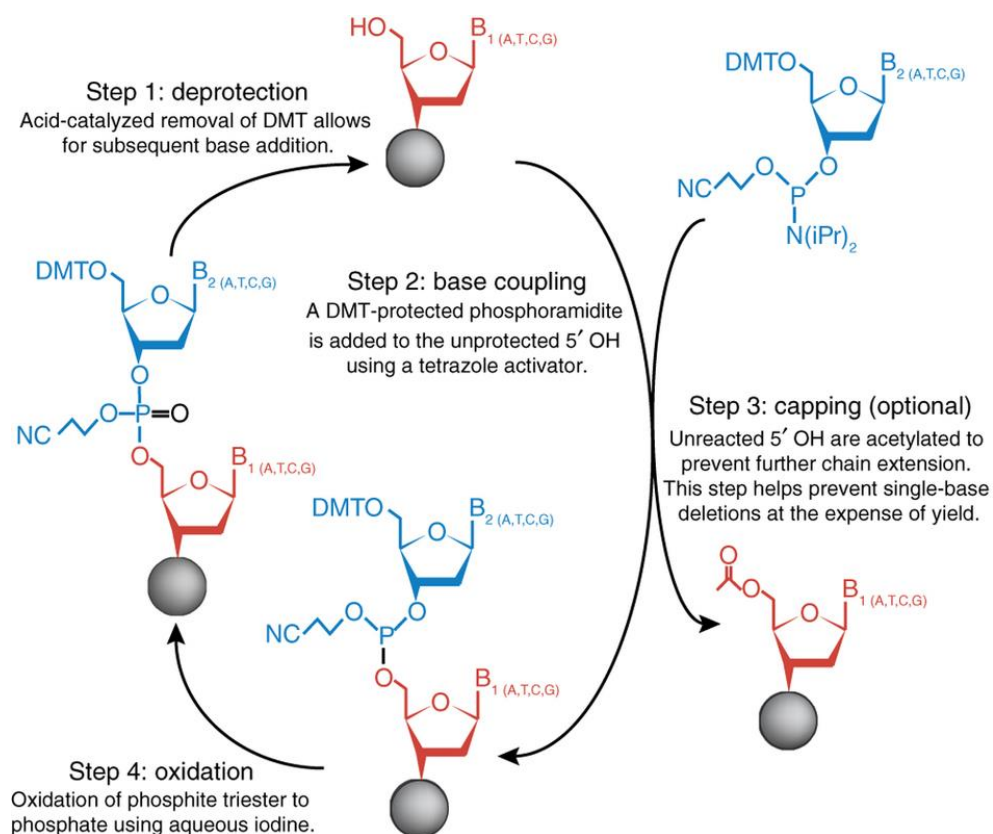


**Figure 3.1** Phosphoramidite chemistry (Kosuri et al., 2014).

In this study, DNA library with **5'-AAGGGCTGGCTGGGATGGA-N<sub>42</sub>-TCACTCCACGGACCCCACT-3'** sequence was synthesized from 3' to 5' direction by ABI 3400 DNA synthesizer with chemical method explained above. With length of 80 bases, the yield given by synthesizer was 45.20% (99%<sup>79</sup>). After deprotection and desalting steps, DNA library was purified with reverse-phase HPLC. The successfully synthesized sequences were separated from not properly synthesized ones which could affect the success of SELEX process. At the end of synthesis, completely and successfully synthesized DNA had dimethoxytrityl (DMT) group on the 5' end of sequences. The introduction of alkyl chains with using amine acetate in mobile phase of HPLC made DNA nonpolar. Not having DMT group on 5' end truncated sequences became polar and eluted from column first. The purification

result of DNA library with reversed-phase ion pairing HPLC was shown in Figure 3.2. The first eluted sequences were not properly synthesized shorter DNA sequences while the second eluted sequences were successfully synthesized DNA library.

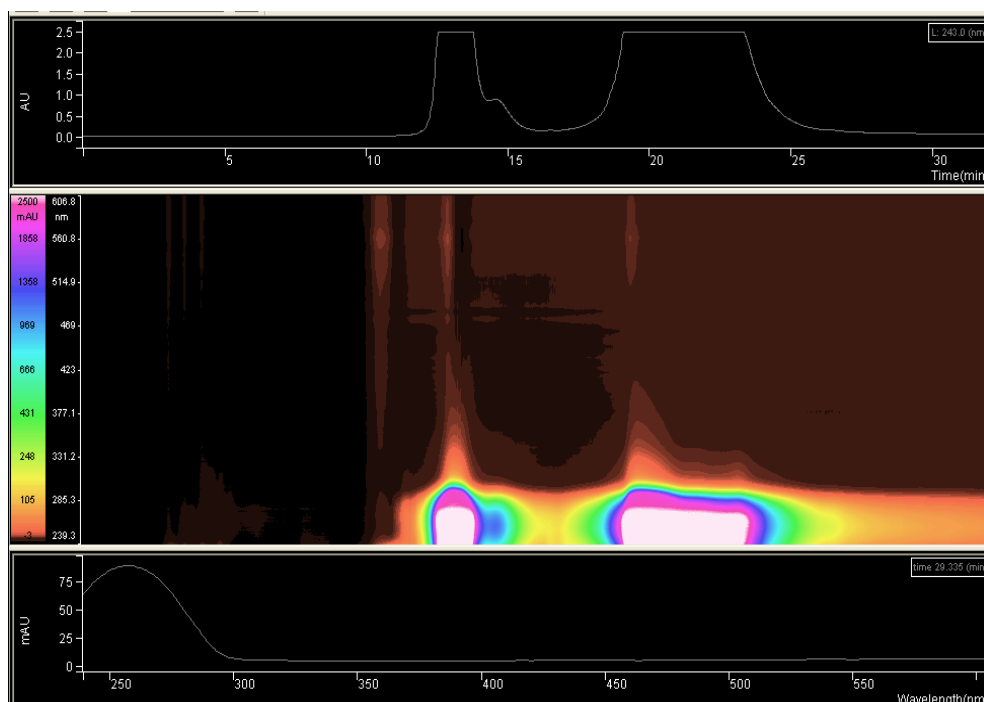


**Figure 3.2** HPLC purification result of DNA library.

As a result, single stranded DNA library having random region with 42 nucleotide length and two primer binding sites were prepared for the starting material in the selection of aptamer.

### 3.1.3 PCR Optimization for T<sub>m</sub> and Primer Concentration

Polymerase chain reaction (PCR) is the most critical step in the selection of aptamers. In order to proceed to selection process properly from the first round of SELEX and to perform aptamer selection correctly certain parameters have to be optimized in this technique. SELEX stands for **S**ystematic **E**volution of **L**igands by **E**xponential **E**nrichment. Exponential enrichment mentioned here is performed by PCR and the success of reaction in one round affects the success of next round throughout SELEX. The amplification of nonspecific and unwanted DNA sequences prevents the amplification of specific sequences that can be aptamer candidates specifically bound to target. By eliminating nonspecific sequences from PCR reaction each round of SELEX ensures a more successful next round. Therefore, before beginning to SELEX annealing temperature and the concentration of primers used in amplification reaction were optimized in this study.

The annealing temperature provides with primers to anneal DNA for the elongation of strands with the help of polymerase enzyme. Decreasing temperature slowly leads to the nonspecific binding of primers to different regions on DNA strand. Thus, annealing temperature is determined based on melting temperature of primers (T<sub>m</sub>) used in reaction and generally it is 3-5°C below the melting temperature of the primers. Not properly determined temperature prevents proper annealing of primers to target DNA in reaction and therefore causes decrease in amplification efficiency of target region or increase in nonspecific amplification of different DNA regions.

In this study, gradient PCR was performed for the determination of optimum annealing temperature. At constant amplification cycle with same PCR reaction mix containing constant DNA and primer concentrations, amplification reactions were performed at different annealing temperatures (60.1, 61.9, 63.0, 64.3, 66.9, 68.4 and 69.9°C). Figure 3.3 shows agarose gel image of PCR products whose amplification reactions were performed at seven different annealing temperatures. While PCR products with annealing temperature above 63°C were shown as weak bands due to

low amplification yield, PCR products with annealing temperature below 63°C were represented as two bands on gel. Therefore, **63°C** was chosen as optimum annealing temperature for further reactions throughout SELEX. As compared with  $T_m$  of primers (Table 3.1), annealing temperature chosen was slightly higher because the hybridization of the primer to DNA occurred under more stringent conditions and thus resulted in enhanced specificity with elimination of nonspecific secondary band in this study.

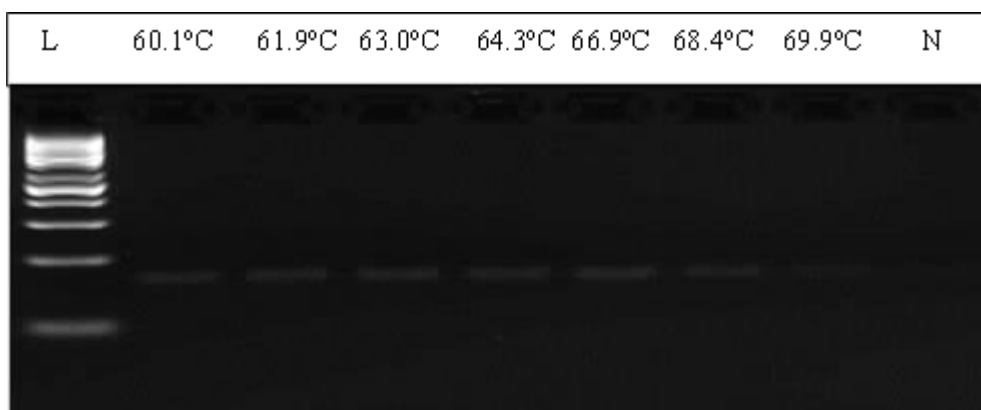


**Figure 3.3** Agarose gel image of seven PCR products whose annealing steps were performed at seven different annealing temperatures (60.1, 61.9, 63.0, 64.3, 66.9, 68.4 and 69.9°C) (L: Ladder, N: negative control).

The concentration of primers was also optimized in this study. Primers at four different concentrations were prepared by diluting 100  $\mu\text{M}$  of stock solutions to 3, 5, 8 and 10  $\mu\text{M}$  and they were used in the amplification reaction of DNA library with optimum annealing temperature. The PCR products amplified at constant number of cycle with same PCR reaction mix containing constant DNA concentration were analyzed by running agarose gel electrophoresis. The gel image of PCR products was shown in Figure 3.4.

As seen, amplification reaction with stock of 10  $\mu\text{M}$  of primers resulted in higher reaction yield so that single band was bright as compared to others. As the stock primers concentration was decreasing, the intensities of bands belonging to the product amplified with these amounts of primers were also decreasing. Therefore, with highest yield, **10  $\mu\text{M}$**  of stock primers concentration was selected as optimum amount of primers in further reactions.

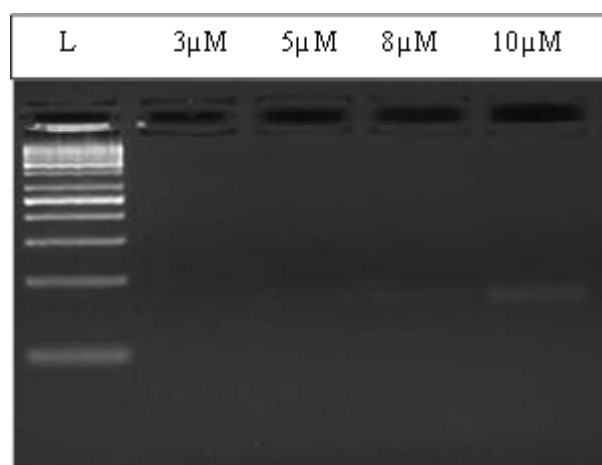


**Figure 3.4** Agarose gel image of four PCR products which were amplified with four different stock primers concentrations (3, 5, 8 and 10  $\mu\text{M}$ ).

### 3.1.4 Preparation of Target Bacterial Cell

Aptamers can be selected for a range of target molecules such as ions, proteins and even for a whole cell. In our study, Cell-SELEX was performed with *S. Enteritidis* as target. During selection process of aptamer, live bacterial cells were used therefore, the maintenance of cell culture was important for the success of process. The cell

surface of bacteria provided many different targets for DNA molecule to bind, especially proteins. The growth conditions such as growth medium, temperature and growth time could change the composition of cell surface by enhancing or preventing the expression of membrane proteins. For example, storing bacterial culture at 37°C for a long time may cause changes in morphology and even lead to cell death. The increase in cell death prevented the enrichment of pool in SELEX properly. Therefore, in order to eliminate the effects of growth conditions on selection process and maintain same composition on cell surface throughout SELEX rounds the growth curve of *S. Enteritidis* was drawn. The number of bacteria grown in TSB at 37°C was measured in terms of absorbance at 600 nm during the course of 6.5 hour cell growth experiment and the curve was drawn as absorbance versus time in minutes. The observed pattern of bacterial growth was exponential as shown in Figure 3.5. The growth equation was evaluated from that curve by using results obtained at the exponential growth phase of bacteria wherein all the cells were dividing regularly at a constant rate (Figure 3.6). Based on equation bacterial culture at early log growth phase was used with optical density of 0.3 measured at a wavelength of 600 nm. The bacterial culture grown for **3 hours** was selected as target bacterial culture in SELEX and also in binding studies.

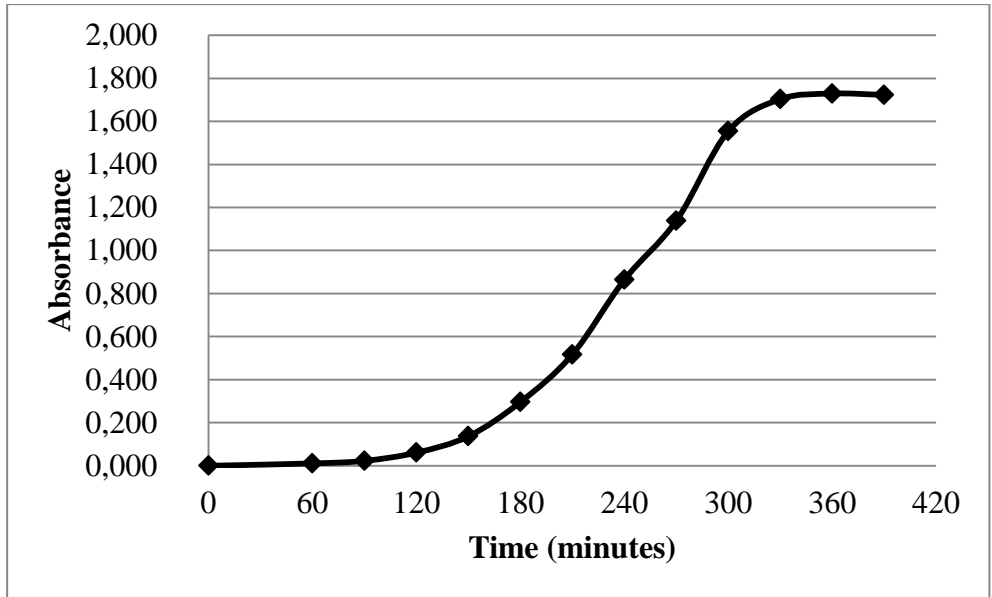


**Figure 3.5** Growth curve of *S. Enteritidis* at 37°C in TSB (The average absorbance at 600 nm taken at intervals of half an hour, n=3).

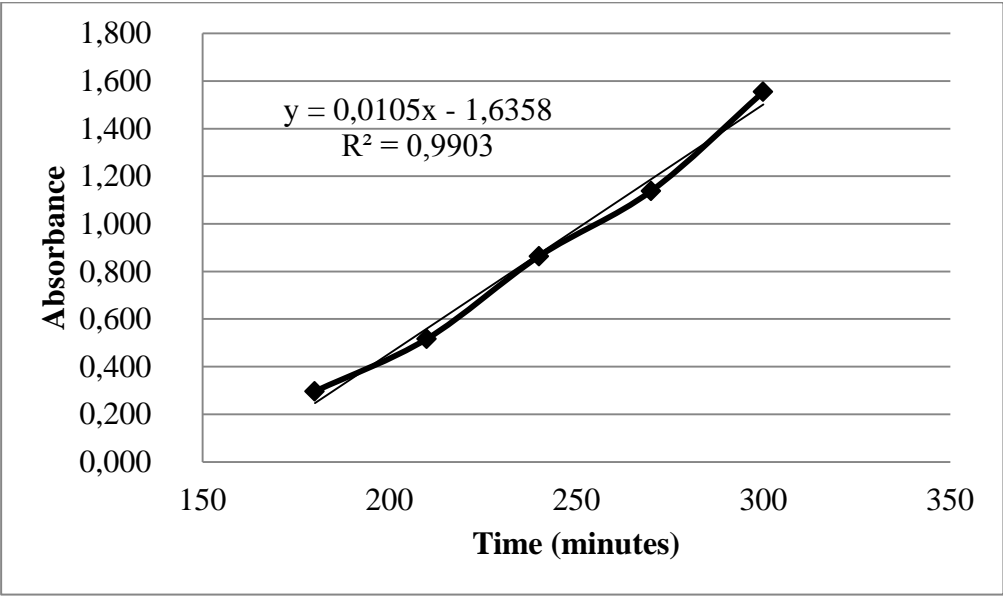


**Figure 3.6** Exponential growth phase of *S. Enteritidis*'s growth curve at 37°C in TSB medium (n=3).

### 3.1.5 SELEX Rounds

In this study, for the selection of aptamer for *S. Enteritidis* whole cell was used instead of membrane proteins or certain molecules on the surface of target cell. Since there was no need to know the exact target previously in SELEX, the surface of target cell provided different molecules for sequences to bind specifically. In addition to ensuring numerous molecules to bind on surface, using whole cell also provided sequences with target molecules at their native state. The molecules, especially proteins, on the surface of bacteria preserved their native structures during the selection process.

In the first round of SELEX, the initial amount of DNA library (10 nmol) and amount of target bacteria (100 million/mL) were selected at their maximum level as compared to the further selection rounds. And throughout the end of SELEX certain parameters were changed gradually in order to increase stringency (Table 2.1). The decrease in cell amount and incubation time, the addition of extra washing steps and the introduction of negative selection applied pressure to the selection of highly specific DNA sequences with high affinity to its target. By increasing stringency, best binders were favored among others. Beside these parameters, optimization of PCR conditions at each round contributed to the selection of best binders.

In preparative PCR of pools eluted after each round, the cycle number was optimized to eliminate nonspecific products. Since the initial DNA library had random region with length of 42 bases, PCR products with shorter or longer sequences were arisen at the end of PCR reaction. In addition to specific sequences these nonspecific ones could be amplified and remain in final pool. The presence of these sequences could affect the success of selection; therefore, they were removed at the amplification step by optimizing PCR cycle number at first. After the completion of each SELEX round, seven reaction tubes were prepared with same eluted pool and the amplification reaction was set at different cycle number for these tubes. The PCR products of cycle 8, 10, 12, 14, 16 and 20 were then analyzed with agarose gel

electrophoresis. As shown in Figure 3.7 and 3.8, PCR products of higher cycle numbers had nonspecific sequences mostly. The presence of second band on agarose gel was generally observed after 12th round. Consequently, the optimized cycle numbers of preparative PCR at each round were summarized at Table 3.2.

**Table 3.2** Optimized cycle numbers of SELEX rounds.

<b>SELEX Rounds</b>	<b>Cycle Number</b>
1 <sup>st</sup>	12
2 <sup>nd</sup>	12
3 <sup>rd</sup>	12
4 <sup>th</sup>	10
5 <sup>th</sup>	12
6 <sup>th</sup>	14
7 <sup>th</sup>	16
8 <sup>th</sup>	14
9 <sup>th</sup>	12
10 <sup>th</sup>	12
11 <sup>th</sup>	10
12 <sup>th</sup>	10

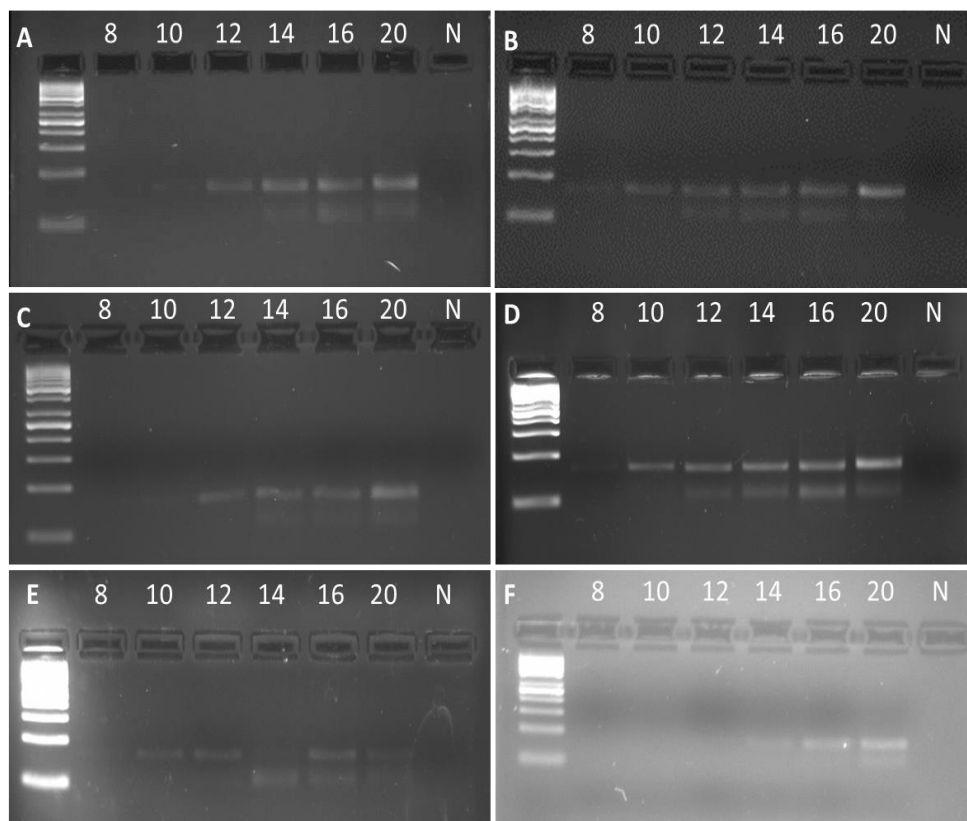


**Figure 3.7** PCR cycle optimization results of pools eluted at A) round 1, B) round 2, C) round 3, D) round 4, E) round 5, F) round 6. Numbers from 8 to 20 represented cycle numbers in PCR and N represented negative control whose reaction mixture contained water instead of DNA.

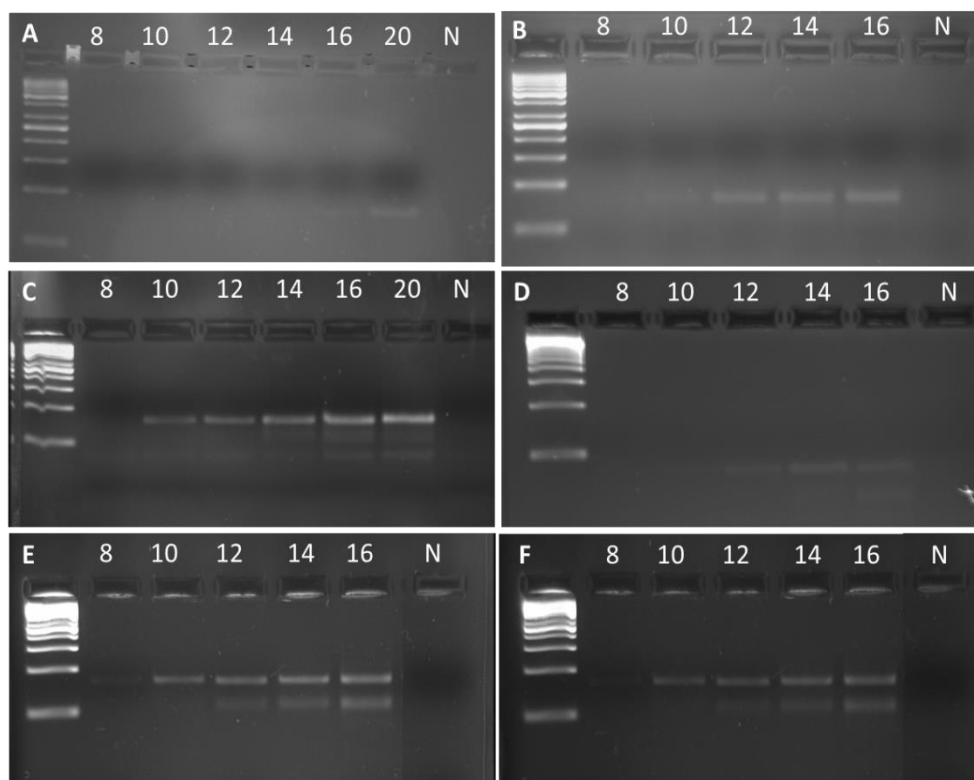


**Figure 3.8** PCR cycle optimization results of pools eluted at A) round 7, B) round 8, C) round 9, D) round 10, E) round 11, F) round 12. Numbers from 8 to 20 represented cycle numbers in PCR and N represented negative control whose reaction mixture contained water instead of DNA.

### 3.1.6 Progress Control of SELEX

Throughout the selection process in SELEX, certain DNA sequences showed more specific binding against target cell as compared with others just due to their structures. By increasing their number by PCR they were enriched in pools and this enrichment caused the evolution of candidate aptamers that bound to target with high affinity and specificity. In order to determine whether selection was completed or not the progress of selection was monitored in this study by two methods, fluorescent

aptamer binding assay and melting curve analyses, explained as follows.

### **3.1.6.1 Fluorescent Aptamer Binding Assay**

For the control of selection process first method was the fluorescent aptamer binding assay which provided elution yield of each round of SELEX. In this assay, initial DNA pools of each round were set to 1 pmole and the portion of DNA molecules bound to *S. Enteritidis* in these pools were determined by measuring relative fluorescence unit after incubation with *S. Enteritidis*. The ratios of bound DNA concentrations to initial pool concentrations were given as elution yields of selection rounds.

Before the calculation of elution yields of SELEX rounds standard curve was constructed with FAM-modified primer (P1-FAM) prepared at 0.01, 0.05, 0.1, 0.5, 1, 5 and 10 pmole. Fluorospectrometer (Nanodrop 3300 Fluorospectrometer, Thermo) was used to measure fluorescence assays. Relative fluorescence units of each concentration of P1-FAM were read as quinary replicates (n=5) and mean units were plotted against concentrations at pmole and  $\mu\text{M}$  units (Figure 3.9).

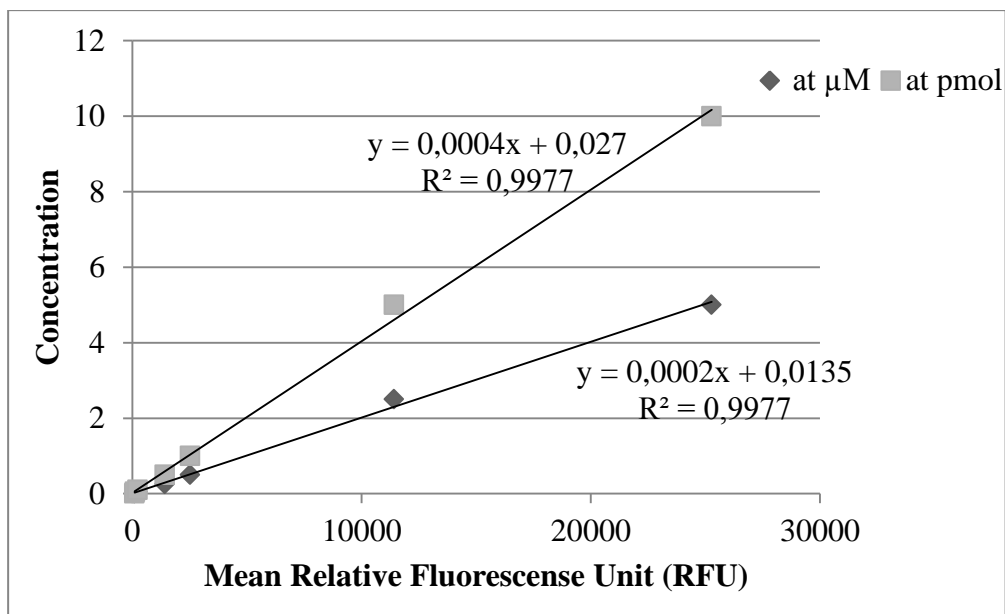


**Figure 3.9** Standard curve of fluorescence labeled forward primer (P1-FAM) constructed with the concentrations at  $\mu\text{M}$  or pmole unit versus relative fluorescence unit (RFU). Seven standard samples (0.01, 0.05, 0.1, 0.5, 1, 5 and 10 pmole) were used with quinary replicates ( $n=5$ ).

After construction of standard curve, pools of twelve SELEX rounds were set to 1 pmole and incubated with  $10^6$  CFU/mL of *S. Enteritidis* at  $4^\circ\text{C}$  for 30 min. Unbound DNA sequences were removed by centrifugation and specifically bound ones were eluted after heat treatment. The relative fluorescence units of bound DNA molecules for each round were measured and concentrations at pmole unit were calculated from standard curve. As explained following formula, the ratio of the eluted pool concentrations to initial pool concentrations gave elution yield of rounds.

$$\text{Elution yield of pools} = \frac{\text{Bound DNA concentration}}{\text{Initial DNA concentration}}$$

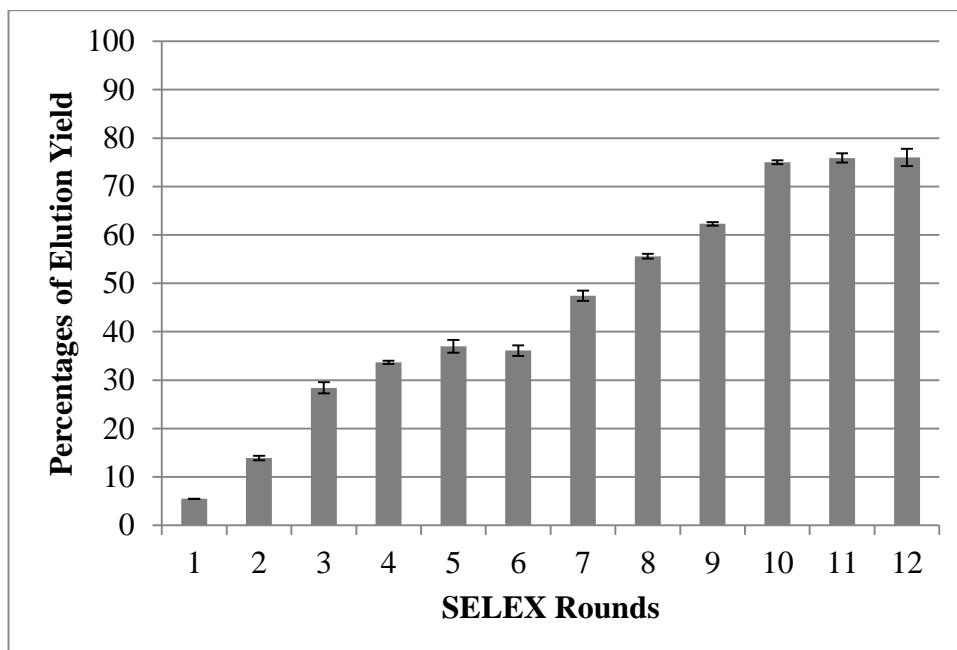


**Figure 3.10** Percentages of elution yield for each round of SELEX. For each round triple replicates of pools were read with fluorospectrometer. Error bars represented standard deviation (SD) with n=3.

As shown in Figure 3.10, the percentages of bound DNA increased from the first round through tenth round of SELEX with a slight decrease at round six. This drop of percentage could be caused by the introduction of negative SELEX step after fifth round. The elimination of unspecific and non-target cell specific DNA sequences in negative selection step could introduce a stringency to SELEX and thus, enhanced the selection of candidate aptamers specifically bound to target cell. Therefore, this stringency could cause a small decrease in the percentage of elution yield at the sixth round. From round 10 till round 12, the amount of bound sequences were approximately same and so there were no increase in the elution yields observed at round 11 and 12. It could be stated that the evolution of DNA pools was terminated and thus, certain sequences which specifically bound to *S. Enteritidis* were dominated in pools. As a result, the progression of SELEX was monitored and

selection process was stopped at **round 12**. This result was also confirmed by another method, melting analyses of pool, as explained below.

### 3.1.6.2 Melting Curve Analyses of DNA Pools

Diversity Standard of Random Oligonucleotides assay, DiStRO, is a melting assay using Real Time PCR to analyze the re-annealing temperature of melted DNA (Schütze *et al*, 2010; Thiel *et al.*, 2012). Based on melting temperatures this method states that with decrease in diversity the melting temperature of DNA shifts to higher temperature. Since best binders are enriched through the end of selection, the overall diversity is reduced meaning that the complexity of DNA library decreases significantly as rounds progress in SELEX.

In this study, the course of selection process in SELEX was monitored by DiStRO assay. The pools eluted after each round were amplified with optimum PCR conditions and reaction mix and after amplification double stranded products were melted at high temperature (95°C). Following an annealing step the temperature was increased from 65°C to 95°C incrementally (with 0.5°C of ramping rate) and the products were again melted at specific melting temperatures. Based on the fluorescence measurements of SYBR Green, diversity was monitored by comparing peaks (Figure 3.11, A), progression of pools on melting curve (Figure 3.11, B) and  $T_m$  of each pool (Table 3.3). As shown in melting peaks (Figure 3.11, A), there were three set of significant drops in the diversity of pools observed at round 7, 8 and 11. For the first 6 rounds of selection the melting temperature of pools remained approximately same and they were around 76°C meaning that the enrichment in pools had not occurred yet. At 7<sup>th</sup> round a selective pressure was introduced to SELEX procedure, which was the increase in washing step from one to two to enhance enrichment. With this pressure, there was a slight shift in melting temperature towards higher temperature as compared with temperature of the first 6

rounds (from 76 to 77°C approximately). This shift was also observed in melting curve (Figure 3.11, B) and indicated that there was a slight loss of complexity in pool as selection progressed from round 6 to 7. Although the melting temperatures of the first six rounds were approximately same, the fluorescence measurement of the first pool (indicated as red color on melting curve) was higher than others. This result was because of the fact that first pool was pre-amplified for 10 cycles before melting curve analyses in RT-PCR experiment.

The most notable decrease in diversity occurred at the 8<sup>th</sup> round. The melting temperature of round 8 was shift to 81.76°C. At this round another selective pressure was introduced besides washing step. The target cell concentration was dropped to 25 million/mL and thus this could cause the shift in T<sub>m</sub> and loss in complexity of pool. Throughout three consecutive rounds (round 8, 9 and 10) there were no significant changes in T<sub>m</sub> and so diversity of pool. The final significant drop in complexity was observed at 11<sup>th</sup> round with the shift at T<sub>m</sub> from 81.76 to 85.06°C. The target concentration was further decreased to 10 million/mL and washing step was increased to three at this round and they were together reasons of loss in complexity in pool. However, although same selective pressure was applied at round 12, there was no change in T<sub>m</sub> of pool. Following 12 selection rounds, diversity was greatly reduced and candidate aptamer sequences were highly enriched in pool, therefore, the selection process was finished at **round 12**.

The iterative selection rounds of SELEX have been generally between 6 and 20 and the number of rounds has been depended on many factors such as types of target, types of library and SELEX variants (Dong *et al.*, 2014). In literature aptamer selections via Cell-SELEX have been performed at possible lowest number (Savory *et al.*, 2014). This is because of that fact that more rounds have led to the enrichment of unspecific sequences preventing effective aptamer selection (Musheev and Krylov, 2006). Certain studies have been indicated that the effectiveness of SELEX and the binding properties of aptamers mostly depend on the performance of amplification step (Schutze *et al.*, 2011). Therefore, selection process in Cell-SELEX has been limited to lower number of rounds. In our study, we finished selection

process at round 12 based on results of binding assay and melting curve analysis via RT-PCR. Proceeding SELEX rounds after 12<sup>th</sup> round may cause failure in aptamer selection against *S. Enteritidis* by increase in nonspecific artifacts amplified in PCR at each round.

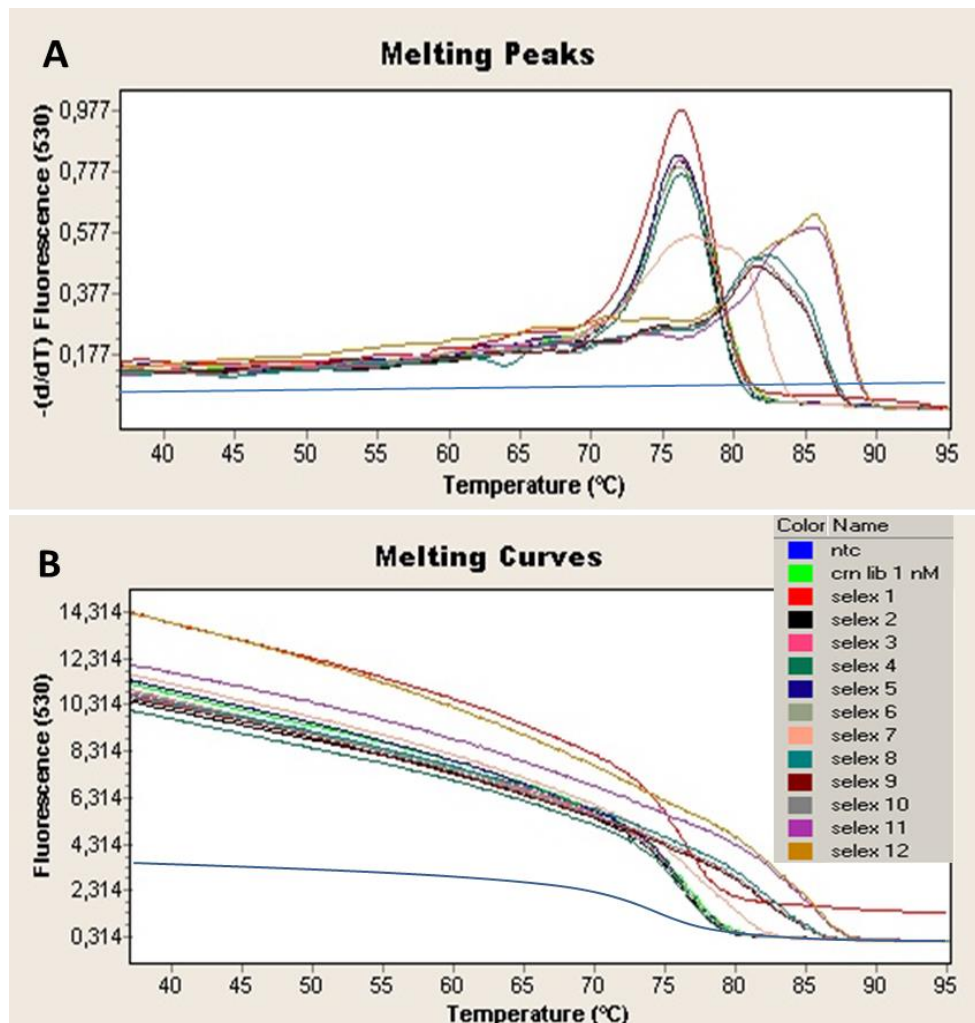


**Figure 3.11** DNA melting temperature analyses of pools by Diversity Standard of Random Oligonucleotides assay in RT-PCR A) Melting peaks of all SELEX pools and DNA library, B) Melting curves of all SELEX pools and DNA library (each pool and library were represented as colors given at right corner of melting curve).

**Table 3.3** Melting temperatures of DNA library and pools at each round.

	<b>T<sub>m</sub> (°C)</b>		<b>T<sub>m</sub> (°C)</b>
DNA Library	76,47		
1 <sup>st</sup> pool	76,36	7 <sup>th</sup> pool	76,78
2 <sup>nd</sup> pool	76,38	8 <sup>th</sup> pool	81,76
3 <sup>rd</sup> pool	76,47	9 <sup>th</sup> pool	81,90
4 <sup>th</sup> pool	76,35	10 <sup>th</sup> pool	82,35
5 <sup>th</sup> pool	76,36	11 <sup>th</sup> pool	85,06
6 <sup>th</sup> pool	76,43	12 <sup>th</sup> pool	85,10

### 3.1.7 Sequence Analyses

At the end of selection, pool of 12<sup>th</sup> SELEX round was sequenced with IonTorrent (Life technologies) sequencing technology. Since starting DNA library had central random region with 42 nucleotides length, at final pool there could be highly variable DNA sequences which could not be sequenced with Sanger Sequencing effectively. All sequence data and relative frequencies of the most abundant sequences were in turn determined by "Next Generation Sequencing". Since the SELEX process selected for the enrichment of molecules with high affinities to the target structure of interest, it was likely to identify good target binding aptamers among the enriched, most abundant DNA sequences. The sequences of round 5, 7 and 12 were sequenced and the summary of results was given at Table 3.4. While total sequenced data was 5.6 megabases at round 5, it was decreased to 1 megabases at 12<sup>th</sup> round due to the elimination of not good binders throughout the selection process. At final pool **12149 sequences** were obtained with average length of 84 base pair. As shown in Figure 3.12, majority of the sequence across total sequence results were approximately 80 bases long. Smaller sequences with length < 50 bases could be primers and barcodes used in sequencing method.

**Table 3.4** Sequence results of pools eluted at rounds 5, 7 and 12.

SELEX Rounds	Bases (M)	$\geq Q20$ (M)	Total Number of Sequences	Mean Read Length (bases)
5	5,6	3,9	70434	80
7	2,1	1,5	26248	82
12	1	0,731	12149	84

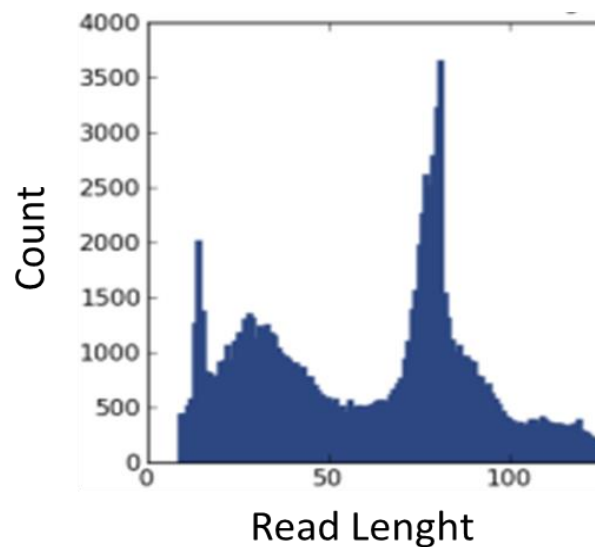


**Figure 3.12** Read length histogram of total sequences: the graph of read length versus their number.

In order to determine the frequencies of certain sequences among total 12149 sequences of round 12 all results were firstly analyzed with MAFFT 7.149 (Kato and Standley, 2013). Figure 3.13 represented the phylogenetic tree of sequences of round 12 drawn by ArchaeopteryxA software of MAFFT multiple sequence

alignment tool. This software clustered unaligned sequences roughly based on their sequence similarity and gave a guide tree as a result. In this study, there were two main branches containing same sequences and so evolved as two candidate aptamers in the selection studies of aptamer for *S. Enteritidis*. In addition to these two main sequence groups, there was one small branch separated from the upper main branch as shown in Figure 3.13. The frequency of the sequences on this small branch was low as compared to that of main branches, however, for the determination of best binder sequences among aptamer candidates the sequence on this branch was selected also for further characterization studies with sequences on two main branches. As a result of frequency analyses with the construction of phylogenetic tree, three aptamer candidates were determined with sequences given at Table 3.5.

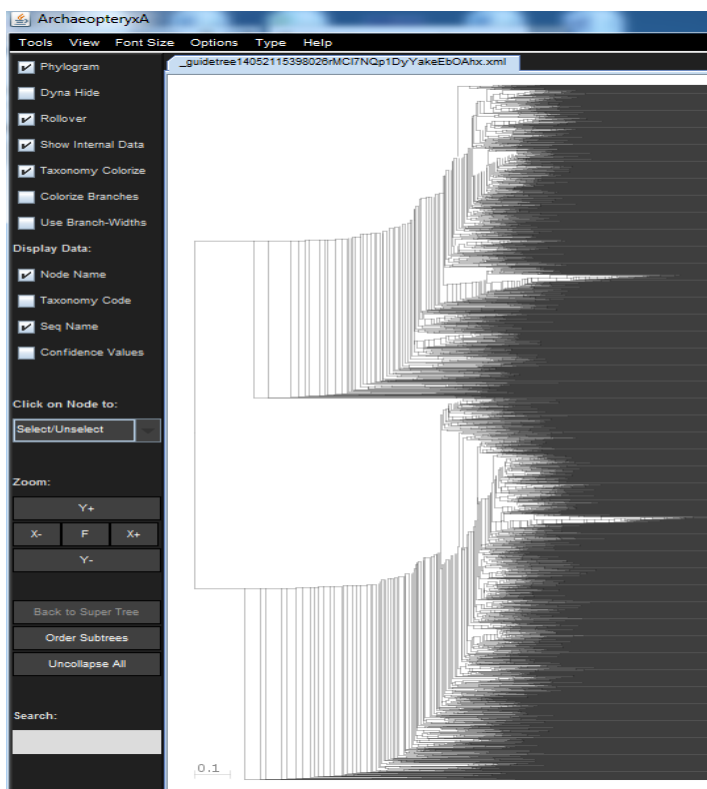


**Figure 3.13** Guide tree of sequence data obtained from SELEX round of 12 via ArchaeopteryxA.

**Table 3.5** Sequence results of candidate aptamers selected for *S. Enteritidis* (bold nucleotides indicated primer regions).

Aptamer candidates	Sequences (at 5'---3'direction)
Crn-1	<b>AAGGGCTGGCTGGGATGGACCCTCCCGAAACGAGCTG</b> <b>TCTCTTAACGGAAGCTAATCTGCCTCACTCCACGGACC</b> <b>CCACT</b>
Crn-2	<b>AAGGGCTGGCTGGGATGGATGTAAGAAGGGAGGAAA</b> <b>GGACCTAAGACCTGCTATATTGCGATCACTCCACGGAC</b> <b>CCCACT</b>
Crn-3	<b>AAGGGCTGGCTGGGATGGATGGATGGCATTACCTATG</b> <b>CGGTAGATTGCCGACGACCACGACTCACTCCACGGACC</b> <b>CCACT</b>

Aptamers are single stranded DNA molecules showing high affinity and specificity to their target molecules. These unique properties are arisen from their three dimensional structures. Therefore, folding into specific structures at selection conditions leads to specific binding of aptamers to target. In this study, candidate aptamers were structurally changed with the change in temperature. The probable secondary structures of these candidate aptamers were analyzed with Nucleic Acid Package (NUPACK) (Dirks *et al.* 2007). At two different temperatures (4 °C and 37°C) candidate aptamers crn-1 and crn-3 showed quietly high differences in their 3D structures along with their thermodynamic properties (Figure 3.14 and 3.16). On the contrary, crn-2 folded into similar structures without depending on temperature difference (Figure 3.15). The effects of change in structure with the change in binding temperature were analyzed at characterization studies on isothermal titration calorimetric results.

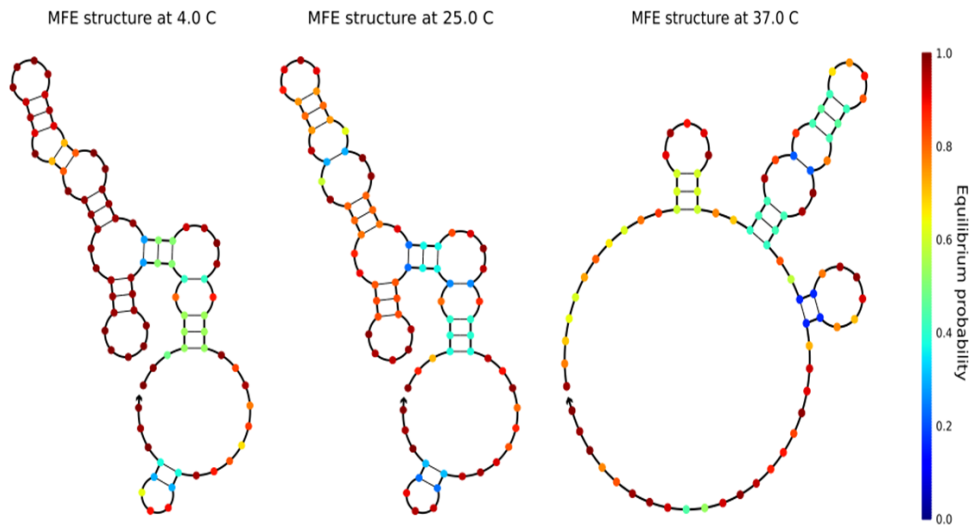


**Figure 3.14** Diagram of minimum free energy secondary structures of crn-1 at 4 °C, 25°C and 37°C drawn by Nupack software

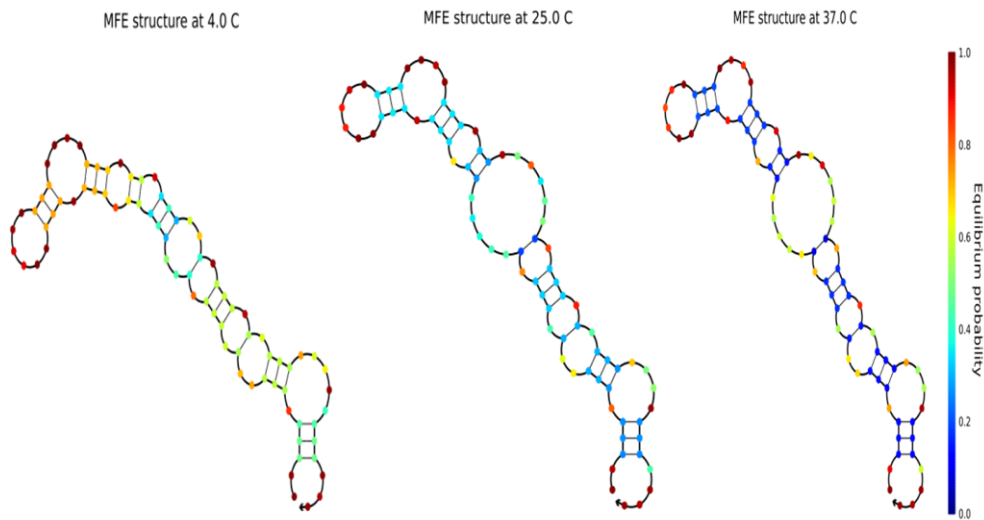


**Figure 3.15** Diagram of minimum free energy secondary structures of crn-2 at 4 °C, 25°C and 37°C drawn by Nupack software.

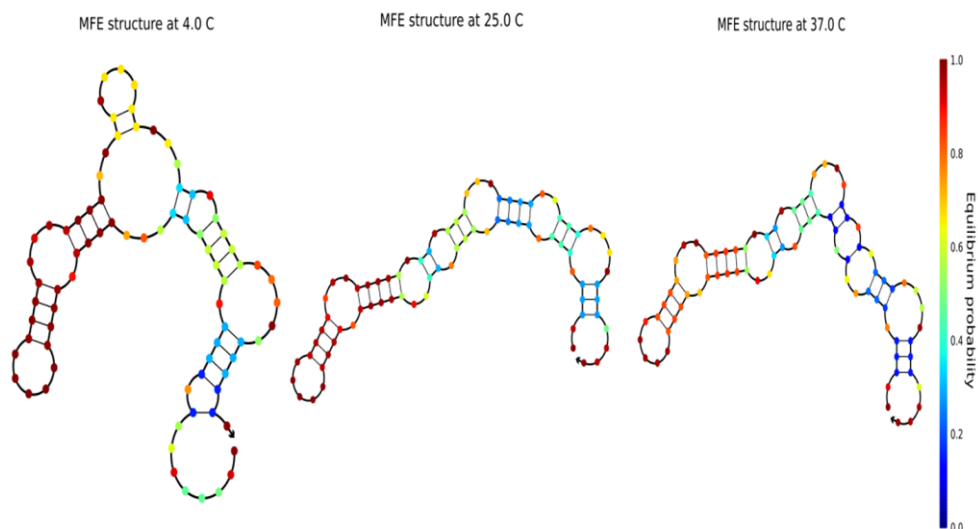


**Figure 3.16** Diagram of minimum free energy secondary structures of crn-3 at 4 °C, 25°C and 37°C drawn by Nupack software.

### 3.1.8 Characterization and Binding Studies of Selected Aptamer

After the completion of SELEX and determination of candidate aptamer sequences based on sequence analyses, they were characterized in terms of their binding specificity and affinity. The nucleotide sequences of good binding aptamers were determined from data obtained by three techniques explained as follows.

These three techniques, confocal imaging, ELAA and calorimetry, were first optimized with the use of *S. aureus* as target and its aptamer sequence (SA-31) taken from literature (Cao *et al.*, 2009). Optimized techniques were then used for the characterization and assessment of binding constant of *S. Enteritidis* aptamers selected in this study.

### 3.1.8.1 Confocal Imaging of Bacteria with Aptamer

Before studying affinity of *S. aureus* and *S. Enteritidis* aptamers to their target cells, the specificity of them were analyzed with the use of Laser scanning confocal microscopy. After incubation of fluorescence modified *S. aureus* aptamer (SA-31-FAM) with its target cell, *S. aureus* and other control cells, *S. Enteritidis* and *E.coli*, the unbounded ones were removed by one washing step. As shown in Figure 3.17, background signals taken from *S. aureus*-aptamer and *E. coli*-aptamer complex were high due to not proper removal of unbound sequences from environment. Washing cell-aptamer complex once was not enough to eliminate unbound sequences and thus another washing step was introduced to get rid of excess sequences.

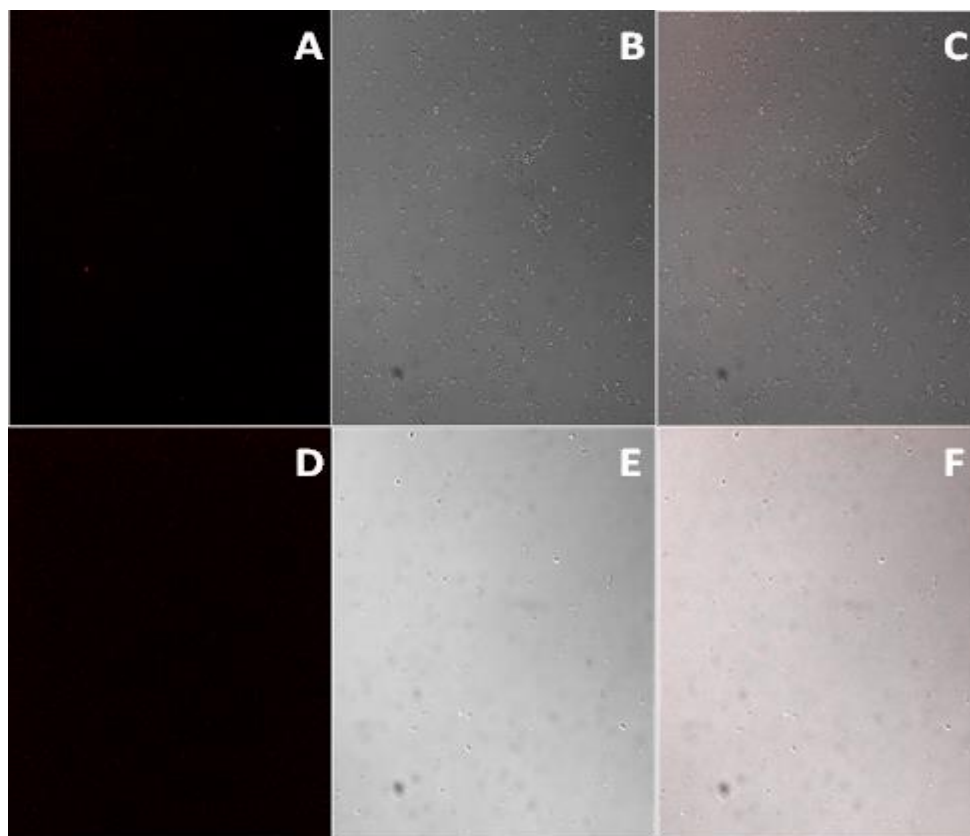


**Figure 3.17** Laser scanning confocal microscope images of *S. aureus* and *E. coli* labelled with *S. aureus* aptamer SA-31(after one washing step) at 488 nm excitation wavelength by plan-neofluar 40X objective. (A) Fluorescence image (B) Optical image (C) Merge of two images of *S. aureus*, (D) Fluorescence image (E) Optical image (F) Merge of two images of *E. coli*.

After washing twice, the cell-aptamer complex for each bacterium was analyzed again with confocal microscope under 488 nm exciting light and visible light. The background signals were very low and thus, signals gathered from slides were belonging to aptamer-target complex. As shown in Figure 3.18, aptamer specific for *S. aureus* bound to its target, *S. aureus*, more significantly as compared to other control cells. While there were some non-specific binding of *S. aureus* aptamer to *E.*

*coli* (observed in Figure 3.18, D-F), binding of aptamer to *S. Enteritidis* was not observed (Figure 3.18, G-I). As a result, it could be stated that aptamer selected for *S. aureus* showed high selectivity to its target. With this optimized procedure, aptamer candidates for *S. Enteritidis* selected in this study were visualized under laser scanning confocal microscope and their specificities were evaluated by comparing their binding properties to target and control cells.

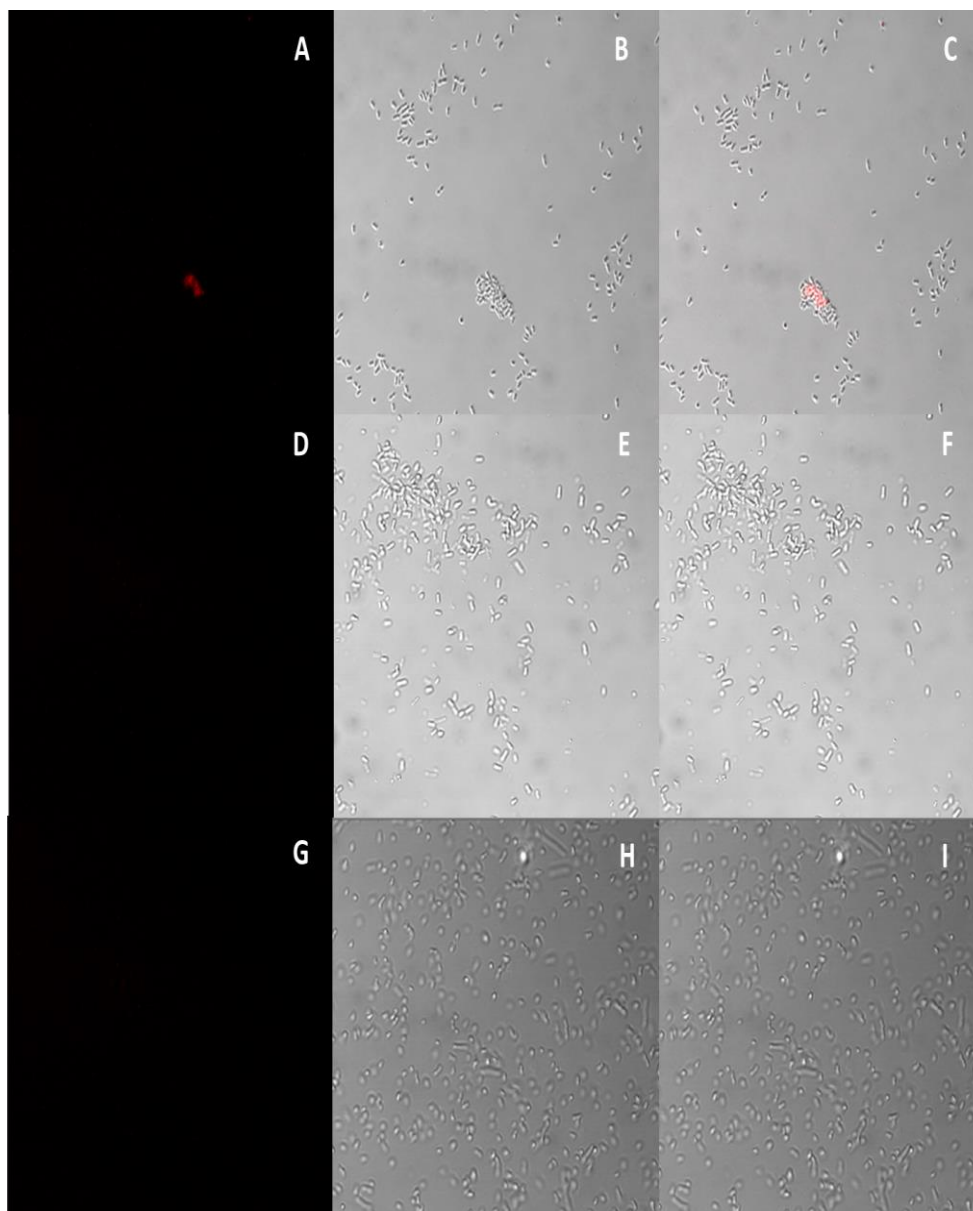


**Figure 3.18** Laser scanning confocal microscope images of three cells bound with *S. aureus* aptamer SA-31 at 488 nm excitation wavelength by plan-neofluar 40X objective. (A) Fluorescence image (B) Optical image (C) Merge of two images of *S. aureus*, (D) Fluorescence image (E) Optical image (F) Merge of two images of *E. coli*, (G) Fluorescence image (H) Optical image (I) Merge of two images of *S. Enteritidis*.

With previously optimized experimental conditions in which *S.aureus* and its aptamer SA-31 was used, confocal imaging experiment was performed for all three fluorescence modified candidate *S.Enteritidis* aptamers and *S.Enteritidis*. In order to evaluate the specificities of these three aptamers *E. coli* and *S. aureus* were used as control cells.

As shown in Figure 3.19 and 3. 20, two candidate aptamers among three bound to *S.Enteritidis* specifically while there were no binding to control cells. The signals gathered from slides containing crn-1-*S.Enteritidis* complex and crn-2-*S.Enteritidis* complex were belonging to specific binding between candidate aptamers and target cell. The fluorescence images taken with plan-neofluar 40X objective at 488 nm were merged with optical images under white light. Binding of aptamers to target cell was easily observed from fluorescence signals coming from cell surface on merged images. Crn-1 and crn-2 showed specificities against *S.Enteritidis* with very low background signals. The control cells, *E.coli* and *S.aureus*, did not bind to crn-1 and crn-2 so that no signals were obtained from control slides. Although two candidate aptamers specifically bound to *S.Enteritidis*, crn-3 did not show any binding to target and control cells (Figure 3.21). There were low signals only coming from backgrounds, the merged image did not show any cells coated with fluorescence modified crn-3. As a result, it could be concluded that crn-1 and crn-2 specifically bound to target cell and they could be determined as aptamers of *S.Enteritidis*. This conclusion was confirmed in the next study, ELISA-like binding assay.

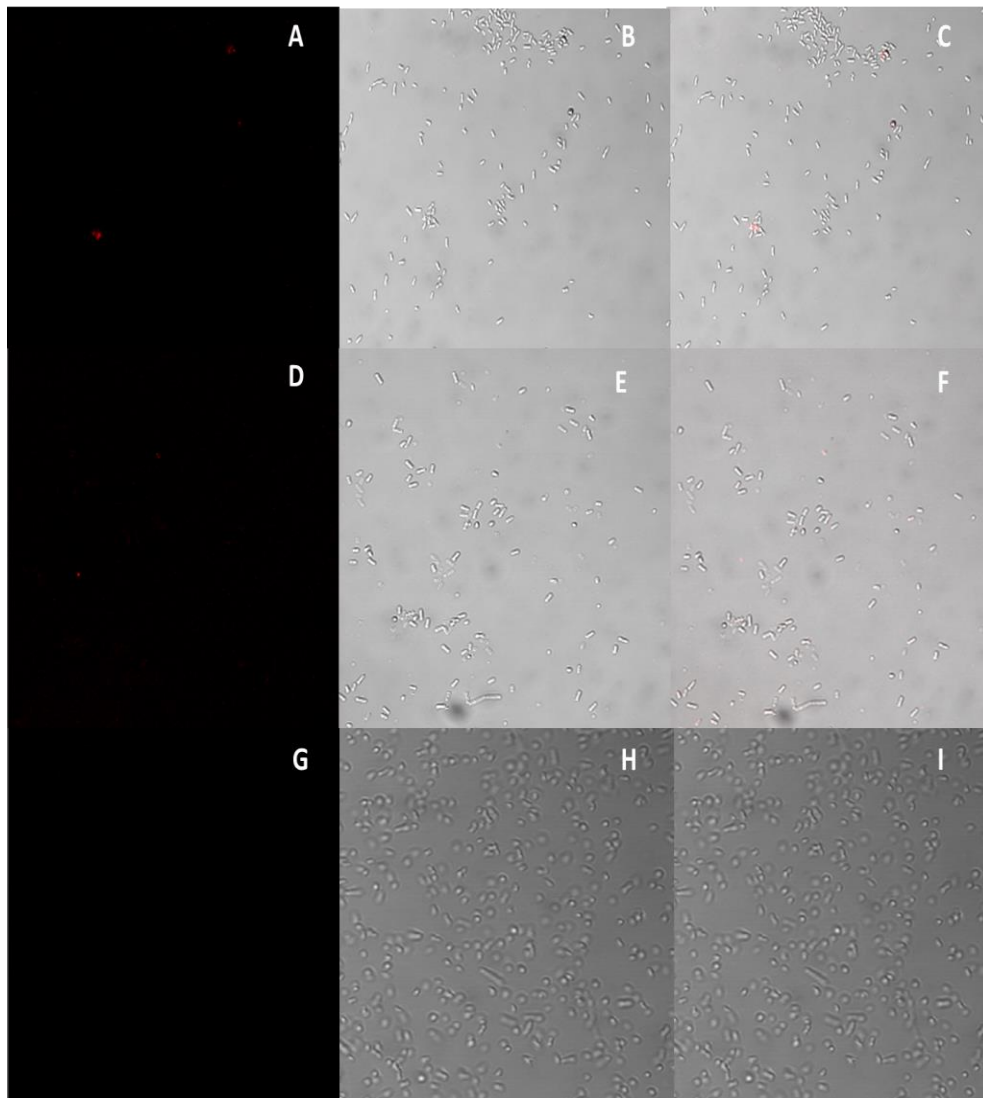


**Figure 3.19** Laser scanning confocal microscope images of three cells bound with *S. Enteritidis* aptamer crn-1 at 488 nm excitation wavelength by plan-neofluar 40X objective. (A) Fluorescence image (B) Optical image (C) Merge of two images of *S. Enteritidis*, (D) Fluorescence image (E) Optical image (F) Merge of two images of *E. coli*, (G) Fluorescence image (H) Optical image (I) Merge of two images of *S. aureus*.

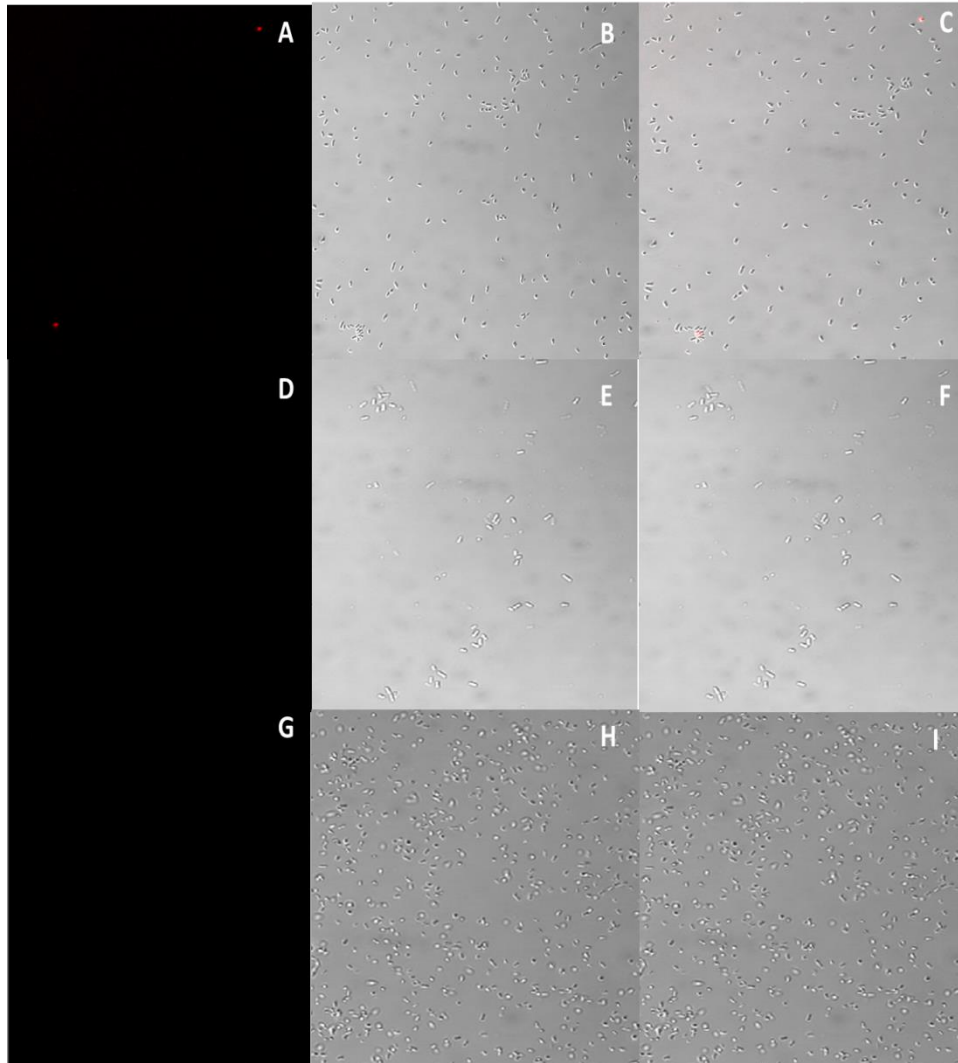


**Figure 3.20** Laser scanning confocal microscope images of three cells bound with *S. Enteritidis* aptamer crn-2 at 488 nm excitation wavelength by plan-neofluar 40X objective. (A) Fluorescence image (B) Optical image (C) Merge of two images of *S. Enteritidis*, (D) Fluorescence image (E) Optical image (F) Merge of two images of *E. coli*, (G) Fluorescence image (H) Optical image (I) Merge of two images of *S. aureus*

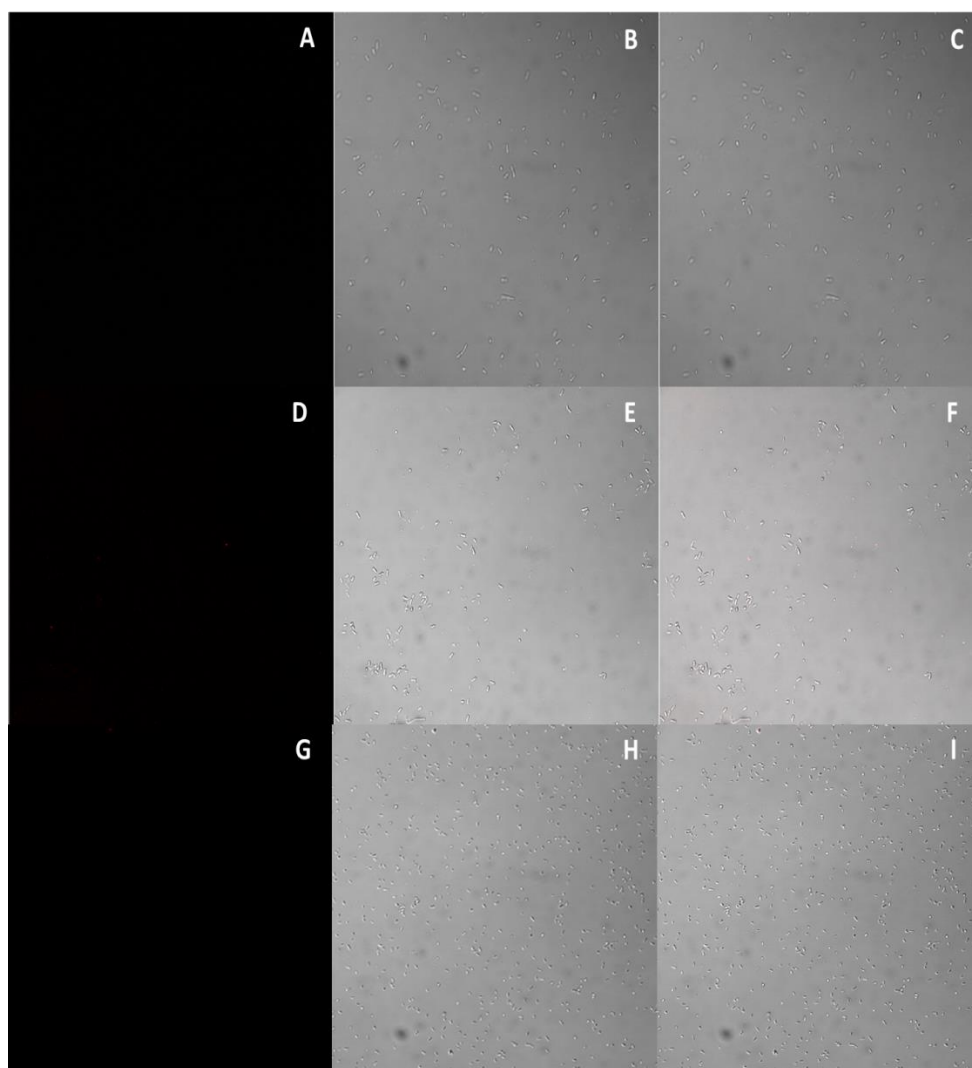


**Figure 3.21** Laser scanning confocal microscope images of three cells bound with *S. Enteritidis* aptamer crn-3 at 488 nm excitation wavelength by plan-neofluar 40X objective. (A) Fluorescence image (B) Optical image (C) Merge of two images of *S. Enteritidis*, (D) Fluorescence image (E) Optical image (F) Merge of two images of *E. coli*, (G) Fluorescence image (H) Optical image (I) Merge of two images of *S. aureus*

### 3.1.8.2 Enzyme-Linked Aptamer Assay (ELAA)

In this study, a common biochemical technique, enzyme-linked immunosorbent assay (ELISA) was used as a base technique for the determination of specificity and affinity of aptamer with a slight modification. Aptamers were used as modular replacements for antibodies in convenient “ELISA-like” formats. Since aptamers had potentially strong binding affinity to the target molecule, **Enzyme Linked Aptamer Assay (ELAA)** was good enough to detect target with high sensitivity and quantify its amount in assay conditions. Figure 3.22 summarized aptamer based assay used in this study schematically.

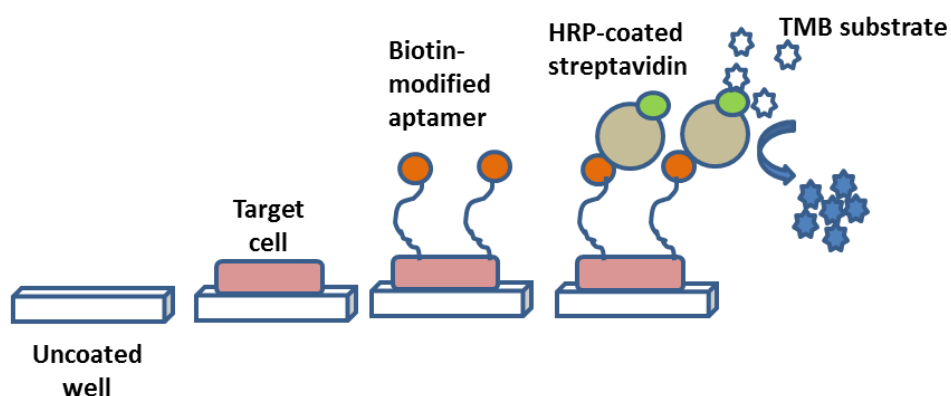


**Figure 3.22** Schematic drawing of aptamer-based ELISA-like assay.

In the assay certain amount of target and control cells were inoculated to uncoated wells of 96 well plate. The bacterial cells were set bottom of wells by centrifugation force and they were incubated with biotin modified aptamers. Aptamer sequences captured by cells then bonded to streptavidin beads which were conjugated with horse radish peroxidase (HRP). With the addition of 3, 3', 5, 5'-tetramethylbenzidine

(TMB) substrate to enzyme surface oxidation reaction took place and the formation of blue color was observed in wells. Being a chromogenic substance, TMB was oxidized with oxygen radicals in enzymatic reaction given at Figure 3.23. The enzymatic reaction catalyzed by HRP produced an intermediate product which finally gave blue color with maximum absorbance at 370 nm.

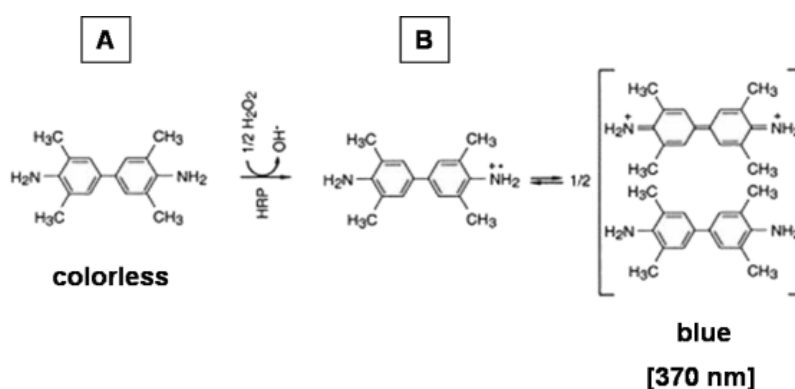


**Figure 3.23** Oxidation reaction of TMB as a substrate of HRP. A. TMB. B. Oxidation product (Muhammad *et al.* 2011).

Optimization experiments were performed with the use of *S. aureus* and its aptamer SA-31. Since wells of plate were uncoated, the initial amount of inoculated cells diminished gradually throughout washing steps in assay procedure. In order to control the cell amounts remained in each well after each round of washing step the turbidities of cells were measured at 600 nm. Although washing wells resulted in the loss of bacterial cell at each concentration as shown in Figure 3.24, these slight decreases in cell amounts were not significant to affect the results of aptamer based assay. There were enough cells remained in wells for aptamer to bind and thus to perform aptamer based enzyme linked assay.

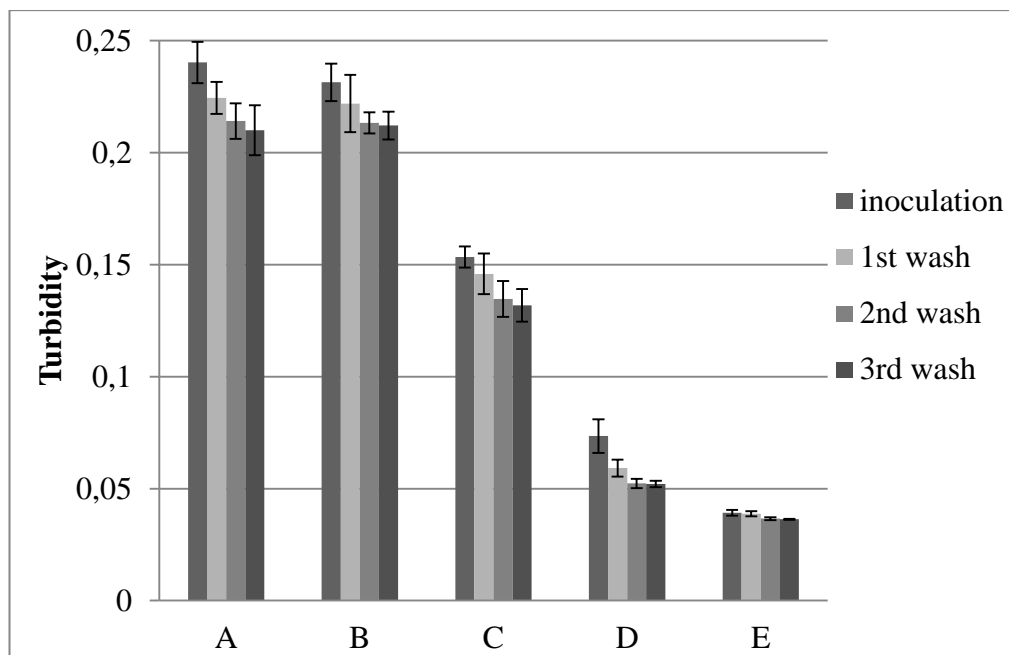


**Figure 3.24** Turbidity measurements of bacterial cells at different amounts after washing steps. A) *S. aureus* at  $10^7$  CFU/mL, B) *S. aureus* at  $10^6$  CFU/mL, C) *S. aureus* at  $10^5$  CFU/mL, D) *S. aureus* at  $10^4$  CFU/mL, E) washing buffer without cell used as control. Error bars represented standard error deviations with  $n=3$ .

In the first assay, while target and control cell amounts were kept constant at  $10^6$  CFU/mL, biotin modified aptamer was used at four different concentrations in order to determine optimum aptamer amount for the characterization in further calorimetric analyses (Figure 3.25). Assays constructed for that study were given in Figure 3.25 as;

A;  $10^6$  CFU/mL of *S. aureus*, **1  $\mu$ M** of Biotin-SA-31, strep-HRP, TMB

B;  $10^6$  CFU/mL of *S. aureus*, **5  $\mu$ M** of Biotin-SA-31, strep-HRP, TMB

C;  $10^6$  CFU/mL of *S. aureus*, **10  $\mu$ M** of Biotin-SA-31, strep-HRP, TMB

D;  $10^6$  CFU/mL of *S. aureus*, **20  $\mu$ M** of Biotin-SA-31, strep-HRP, TMB

E; Control 1: **10  $\mu\text{M}$**  of Biotin-SA-31, strep-HRP, TMB

F; Control 2:  **$10^6$  CFU/mL** of *S. aureus*, strep-HRP, TMB

G; Control 3: only TMB

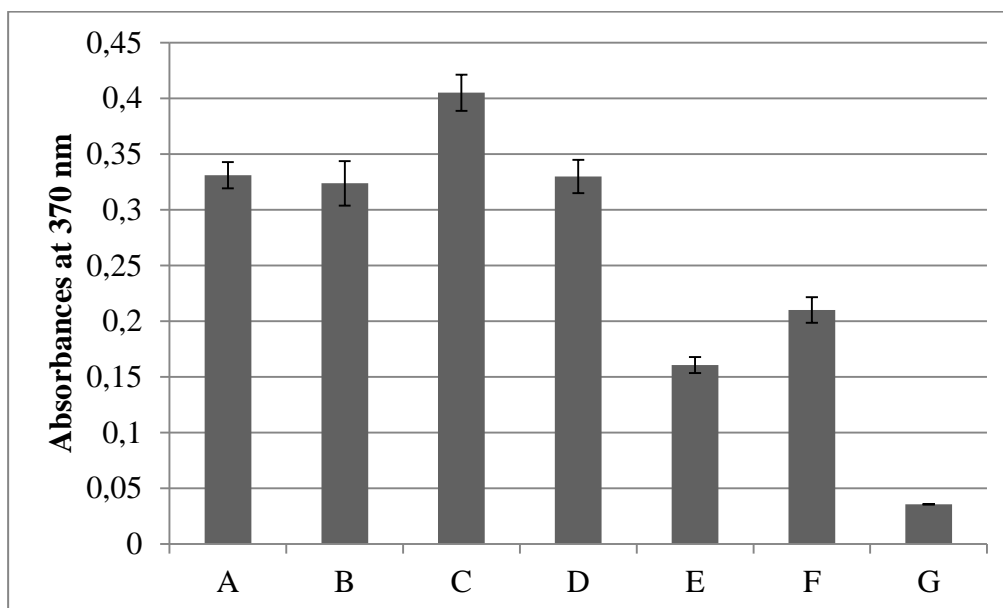


**Figure 3.25** Absorbance readings of different concentrations of SA-31 at constant cell amount ( $10^6$  CFU/mL of *S. aureus*). A) 1  $\mu\text{M}$ , B) 5  $\mu\text{M}$ , C) 10  $\mu\text{M}$ , D) 20  $\mu\text{M}$ , E) Control 1, F) Control 2, G) Control 3. Error bars represented standard deviations with  $n=3$ .

When compared with other three concentrations (1, 5 and 20  $\mu\text{M}$ ), assay constructed with 10  $\mu\text{M}$  of SA31 (Assay C) gave higher absorbance in ELAA. Lower amounts of aptamer in assay were not enough to bind to its specific target molecule on cell surface completely. Thus, they could not provide significant amount of enzymatic

reaction although target cell amount was kept same against four different aptamer concentrations. Assay with highest amount of aptamer (Assay D, 20  $\mu\text{M}$ ) also resulted in the formation of blue color. Higher absorbance reading could be expected as compared with other concentrations due to the usage of higher aptamer concentration; however, absorbance of assay constructed with 20  $\mu\text{M}$  of aptamer was approximately same with that of 1 and 5  $\mu\text{M}$  of aptamers. This may be resulted from the fact that excess amount of aptamer competed to bind to target molecules on cell surface and most of them were eliminated from surface by washing step without reaching to saturation of binding to its target. As a final decision, **10  $\mu\text{M}$**  of *S. aureus* aptamer SA31 concentration was selected to be used in further characterization study. For this assay, three different control wells were formed (E, F and G in Figure 3.25). In the first control well (E), all components of ELISA liked assay were used except cells as a target molecule for aptamer. Since there was not specific structure for aptamer binding, many DNA sequences added to well were removed by washing. The oxidation reaction catalyzed by HRP could not result in the formation of blue color significantly. The second control well (F) contained target cell but not aptamer. No color formation could be expected from this control due to the absence of aptamer as reporter agent for capture of target cells; however, it gave higher absorbance compared with other controls. This may be due to the fact that the cell surface of bacteria provided nonspecific binding site for streptavidin beads coated with HRP and enzymatic reaction could take place leading to color formation. The absorbance from third control (G) only belonged to TMB substrate at 370 nm. Without enzyme TMB was not oxidized, thus it was regarded as background signal.

In the second assay, different cell amounts were tested against constant concentration of SA31, 10  $\mu$ M, which was determined previously as optimum aptamer amount for further study. The aim of this assay was to determine the minimum amount of target cells that could be detected specifically with aptamer. Assays constructed for that study were given in Figure 3.26 as;

A;  **$10^3$  CFU/mL** of *S. aureus*, 10  $\mu$ M of Biotin-SA-31, strep-HRP, TMB

B;  **$10^4$  CFU/mL** of *S. aureus*, 10  $\mu$ M of Biotin-SA-31, strep-HRP, TMB

C;  **$10^5$  CFU/mL** of *S. aureus*, 10  $\mu$ M of Biotin-SA-31, strep-HRP, TMB

D;  **$10^6$  CFU/mL** of *S. aureus*, 10  $\mu$ M of Biotin-SA-31, strep-HRP, TMB

E;  **$10^7$  CFU/mL** of *S. aureus*, 10  $\mu$ M of Biotin-SA-31, strep-HRP, TMB

F; Control 1: only  $10^6$  CFU/mL of *S. aureus*

G; Control 2: only TMB

H; Control 3:  $10^6$  CFU/mL of *S. aureus*, strep-HRP, TMB

I; Control 4:  **$10^6$  CFU/mL of *E.coli***, 10  $\mu$ M of Biotin-SA-31, strep-HRP, TMB

J; Control 5:  **$10^6$  CFU/mL of *S. Enteritidis***, 10  $\mu$ M of Biotin-SA-31, strep-HRP, TMB

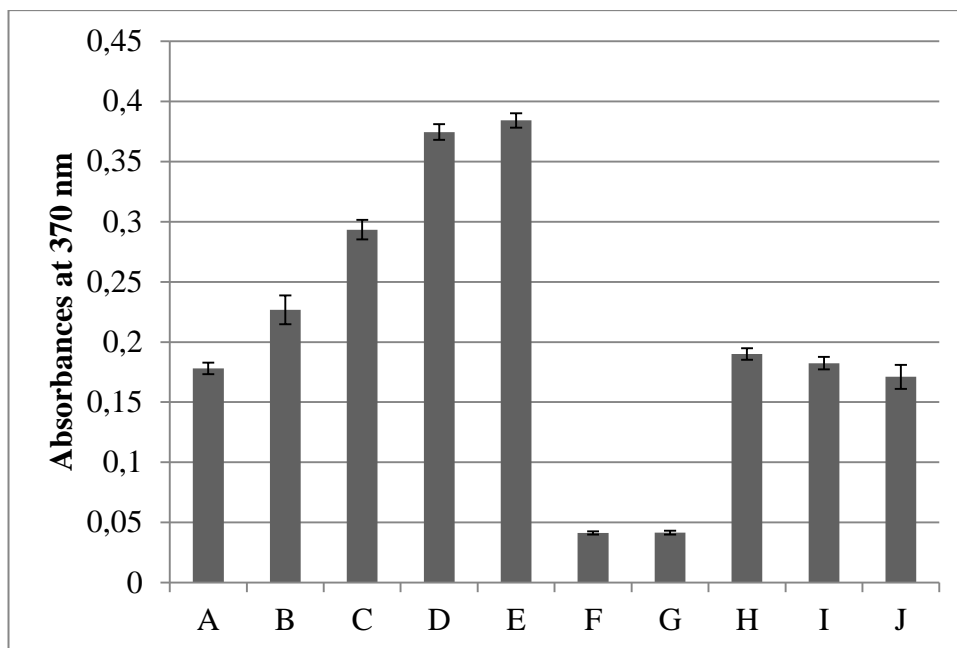


**Figure 3.26** Absorbance readings of different cell amounts at constant SA-31 concentration (10  $\mu$ M). A)  $10^3$  CFU/mL of *S. aureus*, B)  $10^4$  CFU/mL of *S. aureus*, C)  $10^5$  CFU/mL of *S. aureus*, D)  $10^6$  CFU/mL of *S. aureus*, E)  $10^7$  CFU/mL of *S. aureus*, F) Control 1, G) Control 2, H) Control 3, I) Control 4 and J) Control 5. Error bars represented standard deviations with n=3.

As shown in the Figure 3.26, with the increasing amount of *S. aureus* as target cell, absorbance values at 370 nm resulting from the formation of blue color increased until cell amount of  $10^6$  CFU/mL and then remained approximately constant though cell amount continued to increase in assay. This result showed similarity with general reaction rate of enzyme-substrate complex. When enzymatic reaction rate is analyzed at constant enzyme amount, the increase in substrate amount leads to the increase in reaction rate up to a point above which any further increase in substrate concentration produces no significant change in reaction rate. In our assay, aptamer molecules and target cell acted as enzyme and its substrate, respectively. At constant aptamer concentration, absorbance reading increased with increasing cell amount. However, above cell amount of  $10^6$  CFU/mL binding reaction between aptamer and

cell reached its plateau and thus no further increase in absorbance was observed due to the saturation of cell binding sites with aptamer.

Moreover, the lowest amount of cell that could be detected with SA31 specifically was determined as  $10^4$  CFU/mL from Figure 3.26. The cell amounts lower than  $10^4$  CFU/mL behaved like non-target cells with nonspecific aptamer binding. Absorbance result of *S. aureus* at  $10^3$  CFU/mL was close statistically to those of *E. coli* and *S. Enteritidis* at  $10^6$  CFU/mL.

In addition, specificity of *S. aureus* aptamer was tested with two control wells. These two control wells were inoculated separately with *E. coli* and *S. Enteritidis* which were not specific target of aptamer used in assay. The results given at Figure 3.26 represented that although control cells were used at concentration of  $10^6$  CFU/mL, they yielded lower absorbance as compared with that of target cell at  $10^4$  CFU/mL. Since aptamer used in assay was not specific for *E. coli* and *S. Enteritidis*, nonspecific binding resulted in poor absorbance result in spite of higher cell amounts. Furthermore, another control assay was constructed with components including target *S. aureus* cell at  $10^6$  CFU/mL, streptavidin beads coated with HRP and TMB but not aptamer. The absorbance read from this control well was lower than that of well contained same amount of target cell with aptamer. The presence of aptamer modified with biotin molecule provided specific binding of streptavidin beads coated with enzyme and thus it brought more catalytic reaction of substrate on target cell. As a result, the specificity and affinity of *S. aureus* aptamer to *S. aureus* cell was shown clearly.

As explained previously, this optimum assay procedure was applied to the characterization study of *S. Enteritidis* aptamers selected in this study.

First of all, in order to control whether cell amounts in wells were diminished by washing steps, absorbance values of *S. Enteritidis* ( $10^7$ ,  $10^6$ ,  $10^5$ ,  $10^4$  and  $10^3$  CFU/mL) at 600 nm were measured after inoculation of cells and washing steps (Figure 3.27). As compared with the turbidity of inoculation, each washing step

led to decrease in cell amounts without depending on initial concentrations, however, these decreasing cell amounts were not at critical level that may affect further experiment. The lowest amount of cell,  $10^3$  CFU/mL of *S. Enteritidis*, was still measurable and distinguishable when compared with absorbance of wash buffer without containing cell. From these results it was clearly stated that there were still sufficient amount of cells remained in wells for aptamer based assay.

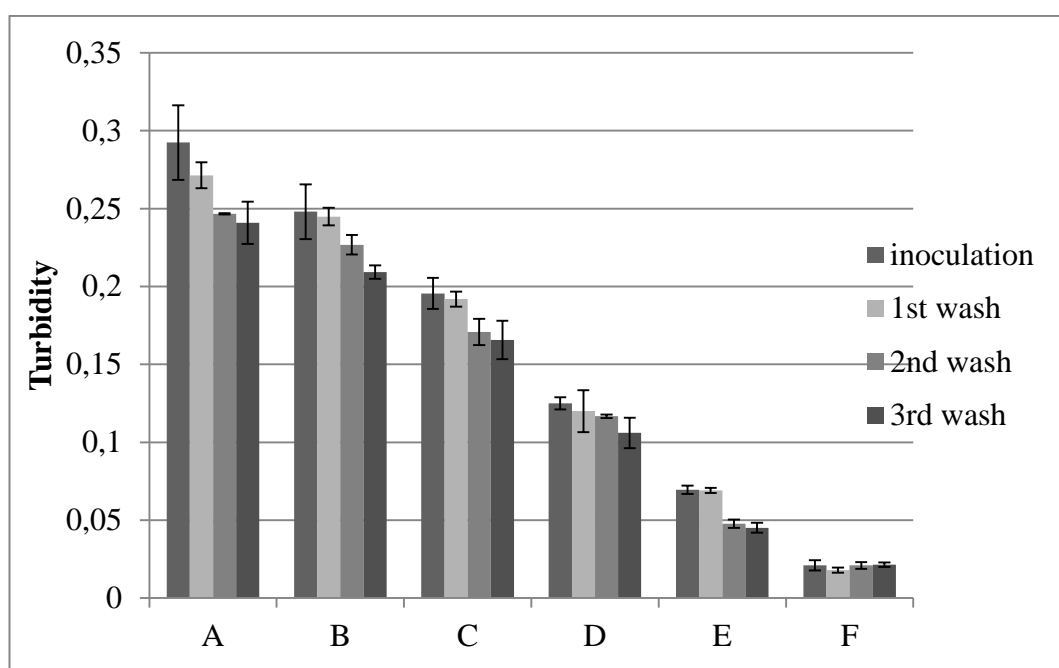


**Figure 3.27** Turbidity measurements of bacterial cells at different amounts after washing steps. A) *S. Enteritidis* at  $10^7$  CFU/mL, B) *S. Enteritidis* at  $10^6$  CFU/mL, C) *S. Enteritidis* at  $10^5$  CFU/mL, D) *S. Enteritidis* at  $10^4$  CFU/mL, E) *S. Enteritidis* at  $10^3$  CFU/mL, F) washing buffer without cell used as control. Error bars represented standard deviations with n=3.

In the first aptamer based assay, four different concentrations of crn-1, crn-2 and crn-3 were incubated with  $10^6$  CFU/mL of *S. Enteritidis* and optimum concentration of each candidate aptamer for efficient ELAA were determined. Moreover, their binding properties were evaluated by comparing absorbance measurement differences between three candidate aptamers. Three control wells were prepared.

The first one was constructed with biotin modified aptamers and HRP coated streptavidin. In the second one aptamers were not used instead only *S. Enteritidis* and HRP coated streptavidin were used for the unspecific binding control of streptavidin to cells. The third control contained only TMB to evaluate absorbance coming from background. Assays constructed for that study were given in Figure 3.28 as;

A;  $10^6$  CFU/mL of *S. Enteritidis*, **1  $\mu$ M of biotin crn-1/crn-2/crn-3**, strep-HRP, TMB

B;  $10^6$  CFU/mL of *S. Enteritidis*, **5  $\mu$ M of biotin crn-1/crn-2/crn-3**, strep-HRP, TMB

C;  $10^6$  CFU/mL of *S. Enteritidis*, **10  $\mu$ M of biotin crn-1/crn-2/crn-3**, strep-HRP, TMB

D;  $10^6$  CFU/mL of *S. Enteritidis*, **20  $\mu$ M of biotin crn-1/crn-2/crn-3**, strep-HRP, TMB

E; Control 1: 10  $\mu$ M of biotin crn-1/crn-2/crn-3, strep-HRP, TMB

F; Control 2:  $10^6$  CFU/mL of *S. Enteritidis*, strep-HRP, TMB

G; Control 3: only TMB

In this assay, the change in concentrations from 1 to 20  $\mu$ M of crn-1 and crn-2 showed differences in their absorbance measurements, while, there were no significant changes in well containing cell with crn-3. The change in the concentrations of crn-3 did not yield a change in binding affinities of crn-3 to

*S. Enteritidis* in fact; control assay constructed without aptamers gave approximately same absorbance measurement with that constructed with crn-3 (Figure 3.28). Although there was no biotin modified aptamer, nonspecific binding of HRP coated streptavidin to *S. Enteritidis* took place in control assay. Since there were no clear discriminations on measurement between crn-3 and control and also within different concentrations of crn-3, it could be stated that crn-3 had no affinity to *S. Enteritidis* and no binding reaction could take place between crn-3 and target cell. Out of crn-3, other two candidate aptamers, crn-1 and crn-2, showed affinities to target cell and increase in concentrations up to 10  $\mu\text{M}$  went parallel with increase in absorbance measurements. If binding capacities of crn-1 and crn-2 were compared at 1, 5 and 10  $\mu\text{M}$ , it could be easily observed that crn-2 showed more binding based on higher absorbance measurements.

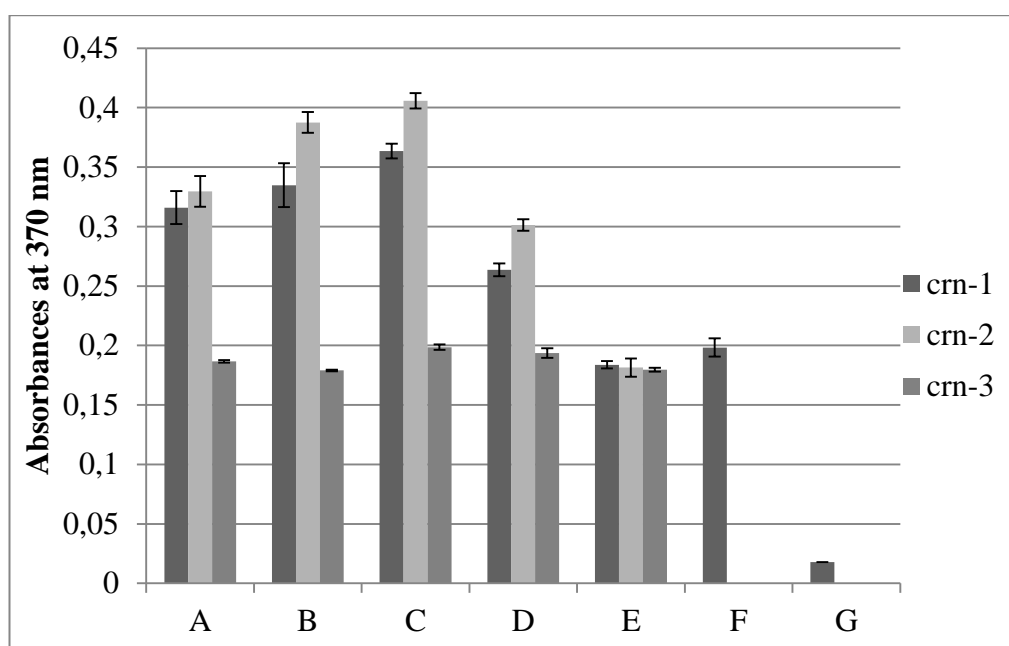


**Figure 3.28** Absorbance readings of different concentrations of crn-1, crn-2 and crn-3 at constant cell amount ( $10^6$  CFU/mL of *S. Enteritidis*). A) 1  $\mu\text{M}$ , B) 5  $\mu\text{M}$ , C) 10  $\mu\text{M}$ , D) 20  $\mu\text{M}$ , E) Control 1, F) Control 2, G) Control 3. Error bars represented standard deviations with n=3.

At 20  $\mu\text{M}$ , binding affinities of both crn-1 and crn-2 decreased below that at 1  $\mu\text{M}$ . Leading to lower absorbance measurements due to lower amount of bindings at high concentrations of crn-1 and crn-2 could be explained by inhibition of aptamer binding effectively to targets at higher amount. Excess amount of sequences could compete for binding and they were easily removed by washing from surface of cell.

These results along with confocal microscopy data indicated that two sequences, **crn-1 and crn-2, were selected as DNA aptamers against *S. Enteritidis*** and they could be characterized in further studies to determine their affinities to target via measuring  $K_d$ . Also, **10  $\mu\text{M}$**  of crn-1 and crn-2 were selected for the next aptamer based ELISA like assay in which lowest detection limits of assays were evaluated.

The purpose of second assay was the determination of lowest amount of *S. Enteritidis*, which could be captured by crn-1 and crn-2 with clear discrimination of not binding to control cells. In this assay, 10  $\mu\text{M}$  of crn-1 and crn-2 were incubated with different amounts of target cell and also with  $10^6$  CFU/mL of two control cells. After removal of unbound, HRP coated streptavidin was added to wells for binding to biotin modified aptamers. With the addition of substrate TMB, enzymatic reaction took place and products with blue color were produced. The measurement of absorbance at 370 nm gave data about binding affinity and specificity of crn-1 and crn-2 against target and control cells. Assays constructed for that study were given in Figure 3.29 as;

A;  **$10^3$  CFU/mL of *S. Enteritidis***, 10  $\mu\text{M}$  of biotin crn-1, strep-HRP, TMB

B;  **$10^4$  CFU/mL of *S. Enteritidis***, 10  $\mu\text{M}$  of biotin crn-1 strep-HRP, TMB

C;  **$10^5$  CFU/mL of *S. Enteritidis***, 10  $\mu\text{M}$  of biotin crn-1, strep-HRP, TMB

D;  **$10^6$  CFU/mL of *S. Enteritidis***, 10  $\mu\text{M}$  of biotin crn-1, strep-HRP, TMB

E;  **$10^7$  CFU/mL of *S. Enteritidis***, 10  $\mu\text{M}$  of biotin crn-1, strep-HRP, TMB

F; Control 1:  $10^6$  CFU/mL of *S. Enteritidis*

G; Control 2: only TMB

H; Control 3:  $10^6$  CFU/mL of *S. Enteritidis*, strep-HRP, TMB

I; Control 4:  $10^6$  CFU/mL of *E. coli*, 10  $\mu$ M of biotin crn-1, strep-HRP, TMB

J; Control 5:  $10^6$  CFU/mL of *S. aureus*, 10  $\mu$ M of biotin crn-1, strep-HRP, TMB

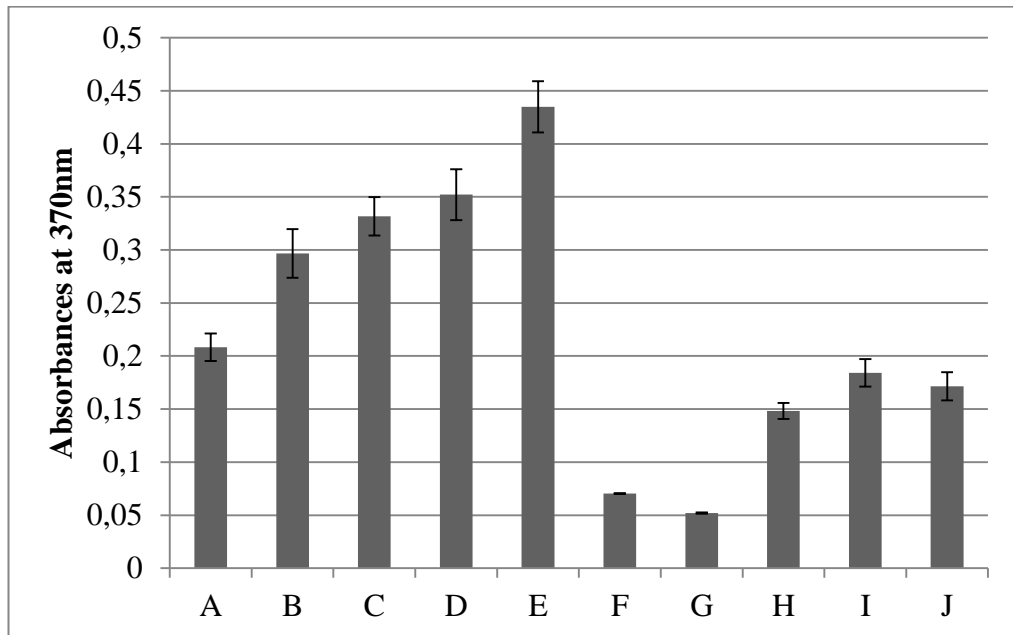


**Figure 3.1** Absorbance readings of different *S. Enteritidis* amount at constant crn-1 concentration (10  $\mu$ M). A)  $10^3$  CFU/mL of *S. Enteritidis*, B)  $10^4$  CFU/mL of *S. Enteritidis*, C)  $10^5$  CFU/mL of *S. Enteritidis*, D)  $10^6$  CFU/mL of *S. Enteritidis*, E)  $10^7$  CFU/mL of *S. Enteritidis*, F) Control 1, G) Control 2, H) Control 3, I) Control 4 and J) Control 5. Error bars represented standard deviations with n=3.

As shown in Figure 3.29 at constant crn-1 concentration the change in *S. Enteritidis* amount led to change in absorbance measurements. The absorbance of assay constructed with  $10^3$  CFU/mL of *S. Enteritidis* and 10  $\mu$ M of crn-1 was higher than

those constructed with  $10^6$  CFU/mL of *S. aureus* and *E. coli*. Although target cell amount was lower as compared with control cells, binding of biotin modified crn-1 to its target cell was higher due to the specificity of crn-1 to *S. Enteritidis*. Therefore, it could be stated that the lowest amount of *S. Enteritidis* that was detected with crn-1 specifically was determined as  **$10^3$  CFU/mL**. The increase in target cell amount was easily observed with the increase in absorbance measurement due to increase in binding of crn-1 to target. In addition to the determination aptamer specificity and the lowest amount of cell captured by crn-1 this assay also clarified that without the use of aptamer HRP modified streptavidin bound to cell surface nonspecifically. In control well which contained only  $10^6$  CFU/mL of *S. Enteritidis* and streptavidin-HRP complex, addition of TMB yielded an enzymatic reaction. However, product formation was lower than well containing  $10^6$  CFU/mL of *S. Enteritidis*, crn-1 and streptavidin-HRP complex. This result indicated the nonspecific binding of streptavidin to cell surface. However, the use of aptamer resulted in more and specific binding reaction.

Similar results were obtained from the third assay which was constructed with crn-2 (Figure 3.30). Assays constructed for that study were given in Figure 3.30 as;

A;  **$10^3$  CFU/mL of *S. Enteritidis***, 10  $\mu$ M of biotin crn-2, strep-HRP, TMB

B;  **$10^4$  CFU/mL of *S. Enteritidis***, 10  $\mu$ M of biotin crn-2 strep-HRP, TMB

C;  **$10^5$ CFU/mL of *S. Enteritidis***, 10  $\mu$ M of biotin crn-2, strep-HRP, TMB

D;  **$10^6$  CFU/mL of *S. Enteritidis***, 10  $\mu$ M of biotin crn-2, strep-HRP, TMB

E;  **$10^7$  CFU/mL of *S. Enteritidis***, 10  $\mu$ M of biotin crn-2, strep-HRP, TMB

F; Control 1:  $10^6$  CFU/mL of *S. Enteritidis*

G; Control 2: only TMB

H; Control 3:  $10^6$  CFU/mL of *S. Enteritidis*, strep-HRP, TMB

I; Control 4:  $10^6$  CFU/mL of *E. coli*, 10  $\mu$ M of biotin crn-2, strep-HRP, TMB

J; Control 5:  $10^6$  CFU/mL of *S. aureus*, 10  $\mu$ M of biotin crn-2, strep-HRP, TMB

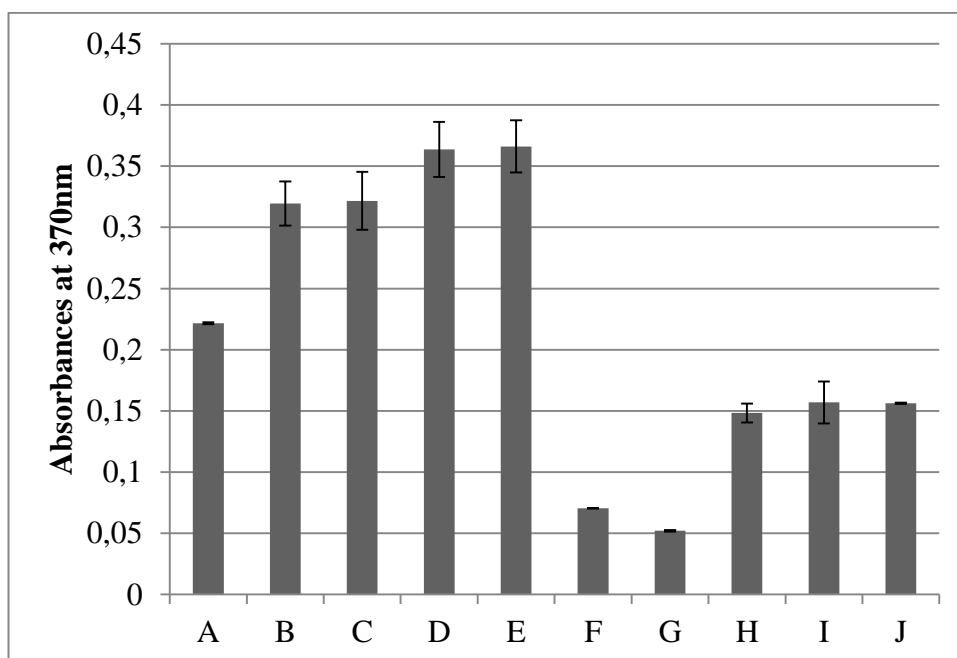


**Figure 3.29** Absorbance readings of different *S. Enteritidis* amount at constant crn-2 concentration (10  $\mu$ M). A)  $10^3$  CFU/mL of *S. Enteritidis*, B)  $10^4$  CFU/mL of *S. Enteritidis*, C)  $10^5$  CFU/mL of *S. Enteritidis*, D)  $10^6$  CFU/mL of *S. Enteritidis*, E)  $10^7$  CFU/mL of *S. Enteritidis*, F) Control 1, G) Control 2, H) Control 3, I) Control 4 and J) Control 5. Error bars represented standard deviations with n=3.

The lowest amount of target cell that could be detected by crn-2 in this assay condition was  $10^3$  CFU/mL. This aptamer sequence like crn-1 bound to *E.coli* and *S.aureus* nonspecifically. However these nonspecific bindings were not resulted from crn-2 binding to these cells, but from nonspecific binding of streptavidin-HRP conjugates to *E.coli* and *S.aureus*. This conclusion was made because other control well containing target cell and streptavidin-HRP conjugate without crn-2 resulted in

enzymatic reaction and yielded approximately same amount of products as two control wells containing *E.coli* and *S.aureus*. The nonspecific bindings of strep-HRP conjugates to cell surface were eliminated by specific binding of crn-1 (Figure 3.29) and crn-2 (Figure 3.30) to their target cell.

With the data from confocal microscope and ELAA, **crn-1 and crn-2, were identified as DNA aptamers against *S. Enteritidis*.**

### **3.1.8.3 Protein Assay of Cell Membrane Proteins**

After the characterization of selected aptamer sequences with confocal microscope and ELAA, the next step was the determination of binding affinities of selected sequences. For this analysis, isothermal titration calorimeter was chosen with the use of membrane proteins as target. For MicroCal VP-ITC provided by Molecular Biology and Biotechnology R&D Center, both target and aptamer sequences had concentrations at molar unit. Therefore, as target of aptamer binding membrane fractions were used instead of whole cell. The extraction of membrane proteins was performed with carbonate extraction method (Molloy, 2008). Basically, with the use of sodium carbonate solution alkaline environment was prepared which provided the solubilization of membrane associated proteins. After the extraction of membrane fractions of *S. Enteritidis*, *S. aureus* and *E.coli*, they were analyzed with Protein 80 Assay of Bioanalyzer (Agilent 2100 Bioanalyzer, Agilent Technologies, Inc., US). The fluorescence of each protein bands were detected and translated into gel-like images and electropherograms. The peaks and intensities represented molecular weight and concentration of separated fragments, respectively. Figure 3.31 represented pseudo gel image of protein bands extracted from three different bacteria. The variety of proteins among bacteria was easily observed from band distributions. This result was also confirmed with electropherograms of fractions belonging to three bacteria (Figure 3.32). The reproducibility of size and concentration results was analyzed with triple replicates. The mean concentrations of total proteins, main protein sizes and their percentages were given for three bacteria at Table 3.6.

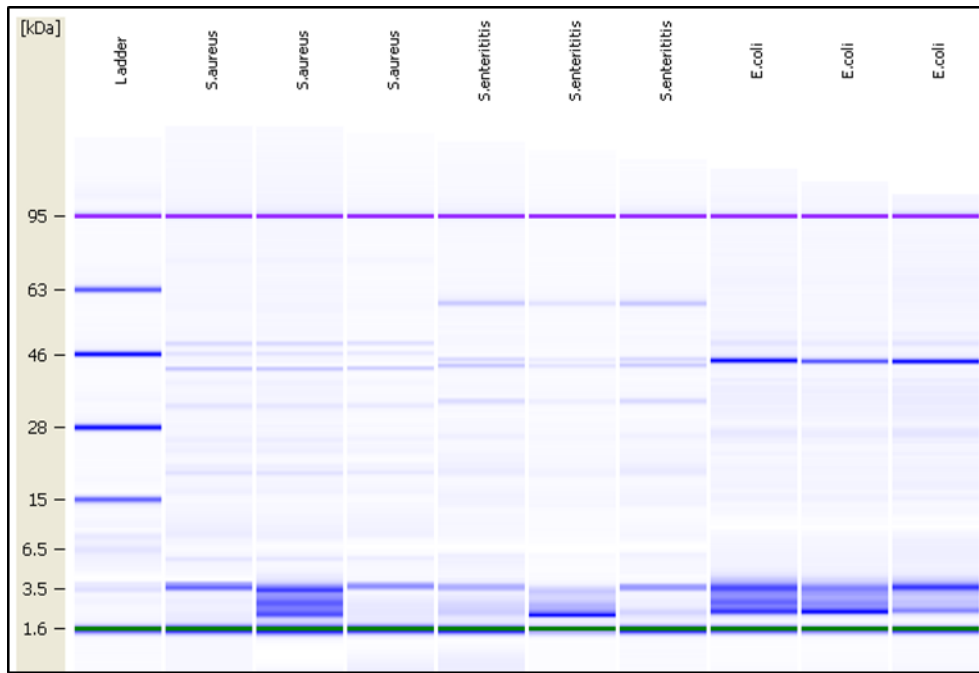


**Figure 3.30** Gel-like images of membrane fractions extracted from *S. Enteritidis*, *S. aureus*, *E. coli*. Triple replicates were loaded for each bacterium in Bioanalyzer. kDa represented molecular weight of proteins.

**Table 3.6** Mean concentrations of total proteins, main protein sizes and their percentages.

<b>Bacteria</b>	<b>Mean concentration (ng/μL)</b>	<b>Standard deviation (ng/μL)</b>	<b>CV (%)</b>	<b>Main protein sizes (kDa)</b>	<b>Relative percentages in total protein (%)</b>
<i>S. aureus</i>	375.53	44.85	11.94	5.8	13.1
				9.2	14.6
				19.8	10.6
				33.3	8.7
				42.6	13.1
				48.9	8.4
<i>S. Enteritidis</i>	275.9	10.61	3.84	19.9	14.2
				34.5	14.3
				43.3	18.8
				44.8	10.4
				59.5	23.0
<i>E.coli</i>	616.77	59.08	9.58	27.1	8.7
				32.1	3.7
				44.4	55.0
				48.9	5.3

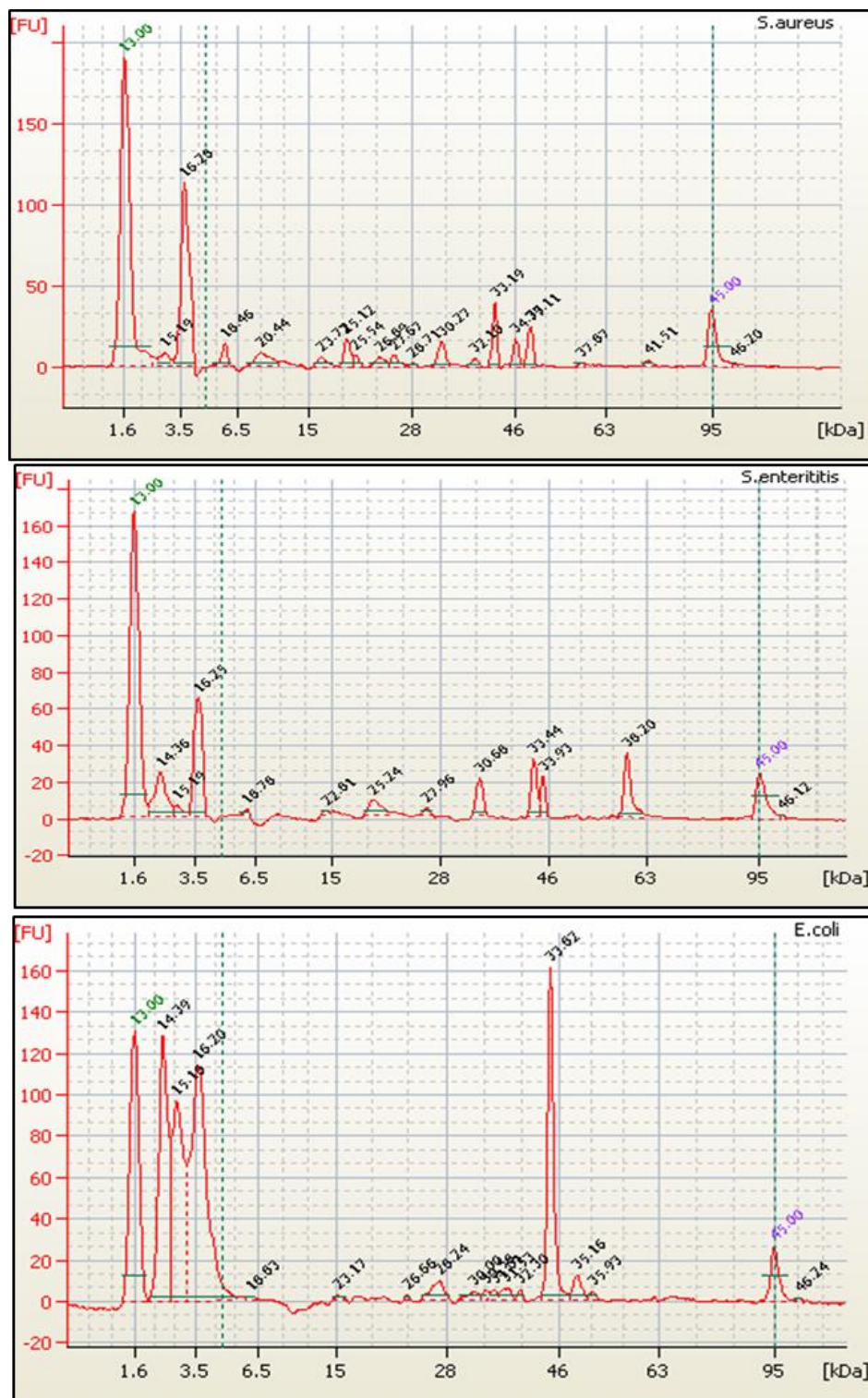


**Figure 3.31** Electropherograms of membrane proteins extracted from *S. Enteritidis*, *S. aureus* and *E. coli* by carbonate extraction method. kDa and FU represented molecular weight of proteins and fluorescence unit.

### 3.1.8.4 Isothermal Titration Calorimeter Analysis

After evaluating the specificity of *S. aureus* and *S. Enteritidis* aptamers to their target cells, *S. aureus* and *S. Enteritidis*, their binding affinities were determined by using isothermal titration calorimetry (ITC).

ITC is a technique that measures the heat generated or absorbed when two molecules interact with each other. It gives quantitative measurements of binding parameters; association constant ( $K_a$ ), the stoichiometry ( $n$ ), and the enthalpy of binding ( $\Delta H$ ) directly. The free energy ( $\Delta G$ ) and entropy ( $\Delta S$ ) of binding are determined from the association constant (Duff *et al.*, 2011). In order to determine how strong or weak binding interaction occurs between aptamer candidates and target molecules, estimation of association constant,  $K_a$ , plays important roles (Jing and Bowser, 2011). From this binding constant dissociation constant ( $K_d$ ) can be calculated by taking reciprocal of  $K_a$  ( $K_d = 1/K_a$ ). Higher  $K_a$  values correspond to lower  $K_d$  values meaning that the binding between molecules are very strong. In addition to  $K_a$ , the stoichiometry represented by  $n$  also gives valuable information about binding mechanism. The  $n$  basically explains the number of binding sites present on macromolecules for binding of ligands. If only one binding site is present on surface, the stoichiometry is 1. ITC analyses also give the change in enthalpy ( $\Delta H$ ). The enthalpy change is the measure of the energy content of the bonds broken and created meaning that the amount of heat released or absorbed during the binding reaction. Generally, the major source contributing to enthalpy change is the hydrogen bonds between molecules. The final parameter given by ITC is the change in entropy ( $\Delta S$ ). The entropy is the measure of disorder in closed system. It changes in reversible processes in which energy can only be transferred in one direction from an ordered state to a disordered state. Therefore, if the system has higher entropy, its randomness is high with lower availability of energy to do work (Pierce *et al.*, 1999).

In this study ITC was used to determine the dissociation constant ( $K_d$ ) of aptamers for the determination of best binding aptamer to its target among candidate aptamers selected in SELEX process. VP ITC titration calorimeter (MicroCal, Northampton,

MA) was used at certain parameters. Assay parameters were previously optimized with *S. aureus* aptamer SA-31 and its target *S. aureus*. As a binding model with n=1;



Then, binding parameters were calculated from the following equations.

$$Ka = [TA]/[T][A]$$

$$Kd = [T][A]/[TA]$$

$$Kd = 1/Ka$$

$$\Delta G = \Delta H - T\Delta S$$

$$\Delta G = -RT\ln Ka$$

In the first experiment, 10  $\mu$ M of *S. aureus* aptamer SA-31 and 50  $\mu$ M of membrane proteins were prepared in 1 X PBS (pH 7) which was previously degassed and filter sterilized in order to remove bubbles and dust particles from buffer. Since air bubbles remaining in either sample cell or syringe interfere with the feedback circuit and result in poor baselines, they were removed from buffer which was used in the preparation of ligand and macromolecule. The pH of aptamer and membrane fraction solutions was measured with microprobe. In order to eliminate heat difference due to pH difference the pH values of these two solutions were adjusted to be approximately same with  $\pm 0.05$  differences. The titration was performed at 4°C with 300 rpm stirring speed to provide good mixing between aptamer and target membrane fraction. As shown in Figure 3.33, the heat changes upon each injection of membrane proteins into aptamer solution were poor within the range of 0 to -2kcal/mole. There was no binding reaction observed between aptamer (SA31) and *S. aureus* membrane proteins at 4 °C.

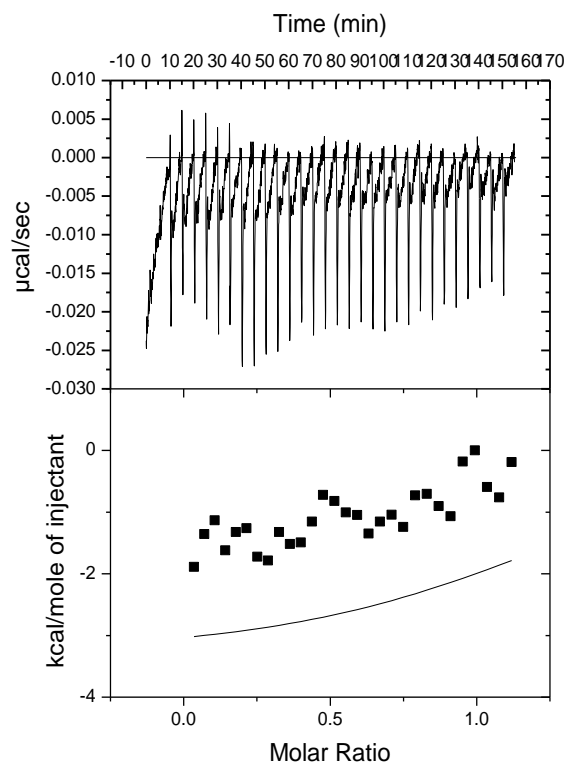


**Figure 3.32** Binding experiment of *S. aureus* aptamer SA-31 and *S. aureus* membrane fractions via ITC at 4°C; Raw ITC data (upper graph), Thermalgram of titrating SA31 with membrane fraction (lower graph).

The second experiment was performed at 25 °C with same parameters. As given above, a one-site interaction model was suited to *S. aureus* aptamer binding to its target. Analyses shown in Figure 3.34 indicated that with  $n=1$ , the binding reaction between aptamer and its target was exothermic reaction in which heat was released. This specific binding reaction occurred spontaneously so that led to higher entropy ( $\Delta S > 0$ ). Since heat was lost in the binding reaction between aptamer and its target, the enthalpy of reaction decreased ( $\Delta H < 0$ ). The quantitative data given by software ORIGIN was tabulated at Table 3.7 With the use of these data the association constant ( $K_a$ ) and change in free energy ( $\Delta G$ ) were calculated by

following formulas in which R was the gas constant ( $1.986 \text{ cal K}^{-1} \text{ mol}^{-1}$ ) and T was the temperature in K.

$$\Delta G = \Delta H - T\Delta S$$

$$\Delta G = -RT \ln K_a$$

At  $25^\circ\text{C}$  (293 K) the binding constant  $K_a$  and  $\Delta G$  between aptamer and *S. aureus* membrane fraction were  $1.56 \times 10^6 \text{ M}^{-1}$  and  $-8445,8 \text{ cal/mol}$ , respectively. The data suggested that the binding reaction of aptamer at  $25^\circ\text{C}$  occurred spontaneously and *S. aureus* aptamer showed affinity at  $\mu\text{M}$  level with one binding site on membrane fraction.

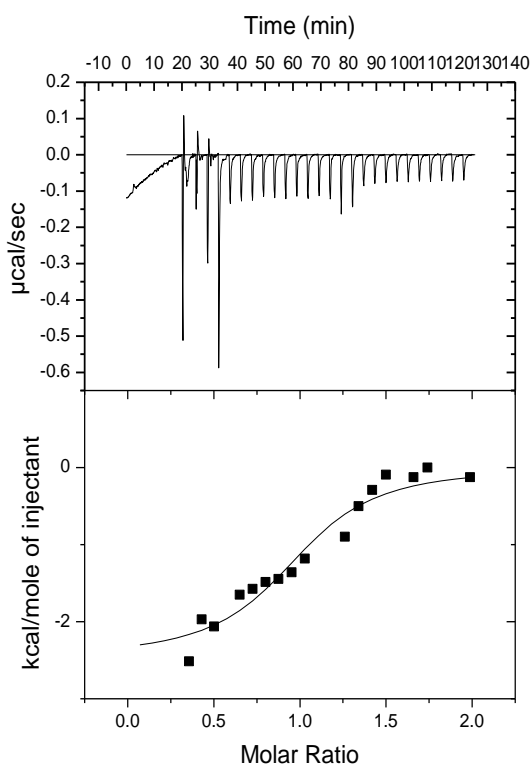


**Figure 3.33** Binding experiment of *S. aureus* aptamer SA-31 and *S. aureus* membrane fraction via ITC at  $25^\circ\text{C}$ ; A) Raw ITC data, B) Thermalgram of titrating SA-31 with membrane fraction.

In the third experiment, parameters of run were kept constant except the reaction temperature again in order to evaluate the effect of binding temperature on binding mechanism and  $K_a$ . The binding reaction was set as 37°C which was the selection temperature of *S. aureus* aptamer for *S. aureus* in literature (Cao *et al.*, 2009). As shown in Figure 3.35 and data given at Table 3.7, the reaction between aptamer and its target membrane fractions gave also one-site binding model at 37°C. The apparent association constant,  $K_a$ , was  $1.03 \times 10^6 \text{ M}^{-1}$  and  $\Delta G$  between SA-31 and target at 37°C was determined to be:  $\Delta G = -8531.5 \text{ cal/mol}$ . As compared with affinity constant and free energy change of reaction at 25°C, binding reaction at 37°C gave similar results. These close apparent association constants were correlated with similar possible minimum free energy structures of *S. aureus* aptamer at two different temperatures. As represented in Figure 3.37, the minimum free energy structures of aptamer at 25°C and 37°C were same with small equilibrium probability differences. Having same folding at these temperatures provided aptamer to have same binding mechanisms because specific binding of aptamer to its target with high affinity was only due to its unique 3D structure. As mentioned in the first experiment, there was no binding occurred between SA31 and *S.aureus* membrane fractions at 4 °C. The possible structure of SA31 at 4 °C was quietly different as compared with structures at 25°C and 37°C. This difference in structure could be the reason of nonbinding of SA-31 at 4 °C.

Results of these three experiments were corrected with result of heat of dilution data. Control experiment was performed by titrating membrane fractions in syringe into buffer solution without aptamer in cell. Data of heat of dilution was subtracted from data of three experiments before evaluating binding parameters. As shown in Figure 3.36, heat released by dilution and mixing of solution was negligible with very poor heat change at each titration. Therefore, after subtraction of this result from experimental results it could be concluded that changes in heat upon titration of membrane fraction into aptamer solution were resulted from binding reaction between ligand and aptamer.

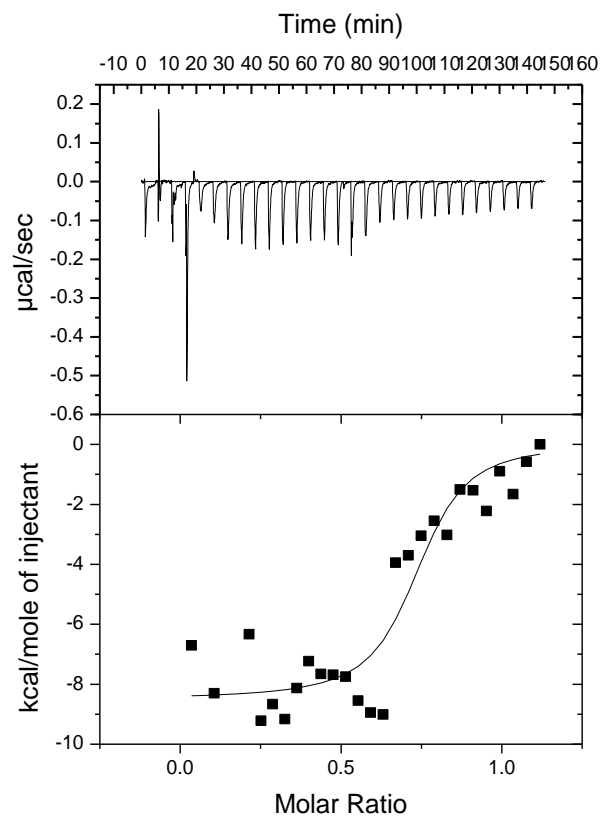


**Figure 3.34** Binding experiment of *S. aureus* aptamer SA-31 and *S. aureus* membrane fraction via ITC at 37°C; A) Raw ITC data, B) Thermalgram of titrating SA-31 with membrane fraction.

**Table 3.7** Thermodynamic parameters of binding reaction between SA-31 and *S. aureus* membrane fractions (in 10 mM of PBS at pH 7) at different temperatures with one site binding model.

Binding reaction	$\Delta H$ (cal/mol)	$\Delta G$ (cal/mol)	$K_a$ ( $M^{-1}$ )	$K_d$ (M)	Stoichiometry (N)
at 4°C	-	-	-	-	-
at 25°C	-2456	-8445.8	$1.56 \times 10^6$	$0.625 \times 10^{-6}$	0.997
at 37°C	-9911	-8531.5	$1.03 \times 10^6$	$0.971 \times 10^{-6}$	0.923

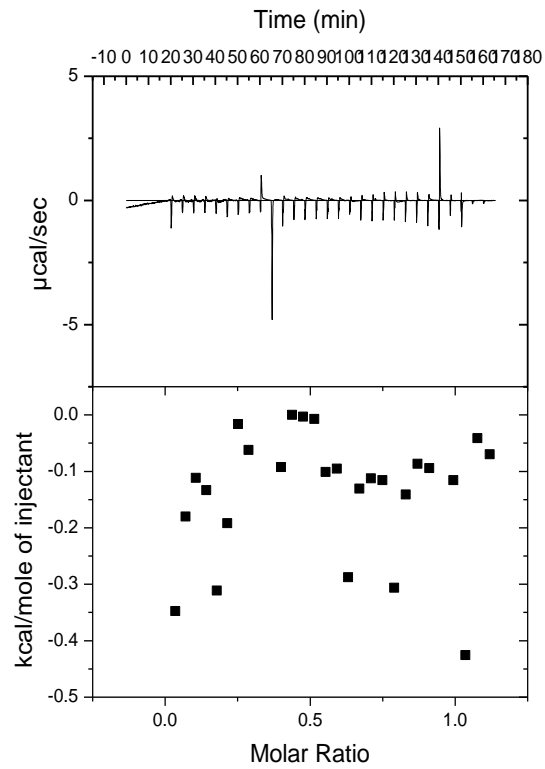


**Figure 3.35** Heat of dilution experiment: Titration of membrane fractions of *S. aureus* into PBS solution. A) Raw ITC data, B) Thermalgram of titrating buffer solution with membrane fraction.

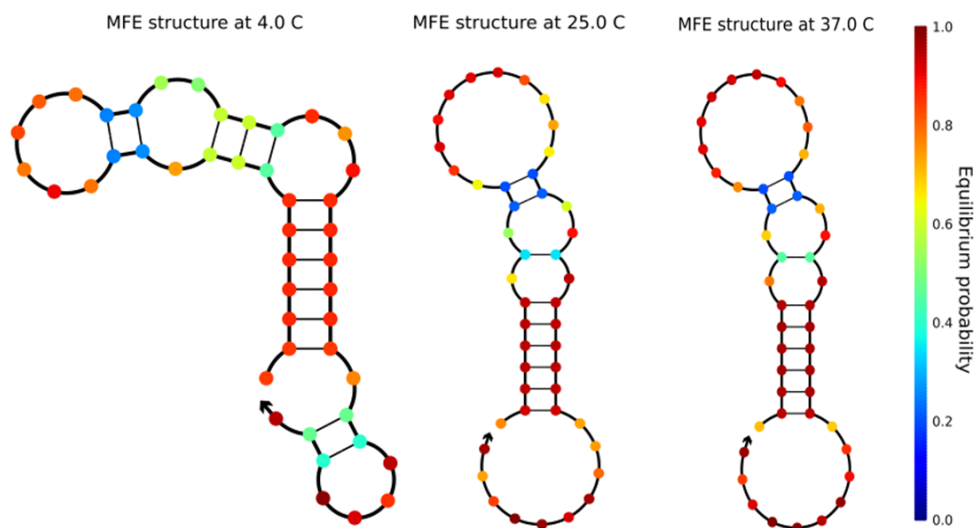


**Figure 3.36** Possible minimum free energy structures of *S. aureus* aptamer (SA-31) at 4°C, 25°C and 37°C drawn by Nupack software.

Same binding studies were performed with *S. Enteritidis* and two aptamers selected in this study. The titration parameters (injection number, initial delay, stirring speed, volume of titration, duration of each titration and spacing between titrations) were standardized with the use of SA-31 and *S. aureus* membrane fractions as mentioned and applied to the titration studies of two *S. Enteritidis* aptamers, crn-1 and crn-2.

In the first experiment, 10  $\mu\text{M}$  of crn-1 and 50  $\mu\text{M}$  of membrane proteins of *S. Enteritidis* were prepared in 1 X PBS (pH 7) which was previously degassed and filter sterilized to remove bubbles and dust particles from buffer. The membrane fractions in syringe were then titrated into crn-1 solutions in sample cell at 4°C. In this study, the aim was to find apparent  $K_a$  of binding reaction between crn-1 and membrane fraction of *S. Enteritidis*. Therefore, titration was performed at 4°C which was the temperature of selection process in SELEX. Raw ITC data and thermalgram of titrating crn-1 with membrane fraction were given at Figure 3.38. According to data and thermodynamic parameters, binding reaction between crn-1 and membrane

fractions of *S. Enteritidis* at 4 °C gave one site binding model with  $n=1$ . The apparent association constant ( $K_a$ ) and  $\Delta G$  between *crn-1* and target at 4°C were calculated as  $1.03 \times 10^6 \text{ M}^{-1}$  and -8535.5 cal/mol, respectively.

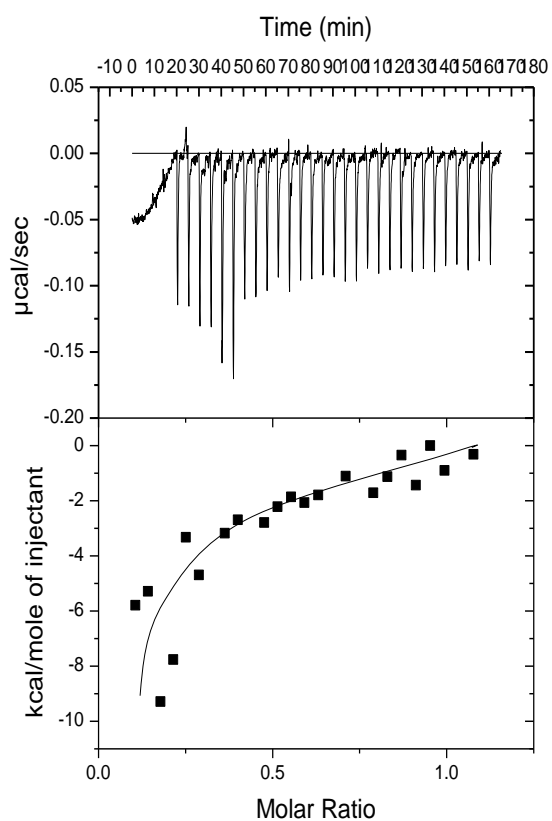


**Figure 3.37** Binding experiment of *crn-1* and *S. Enteritidis* membrane fraction via ITC at 4°C; A) Raw ITC data, B) Thermalgram of titrating *crn-1* with membrane fraction.

In the second experiment, the effect of temperature on binding reaction between crn-1 and membrane fraction of *S. Enteritidis* was evaluated isothermally. As shown in Figure 3.14, the possible minimum free energy structure of crn-1 at 4°C was quite different from the structure at 37°C. Since binding of aptamer to its target is only due to its three dimensional structure, the change in structure due to the change in temperature was expected to affect binding reaction. As shown in Figure 3.39, the titration of membrane fraction at 37°C did not yield a binding reaction between crn-1 and membrane fractions. At this temperature, the structure of crn-1 was not suitable to bind specific region of target in membrane fractions. This result was also confirmed in capillary studies in which these two different temperatures were used in the incubation period of cells in constructed capillaries.

After measuring apparent binding constant of crn-1 and evaluating the effect of temperature on binding reaction between crn-1 and membrane fractions of *S. Enteritidis*, same experiments were performed for binding characterization of crn-2. First experiment was performed with 10 µM of crn-2 and 50 µM of membrane fractions of *S. Enteritidis* for the determination of binding constant at 4 °C. As shown in Figure 3.40 and thermodynamic parameters calculated from these data, apparent  $K_a$  was found as  $3.24 \times 10^{-6} \text{ M}^{-1}$  and change in free energy was -9241cal/mol. The binding reaction between crn-2 and *S. Enteritidis* was one-site binding reaction with the release of heat ( $\Delta H < 0$ ).

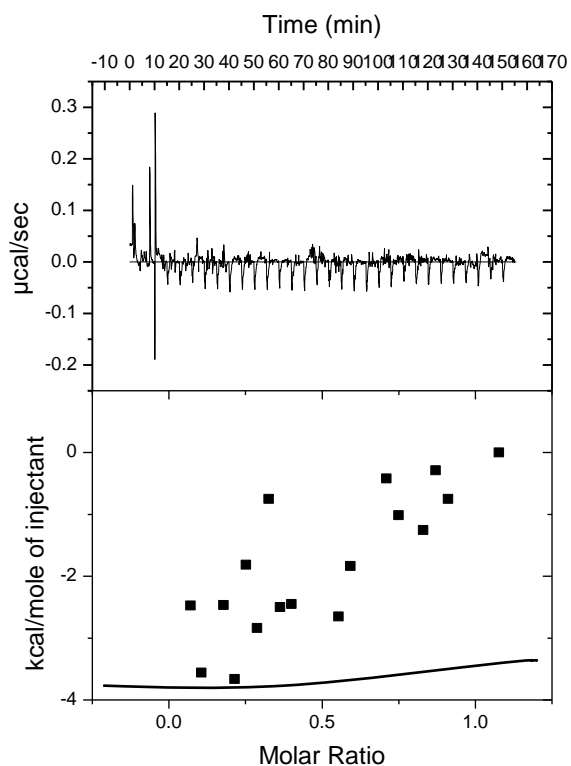


**Figure 3.38** Binding experiment of crn-1 and *S. Enteritidis* membrane fraction via ITC at 37°C; A) Raw ITC data, B) Thermalgram of titrating crn-1 with membrane fraction.

For the evaluation of temperature effect, titration experiment was performed with same parameters as in the first one except temperature in sample cell. In this experiment, temperature of sample cell was set to 37 °C. As observed in Figure 3.15, crn-2 had similar possible free energy structures at 4°C to 37 °C on the contrary to crn-1. Therefore, it was expected from crn-2 to bind its target in membrane fraction at 37°C and thus to have binding profile in titration experiment at 37°C as well.

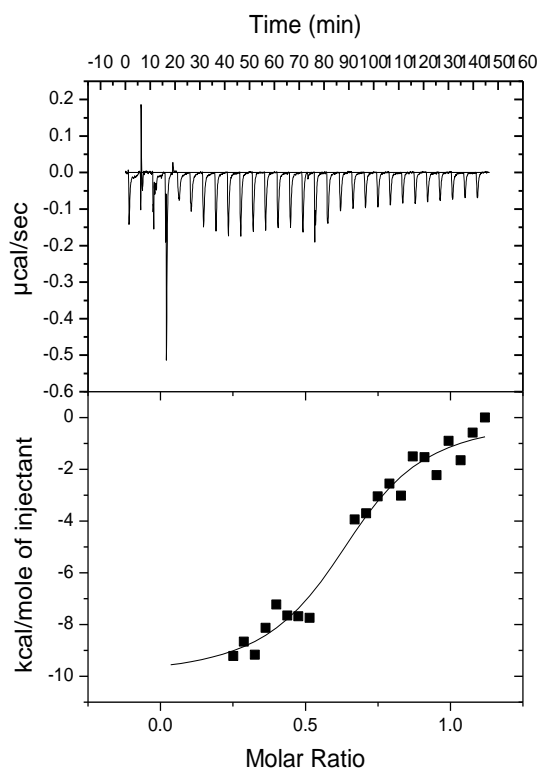


**Figure 3.39** Binding experiment of crn-2 and *S. Enteritidis* membrane fraction via ITC at 4°C; A) Raw ITC data, B) Thermalgram of titrating crn-2 with membrane fraction.

As expected, crn-2 bond to membrane fractions at 37°C with one-site binding model (Figure 3.41). From enthalpy and entropy data, apparent  $K_a$  and change in free energy were calculated as  $5.73 \times 10^6 \text{ M}^{-1}$  and -9617 cal/mol, respectively.

As a summary, two selected aptamers, crn-1 and crn-2, bound to their targets on the outer surface of *S. Enteritidis* with high affinity at  $\mu\text{M}$  level. Thermodynamic parameters of crn-1 and crn-2 were given at Table 3.8. Moreover, crn-2 showed binding at 4°C and 37°C because of its similar structure at these two different temperatures while crn-1 bound to its target only at 4°C.

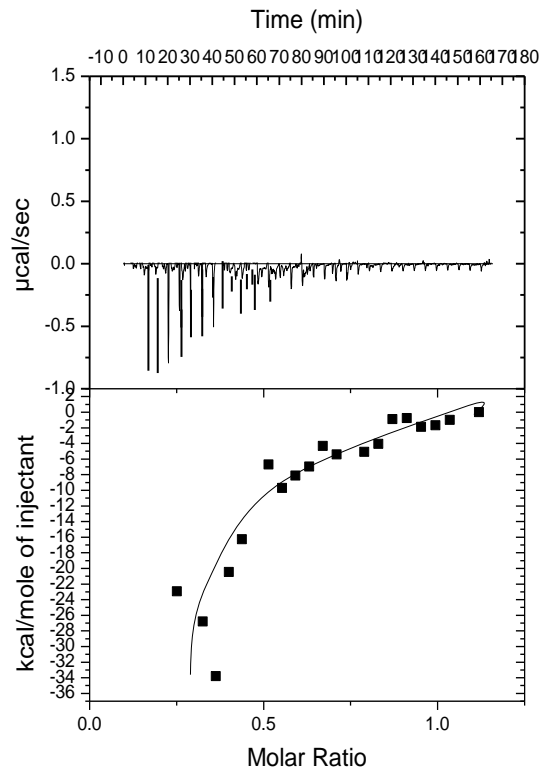


**Figure 3.40** Binding experiment of crn-2 and *S. Enteritidis* membrane fraction via ITC at 37°C; A) Raw ITC data, B) Thermalgram of titrating crn-2 with membrane fraction.

**Table 3.8** Thermodynamic parameters of binding reaction between crn-1/crn-2 and *S. Enteritidis* membrane fractions (in 10 mM of PBS at pH 7) at different temperatures with one site binding model.

Aptamer	Binding reaction	$\Delta H$ (cal/mol)	$\Delta G$ (cal/mol)	$K_a$ ( $M^{-1}$ )	$K_d$ (M)
<b>Crn-1</b>	at 4°C	-9911	-8535.5	$1.03 \times 10^6$	$0.971 \times 10^{-6}$
	at 37°C	-	-	-	-
<b>Crn-2</b>	at 4°C	-10030	--9241	$3.24 \times 10^6$	$0.309 \times 10^{-6}$
	at 37°C	-32650	-9617	$5.73 \times 10^6$	$0.175 \times 10^{-6}$

### 3.2 Construction of Aptamer-Based Sandwich Platform for Bacterial Detection

The two purposes of this study are the selection of DNA aptamer against *S. Enteritidis* and the use of aptamers in the construction of aptamer-based sandwich platform for the detection of *S. Enteritidis*. As explained in the chapter of “Materials and Methods” and shown in Figure 2.1, while the aptamer selection process was performed for *S. Enteritidis*, the construction of platform was optimized with *S. aureus* aptamer SA31 spontaneously. The optimized parameters were, then, used for sandwich type platform constructed with *S. Enteritidis* aptamer for the detection of *S. Enteritidis*.

The construction of sandwich platform with aptamers as receptor and sensing element was composed of four stages in this study; surface coating of standard glass capillary tubes, immobilization of thiol modified aptamer to coated surface, capture of target cell by immobilized aptamer and detection of captured cell by sensing aptamer modified with two different signaling agents. The final figure of aptamer-based sandwich platform was shown in Figure 3.42.

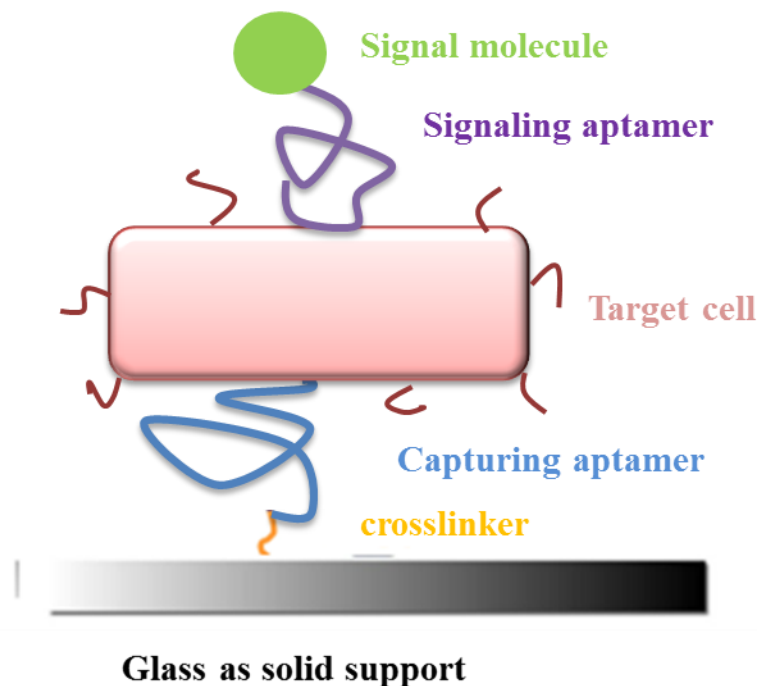


**Figure 3.41** Representative figure of aptamer-based sandwich platform.

Glass capillaries were selected as support materials in this study because they are cheap and easily obtained. In addition, they were able to withstand physical and certain chemical processes and provided a homogeneous surface for immobilization (Basabe-Desmonts *et al.*, 2007).

The construction of the sensing platform began with the surface coating of the support material. The surfaces of glass capillaries were coated with a poly-L-lysine solution. Poly-L-lysine is a cationic polymerized amino acid that changes the negative charges on the glass surface to positive charges. Coating the surface of glass with poly-L-lysine, therefore, makes the surface attractive to negatively charged DNA sequences due to the attraction between opposite charged groups. The negatively charged phosphate groups of DNA were attracted by the positively charged ammonia group of poly-L-lysine.

In literature, there have been many attempts to immobilize DNA molecule to surface of glass which have depended on adsorption (Geng *et al.*, 2009 and Carlson *et al.*, 2014) or covalent attachment of DNA to surface (Zammatteo *et al.*, 2000). The adsorption of DNA to surface is an easy method and it depends on salt concentration and pH of binding solution. A common example in which adsorption is used to attach DNA to support is the spin columns used in DNA isolation technique (Tian *et al.*, 2000). DNA is attached to silica resin in the presence of high salt concentration under low pH and then eluted from silica in the presence of low salt concentration under high pH.

Although adsorption strategy has been applicable for DNA immobilization, covalent attachments of nucleic acids have been widely used in array technologies. Attaching DNA covalently provides certain advantageous over adsorption such as distributing nucleic acids to surface evenly and providing more strong binding between DNA and surface (Zammatteo *et al.*, 2000). Therefore, the covalent attachment was selected as strategy to attach aptamer to surface and for that purpose the surfaces of capillaries were coated with poly-L-lysine solution.

Before coating, capillaries were washed with sodium hydroxide washing solution and then with distilled water to remove dusts, oils and debris which could remain in capillaries after their production. Capillaries were coated with poly-L-lysine solution uniformly by syringe pump at injection speed of 10 $\mu$ L/sec.

The next stage in the construction of platform was the immobilization of thiol modified aptamer to coated surface. For this purpose, a cross linker and a reducing agent were used in capillary platform. N-[ $\epsilon$ -maleimidocaproyloxy] sulfo succinimide ester (Sulfo EMCS) is a water soluble heterobifunctional crosslinker composed of two functional groups; N-hydroxysuccinimide (NHS) ester and maleimide groups. These two groups provide the formation of covalent conjugation between amine and sulfhydryl containing molecules. TCEP (tris (2-carboxyethyl) phosphine) is a reducing agent which breaks disulfide bonds.

In this study, purchased thiol modified aptamers were in oxidized form and before immobilization they were reduced to thiol (-SH) group with the use of TCEP. Sulfo EMCS, in fact, was used for the immobilization of DNA covalently to surface because as a crosslinker it formed more stable bond between aptamer sequences and active group on coated surface. In addition, the formation of undesired crosslinks was eliminated because of its two functional groups that selectively formed covalent bonds (Chrissey *et al.*, 1996). The NHS ester group of crosslinker formed amide bond with N-terminus of lysine on coated surface while maleimide group formed thioether bond with -SH group on modified aptamer.

After immobilization of thiol modified aptamer to surface, next step was the capture of target cell specifically. As mentioned above, poly-L-lysine coating made surface positively charged so that negatively charged DNA molecules were attracted towards surface of platform. However, the presence of positive charges on surface also made cells to attach surface nonspecifically. This nonspecific binding of cell to surface was minimized with the use of surface blocking agents. The immobilization of aptamers to surface was followed by blocking the surface of platform which was not occupied by aptamers. As blocking agents, polyethylene glycol (PEG) and bovine serum albumin (BSA) were applied to surface and their blocking efficiencies were compared in optimization studies.

The last step was the detection of captured cells by sensing aptamers with two signaling strategies. After capturing cells by immobilized aptamers, biotin modified aptamers were applied onto cells to form sandwich type detection assay. Followed by the application of streptavidin conjugated quantum dots, capillaries were visualized under UV light for the detection of *S. Enteritidis* in sandwich type assay. Quantum dots are nanosized fluorescent semiconductor materials made from elements like silicon or germanium, or a compound, such as CdS or CdSe. By changing their size QDs can be visible under ultraviolet (UV), visible and infrared spectra of light (Pietryga *et al.*, 2004; Zhong *et al.* 2003; Zhong *et al.*, 2003; Qu *et al.*, 2002; Kim *et al.*, 2003). In our study, sandwich platforms constructed with QD sensing system

were observed under UV light and signal differences between aptamer-target cell complex and controls were evaluated based on brightness of signal.

In second sensing system, streptavidin conjugated horse radish peroxidase (HRP) were applied to biotin modified aptamers which were previously bound to captured cells. HRP is an enzyme that catalyzes substrate with the presence of hydrogen peroxide as oxidizing agent to produce colored product which can be detected by naked eyes or spectrophotometer. In our study, sandwich platforms constructed with HRP sensing system were observed by the formation of color changes upon addition of substrate of HRP, 3,3',5,5'-tetramethylbenzidine (TMB). The color intensity differences between aptamer-target cell complex and controls were evaluated based on blue color formation.

### **3.2.1 Optimization Studies**

All four stages used in the construction of aptamer based sandwich platform were optimized with *S. aureus* aptamer SA31. Optimization parameters were summarized in the chapter of “Materials and Methods” at Table 2.2.

The first parameter to be optimized was the concentration of thiol modified aptamer which was immobilized to surface. The concentration of biotin modified signaling aptamer was previously determined in Enzyme-Linked Aptamer Assay (ELAA) as 10  $\mu\text{M}$  (Figure 3.25). Among four different concentrations (1, 5, 10 and 20  $\mu\text{M}$ ), the highest absorbance resulted from the enzymatic reaction between HRP and TMB was measured in assay constructed with 10  $\mu\text{M}$  biotin modified SA-31. Therefore, 10  $\mu\text{M}$  of SA-31 was used as signaling agent in sandwich detection platform. In the first capillary experiment, 5  $\mu\text{M}$  of thiol modified SA-31 as capture aptamer was prepared in binding buffer containing Sulfo EMCS (final concentration of 2  $\mu\text{M}$ ) and TCEP (final concentration of 0.1  $\mu\text{M}$ ) and this solution was incubated for 1 hour in capillary previously coated with poly-l-lysine. After incubations in order of capture

SA-31, cells, signal SA-31 and QD conjugated streptavidin and washing steps after each incubation, capillary was visualized under UV light. Beside sandwich platform for *S. aureus* detection, four different control capillaries were prepared as follows.

A; Sandwich platform: 5  $\mu\text{M}$  of thiol-SA-31+  $10^6$  CFU/mL of *S. aureus* + 10  $\mu\text{M}$  of biotin SA-31, strep-QD

B; Control 1:  $10^6$  CFU/mL of *S. aureus* + 10  $\mu\text{M}$  of biotin SA-31, strep-QD

C; Control 2: 5  $\mu\text{M}$  of thiol-SA-31+  $10^6$  CFU/mL of *S. Enteritidis* + 10  $\mu\text{M}$  of biotin SA-31, strep-QD

D; Control 3: 5  $\mu\text{M}$  of thiol-SA-31+  $10^6$  CFU/mL of *E. coli* + 10  $\mu\text{M}$  of biotin SA-31, strep-QD

E; Control 4: 5  $\mu\text{M}$  of thiol-SA-31+ 10  $\mu\text{M}$  of biotin SA-31, strep-QD

In the first control, *S. aureus* was incubated in poly-l-lysine coated surface without immobilized aptamer in order to control the occurrence of unspecific binding of cells to surface. The second and third control capillaries contained non-target cells of SA-31, *S. Enteritidis* and *E. coli*, thus, specificity of SA-31 to *S. aureus* was evaluated. The self-dimer formation between capture and signal SA-31 was controlled in the last control capillary. As shown in Figure 3.43, there were no significant signals in all five capillaries meaning that no specific capturing of cells occurred between capture and signal aptamer in a sandwich manner.

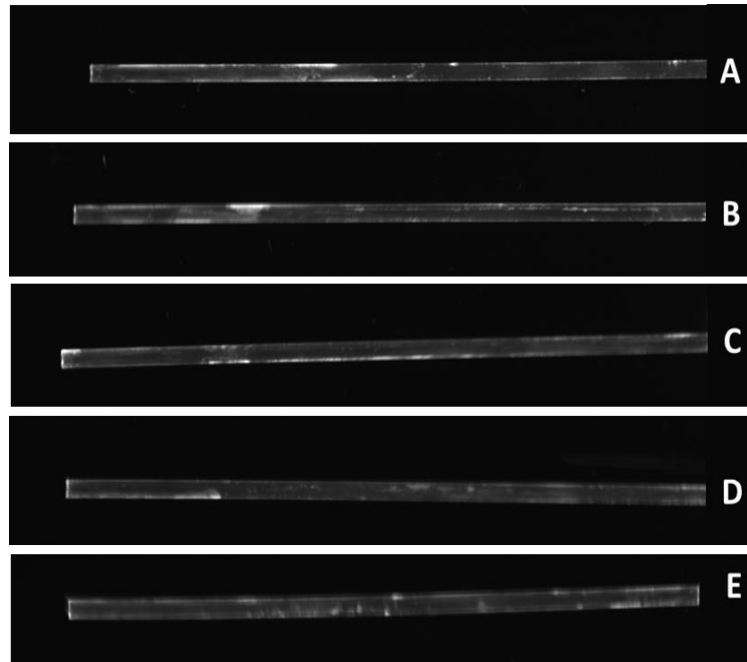


**Figure 3.42** Capillary images of *S. aureus* detection platforms with 5  $\mu\text{M}$  of SA-31 under UV light; A) Sandwich system, B) Unspecific binding control (Control 1) C) Specificity control with *S. Enteritidis* (Control 2), D) Specificity control with *E. coli* (Control 3), E) Sel-dimer control (Control 4).

This result could be due to lower amount of capture aptamer (5  $\mu\text{M}$ ), shorter incubation time (1 hour) or harsh washing steps (50 $\mu\text{L}/\text{sec}$ ). Therefore, the concentration of capture SA-31 was increased to 10  $\mu\text{M}$  in the next study. Sandwich and control capillaries were prepared as follows.

A; Sandwich platform: 10  $\mu\text{M}$  of thiol-SA-31+ 10<sup>6</sup> CFU/mL of *S. aureus* + 10  $\mu\text{M}$  of biotin SA-31, strep-QD

B; Control 1:10<sup>6</sup> CFU/mL of *S. aureus* + 10  $\mu\text{M}$  of biotin SA-31, strep-QD

C; Control 2: 10  $\mu\text{M}$  of thiol-SA-31+ 10<sup>6</sup> CFU/mL of *S. Enteritidis* + 10  $\mu\text{M}$  of biotin SA-31, strep-QD

D; Control 3: 10  $\mu\text{M}$  of thiol-SA-31 +  $10^6$  CFU/mL of *E. coli* + 10  $\mu\text{M}$  of biotin SA-31, strep-QD

E; Control 4: 10  $\mu\text{M}$  of thiol-SA-31 + 10  $\mu\text{M}$  of biotin SA-31, strep-QD

In addition to the increase in capture aptamer concentration, incubation time was changed for proper capturing step. Thiol modified SA-31 was first incubated in tube for 30 min with TCEP and sulfo-EMCS for the reduction of disulfide bonds and formation of thioether bond with  $-\text{SH}$  group on modified aptamer and maleimide group of Sulfo EMCS. Then, aptamer solution was incubated further in capillary for 1 hour to immobilize capture SA-31 via the formation of amide bond with N-terminus of lysine on surface and NHS ester group of Sulfo EMCS.

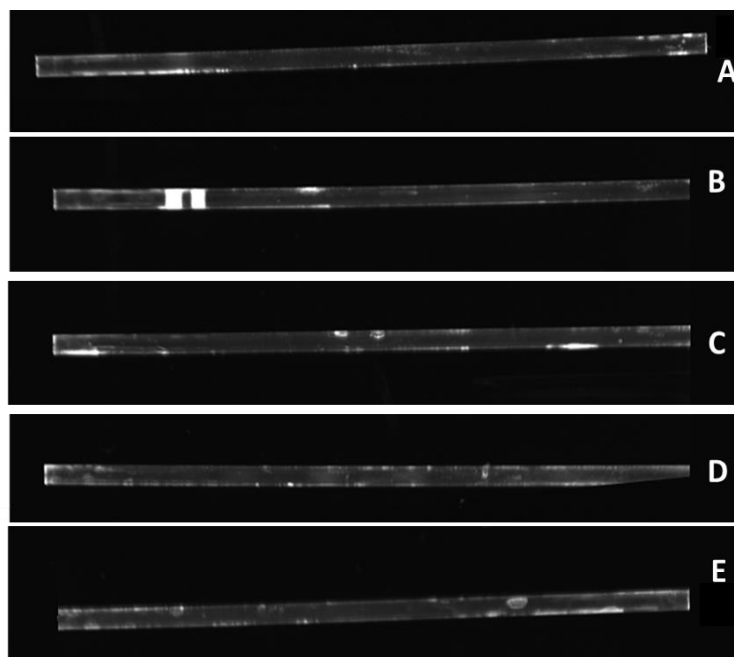


**Figure 3.43** Capillary images of *S. aureus* detection platforms with 10  $\mu$  of SA-31 under UV light; A) Sandwich system, B) Unspecific binding control (Control 1) C) Specificity control with *S. Enteritidis* (Control 2), D) Specificity control with *E. coli* (Control 3), E) Sel-dimer control (Control 4).

As shown in Figure 3.44, slight increases in signals of capillaries were observed after the use of 10  $\mu$ M capture SA-31 and the extension of incubation time from 1 hour to 1 hour 30 min. Nevertheless, signals coming from capillaries were not significant and they were approximately all same so that sandwich detection platform and control capillaries were not discriminated.

However, there were relatively intensive signals coming from the left end of capillaries (Figure 3.44). In the experiments, all solutions were applied to capillaries from right end and poured off from the left end. Thus, the left ends were the outfalls of solutions. One possible explanation of signals from left ends was that captured cells were removed from capillaries and some of them could accumulate at the left

end due to the harsh washing steps. As a result, harsh washing could lead to loss of cells and thus signals from capillaries.

In order to eliminate loss of cells from surface by harsh washing, capillaries were washed with syringe pump at lower speed (10 $\mu$ L/sec). In addition, surface blocking stage was introduced into the construction experiment of sandwich platform. Since cells could bind unspecifically to the poly-l-lysine surface and washing at lower speed could encourage these nonspecific bindings, the surface of poly-l-lysine coated capillary was blocked with blocking agents after immobilization of capture aptamer to surface. Polyethylene glycol (PEG) is water soluble and non-toxic polyether compound and it has been mainly used to minimize protein adsorption to sensing platform (Liu *et al.*, 2013). Bovine serum albumin (BSA) is a serum albumin protein which is one of the most common blocking agents used in ELISA (Xiao and Isaacs, 2012). In our study, PEG and BSA were used as blocking agents to minimize binding of cells unspecifically to surface. Sandwich and control capillaries were prepared as follows.

A; Sandwich platform: 10  $\mu$ M of thiol-SA-31+ 10<sup>6</sup> CFU/mL of *S. aureus* + 10  $\mu$ M of biotin SA-31, strep-QD

B; Control 1:10<sup>6</sup> CFU/mL of *S. aureus* + 10  $\mu$ M of biotin SA-31, strep-QD

C; Control 2: 10  $\mu$ M of thiol-SA-31+ 10<sup>6</sup> CFU/mL of *S. Enteritidis* + 10  $\mu$ M of biotin SA-31, strep-QD

D; Control 3:10  $\mu$ M of thiol-SA-31+ 10<sup>6</sup> CFU/mL of *E. coli* + 10  $\mu$ M of biotin SA-31, strep-QD

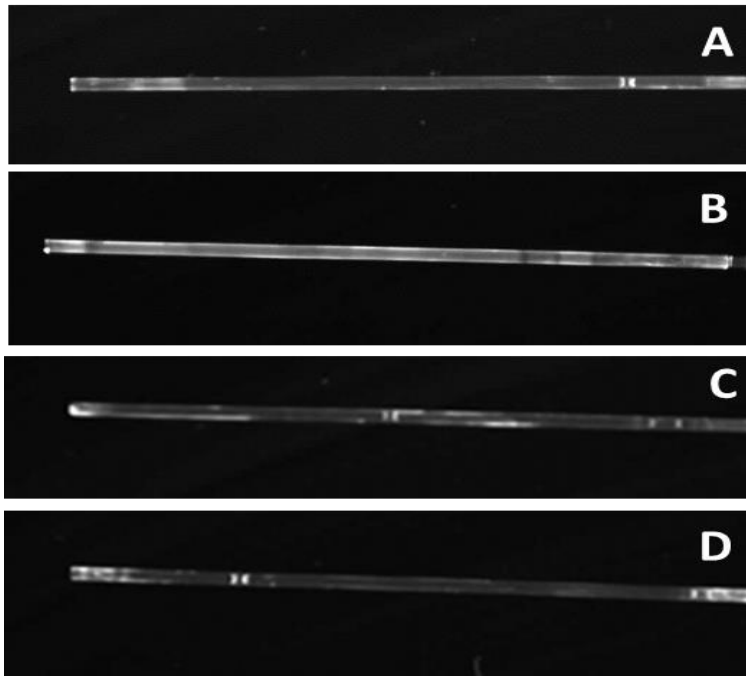
All capillaries were washed at lower speed and surfaces of them were blocked with PEG and 2% of BSA to occupy nonspecific binding regions.

Figure 3.45 represented images of capillaries whose surfaces were blocked with the use of PEG. As observed, the signals coming from sandwich platform increased as compared to those of specificity control capillaries. The specific binding of SA-31 to

*S. aureus* in sandwich platform led to higher signal production upon binding of signaling SA-31. Since *E. coli* and *S. Enteritidis* were not target for SA-31 to bind, control capillaries containing these cells did not give significant signals as compared with signal of sandwich platform.

However, when signals from sandwich platform and unspecific binding control capillary were compared, it was observed that signals were higher in control capillary (B in Figure 3.45). The non specific binding of *S. aureus* to surface was not minimized effectively with PEG blocking step. Poly-l-lysine coated surface without capture aptamer provided more binding side for *S. aureus* although PEG was used as blocking agent. As a result, PEG was evaluated as ineffective blocking agent in this study and another capillary construction study was performed with BSA as blocker.

Capillaries were constructed same with previous study except 2% of BSA was applied in surface blocking stage. The result was represented in Figure 3.46. The specificity control capillaries (C and D) did not give signals as expected. SA-31 selected against *S. aureus* showed specificity meaning that it did not bind to non target cells. Also, the binding of *S. aureus* to coated surface without capture SA-31 was lower than specific binding of it to capture SA-31 immobilized to surface. When signals were compared, it was obviously observed that sandwich platform for *S. aureus* was effectively constructed with lower unspecific binding to of cell to surface. BSA at 2% provided an environment where unspecific binding of target cells was minimized. As a result, it was concluded that BSA was an effective surface blocking agent in our study.



**Figure 3.44** Capillary images of *S. aureus* detection platforms blocked with PEG under UV light; A) Sandwich system, B) Unspecific binding control (Control 1) C) Specificity control with *S. Enteritidis* (Control 2), D) Specificity control with *E. coli* (Control 3).

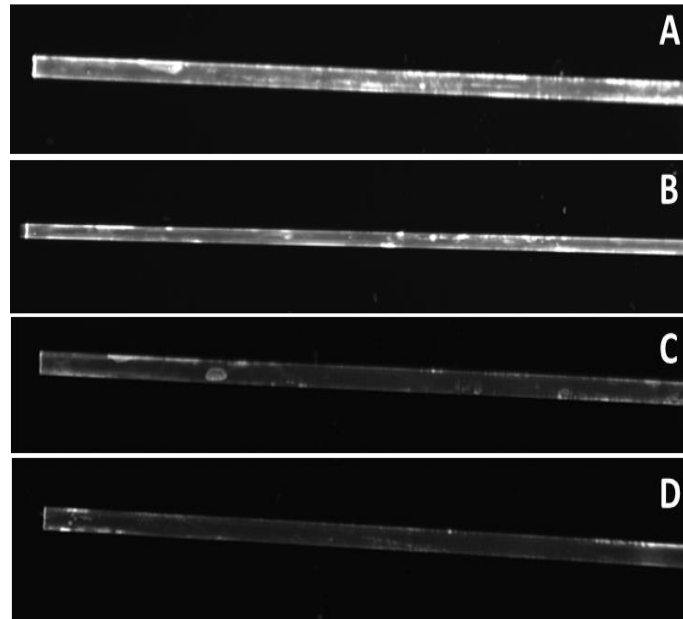


**Figure 3.45** Capillary images of *S. aureus* detection platforms blocked with 2% of BSA under UV light; A) Sandwich system, B) Unspecific binding control (Control 1) C) Specificity control with *S. Enteritidis* (Control 2), D) Specificity control with *E. coli* (Control 3).

For further elimination of unspecific binding of target cell to surface, the concentration of BSA was increased to 5% in the next optimization study. As shown Figure 3.47, signals from unspecificity control capillary (B) was significantly lower than signals from sandwich platform. The increase in concentration of BSA from 2% to 5% further minimized unspecific binding of *S.aureus* to coated surface. Therefore, sandwich platform constructed with specific aptamer for *S. aureus* detection was clearly differentiated from control capillaries by giving highest signal.

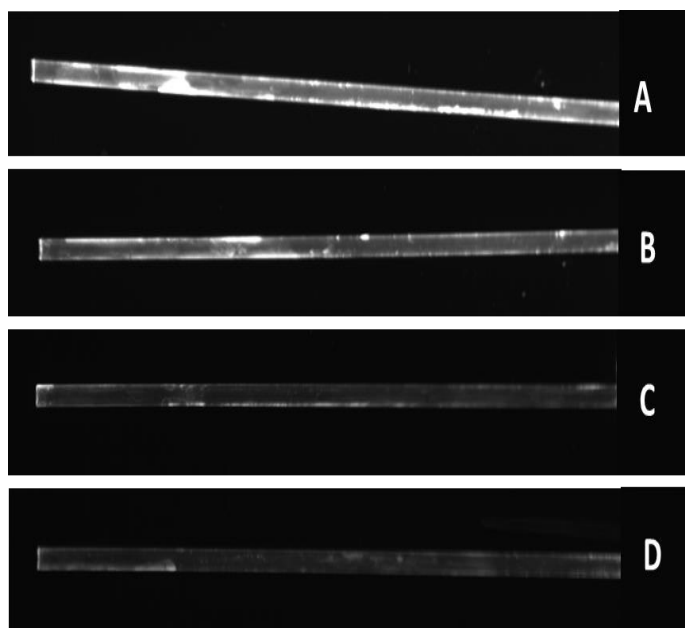


**Figure 3.46** Capillary images of *S. aureus* detection platforms blocked with 5% of BSA under UV light; A) Sandwich system, B) Unspecific binding control (Control 1) C) Specificity control with *S. Enteritidis* (Control 2), D) Specificity control with *E. coli* (Control 3).

As a result of all these studies, optimum parameters for efficient detection platform were found as; **10  $\mu$ M of capture aptamer, 1hour 30 min incubation of capture aptamer, 10  $\mu$ L/sec of injection speed of washing solutions and 5% BSA as blocking agent.**

These optimum parameters were used also for the construction of sandwich platform with the HRP conjugated streptavidin signaling strategy.

In this second signaling strategy, sandwich platform and control capillaries were constructed same with previous capillary studies, however, instead of QD conjugated streptavidin signal molecules, HRP conjugated streptavidin signaling molecules were used. Capillaries were constructed as follows.

A; Sandwich platform: 10  $\mu\text{M}$  of thiol-SA-31+  $10^6$  CFU/mL of *S. aureus* + 10  $\mu\text{M}$  of biotin SA-31, strep-HRP, TMB

B; Control 1:  $10^6$  CFU/mL of *S. aureus* + 10  $\mu\text{M}$  of biotin SA-31, strep-HRP, TMB

C; Control 2: 10  $\mu\text{M}$  of thiol-SA-31+  $10^6$  CFU/mL of *S. Enteritidis* + 10  $\mu\text{M}$  of biotin SA-31, strep-HRP, TMB

D; Control 3: 10  $\mu\text{M}$  of thiol-SA-31+  $10^6$  CFU/mL of *E. coli* + 10  $\mu\text{M}$  of biotin SA-31, strep-HRP, TMB

E; Control 4: 10  $\mu\text{M}$  of thiol-SA-31+ 10  $\mu\text{M}$  of biotin SA-31, strep-HRP, TMB

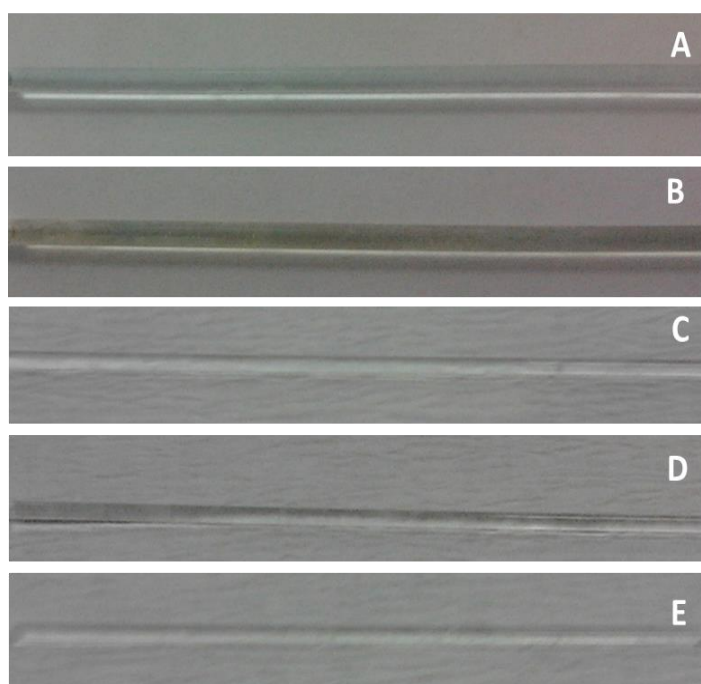


**Figure 3.47** Capillary images of *S. aureus* detection platforms with HRP-strep signaling strategy; A) Sandwich system, B) Unspecific binding control (Control 1) C) Specificity control with *S. Enteritidis* (Control 2), D) Specificity control with *E. coli* (Control 3).

Figure 3.48 represented image of capillaries constructed with HRP-streptavidin signaling strategy and previously optimized parameters. The formation of blue color in sandwich platform indicated the capture of *S. aureus* between surface immobilized SA-31 and biotin modified SA-31 with enzymatic reaction of HRP and TMB. Besides, the unspecific binding control capillary was observed as a slight blue color as compared with sandwich one. The specificity control capillaries containing *S. Enteritidis* and *E. coli* did not produce signal due to the fact that SA-31 was specific for *S. aureus*. Since signals from specific binding of *S. aureus* to its aptamer and that from unspecific binding of cell to surface were very low to be observed with naked eyes, signal amplification strategies were studied in the next experiment. The idea of signal amplification was raised to increase signals for providing clear and easy observation of specific detection of bacteria with naked eyes.

### **3.2.2 Signal Amplification**

One of the major goals in our study was to develop aptamer based sandwich platform for the detection of *S. Enteritidis* with high specificity and sensitivity. The specificity of constructed platform was achieved via the use of aptamer selected against *S. Enteritidis*. For the sensitivity of detection platform two signal amplification strategies were used in our study.

The development of high sensitivity in biosensor technology has required different strategies, different amplification platforms and amplification processes. For example, metal nanoparticles with specific electronic, optical, photophysical and catalytic properties have been effective in signal amplification for detection platform in biosensing processes (Ju, 2012). In literature, nanomaterials based on carbon have been used for the improvement of conductivity to speed up electron transfer (Ju, 2012) or nanomaterials like quantum dots have been used as tag molecules in electrochemiluminescence analysis (Li *et al.*, 2010). The number of QDs on polymer was increased as a result; signals gathered from biosensor have been enhanced.

Therefore, targets at low amounts can be detected with high sensitivity. In the first strategies, ultra-TMB was used as a chromogenic substrate for horseradish peroxidase. It was soluble substrate that yielded a blue color formation when it was oxidized by horseradish peroxidase. The blue color formation was occurred due to the oxygen radical productions from hydrogen peroxide found in an aqueous buffer formulation of soluble ultra-TMB. When compared with standard TMB, ultra-TMB produced higher signal/noise ratio and increased sensitivity of reaction in which it was used.

As shown in Figure 3.49, the signals from sandwich platform increased so that it could be observed easily without any need for specific instrument. As compared with normal TMB (Figure 3.48), the increase in the color intensity upon enzymatic reaction between HRP and ultra-TMB was significant. Beside sandwich platform, signals from unspecificity control capillary also increased. *S. aureus* bond to poly-l-lysine coated surface nonspecifically and labeled with signaling SA-31. After the addition of ultra-TMB, enzymatic reaction generated blue color formation with higher color intensity. However, as the color intensities of sandwich assay and unspecificity control capillary compared, obviously it was higher in sandwich platform. In the specificity control capillary containing *S. Enteritidis*, there were weak signals which could be due to the presence of strep-HRP in capillary after washing step. Since *S. Enteritidis* was not target for SA-31 to bind, biotin modified SA-31 and thus streptavidin conjugated HRP should be removed from control capillaries with washing step. Improper removal of strep-HRP in this capillary, therefore, yielded a slight blue color formation. In other specificity control capillary containing *E.coli* and self-dimer control capillary, there were no signal productions as expected.

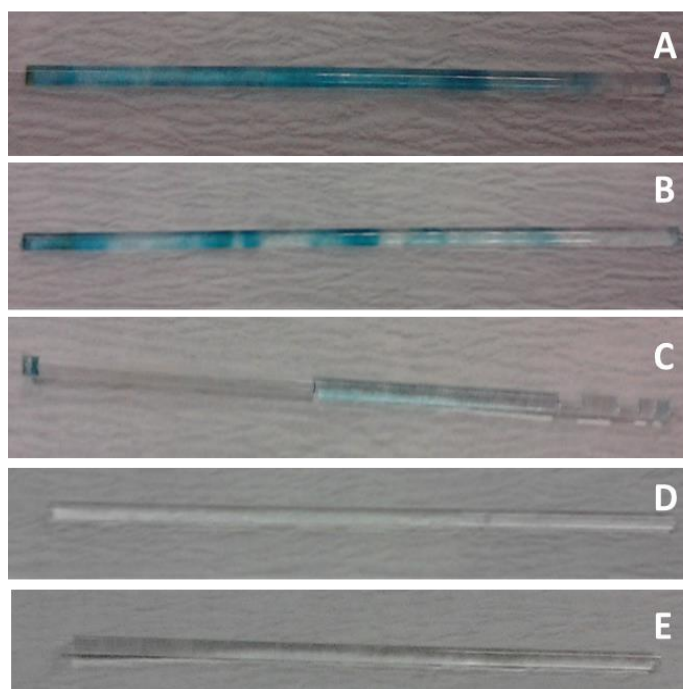


**Figure 3.48** Capillary images of *S. aureus* detection platforms constructed with strep-HRP and ultra-TMB; A) Sandwich system, B) Unspecific binding control (Control 1) C) Specificity control with *S. Enteritidis* (Control 2), D) Specificity control with *E. coli* (Control 3), E) Sel-dimer control (Control 4).

In the second signal amplification strategies, we used streptavidin poly-HRP conjugates (SA-PolyHRP40) with ultra-TMB instead of streptavidin-HRP conjugates which were used in optimization studies. This conjugate was biotin binding protein conjugated with polymers of horseradish peroxidase. Like standard streptavidin HRP conjugates, this complex performed enzymatic reaction between horseradish peroxidase and its substrate TMB. However, unlike standard conjugates the estimated average number of HRP monomer molecules in streptavidin poly-HRP was 200 (40 X 5) as shown in Figure 3.50. Since higher number of enzyme molecules were found on streptavidin bounded biotin molecule more reactions were expected to take place when substrate of enzyme was added to assay. As a result,

signals were amplified upon binding between streptavidin poly-HRP complex and biotin modified aptamer previously bound to target cell was occurred. This signal amplification also brought lower background signal in addition to higher sensitivity to the detection platform.

As shown in Figure 3.51, sandwich platform which was constructed with capture and signal *S.aureus* aptamer and streptavidin conjugated poly HRP with ultra-TMB as signaling strategy showed clear blue color formation with significantly higher color intensity. The unspecific binding of cell to coated surface without capture aptamer was minimized with surface blocking and slower washing step and thus, relatively lower signals were produced at unspecific binding control capillary when compared with signals of sandwich platform.

As a result, aptamer-based sandwich type capillary detection platforms with two different signaling strategies were optimized with the use of *S.aureus* aptamer. These optimum parameters were, then, applied to the construction of detection platform for *S. Enteritidis* with its aptamers selected in this study.

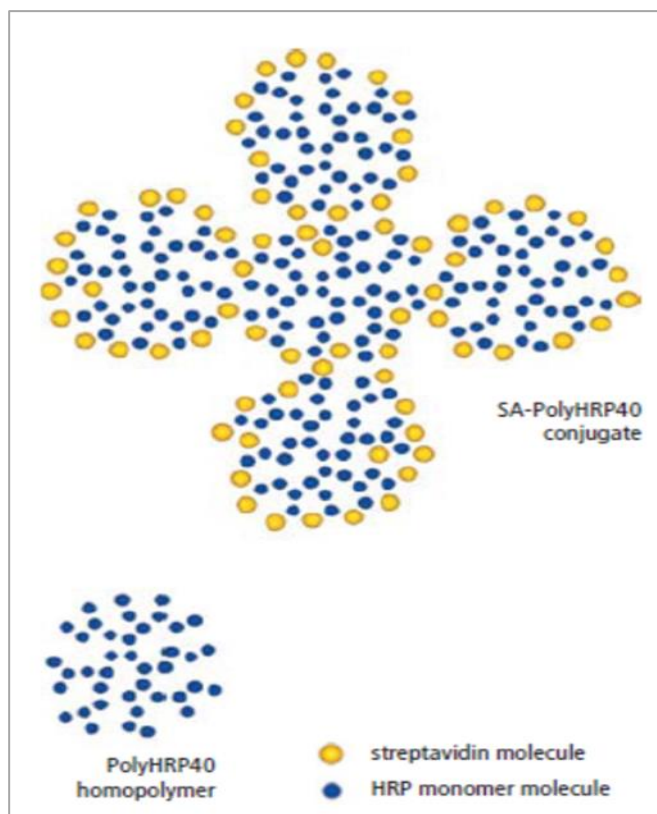


**Figure 3.49** Representative figure of streptavidin Poly-HRP conjugates.

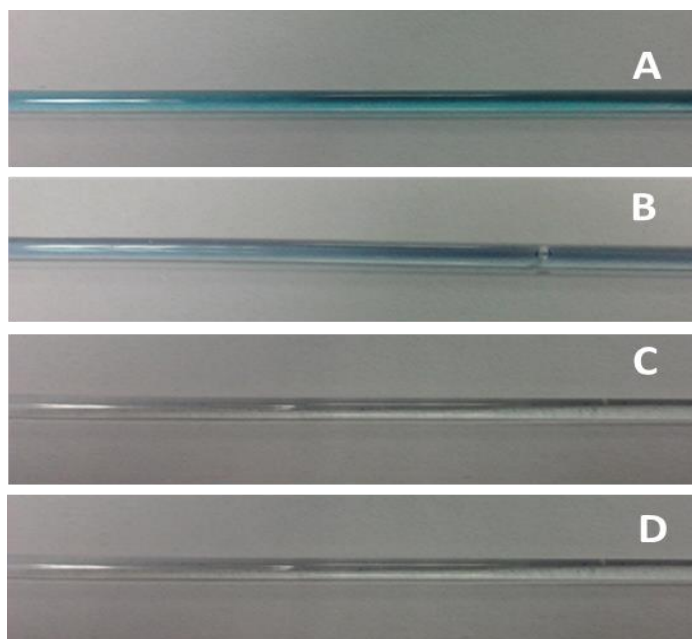


**Figure 3.50** Capillary images of *S. aureus* detection platforms constructed with SA-PolyHRP40 and ultra-TMB; A) Sandwich system, B) Unspecific binding control (Control 1) C) Specificity control with *S. Enteritidis* (Control 2), D) Specificity control with *E. coli* (Control 3).

### 3.2.3 Detection Platforms for *S. Enteritidis*

Aptamer-based sandwich platforms for the detection of *S. Enteritidis* were constructed with crn-1 and crn-2 as capturing and signaling agents in two signaling strategies, QD and HRP. The incubation temperature of *S. Enteritidis* in capillaries was 4°C which was aptamer selection temperature in Cell-SELEX study. Sandwich and control capillaries were prepared for QD signaling as follows.

A; Sandwich platform: 10  $\mu$ M of thiol-crn1/crn-2 +  $10^6$  CFU/mL of *S. Enteritidis* + 10  $\mu$ M of biotin crn1/crn2, strep-QD

B; Control 1:  $10^6$  CFU/mL of *S. Enteritidis*+ 10  $\mu$ M of biotin crn1/crn-2, strep-QD

C; Control 2: 10  $\mu\text{M}$  of thiol-crnl/crn-2+  $10^6$  CFU/mL of *S. aureus* + 10  $\mu\text{M}$  of biotin-crnl/crn-2, strep-QD

D; Control 3:10  $\mu\text{M}$  of thiol-crnl/crn-2 +  $10^6$  CFU/mL of *E. coli* + 10  $\mu\text{M}$  of biotin biotin-crnl/crn-2, strep-QD

For HRP signaling, capillaries were constructed as;

A; Sandwich platform: 10  $\mu\text{M}$  of thiol-crnl/crn-2 +  $10^6$  CFU/mL of *S. Enteritidis* + 10  $\mu\text{M}$  of biotin crnl/crn2, strep-HRP, TMB

B; Control 1: $10^6$  CFU/mL of *S. Enteritidis*+ 10  $\mu\text{M}$  of biotin crnl/crn-2, strep-HRP, TMB

C; Control 2: 10  $\mu\text{M}$  of thiol-crnl/crn-2+  $10^6$  CFU/mL of *S. aureus* + 10  $\mu\text{M}$  of biotin-crnl/crn-2, strep-HRP, TMB

D; Control 3:10  $\mu\text{M}$  of thiol-crnl/crn-2 +  $10^6$  CFU/mL of *E. coli* + 10  $\mu\text{M}$  of biotin biotin-crnl/crn-2, strep-HRP, TMB

The results of capillaries upon capturing and labeling target and control cells with QD signaling strategy were shown in Figure 3.52 for crn-1 and 3.53 for crn-2 while results with HRP signaling strategy were shown in Figure 3.54 for crn-1 and 3.55 for crn-2.

From all results, it was clearly observed that platforms constructed with these two aptamers showed high specificity for the detection of *S. Enteritidis* at 4°C. Crn-1 and crn-2 did not have affinity towards control cells, *E.coli* and *S. aureus*, thus, they made detection platform highly specific for their target *S. Enteritidis*. Although unspecific bindings of *S. Enteritidis* to coated surface without aptamers were observed, they were minimized with surface blocking and slower washing speed as in the platform of *S. aureus*. When signals and color intensities of sandwich platforms of *S. Enteritidis* and unspecific binding control capillaries were compared, obvious differences were observed clearly.

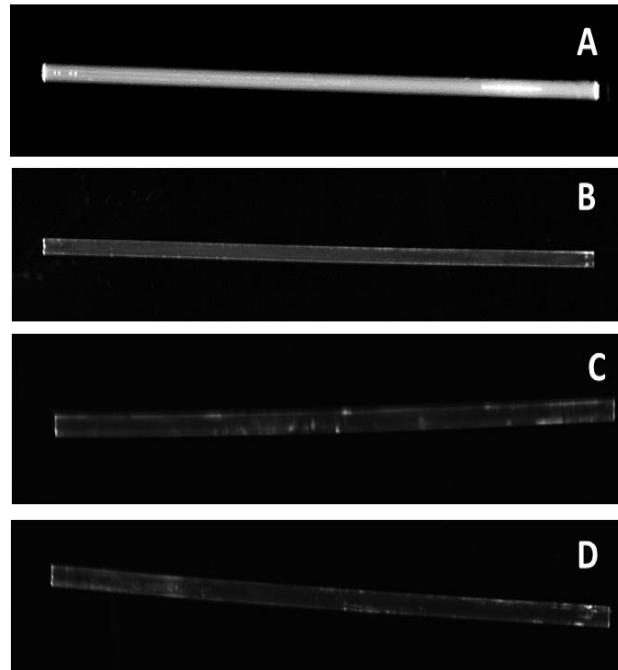


**Figure 3.51** Capillary images of crn-1 based *S. Enteritidis* detection platforms with QD signaling strategy; A) Sandwich system with crn-1, B) Unspecific binding control (Control 1) C) Specificity control with *S. aureus* (Control 2), D) Specificity control with *E. coli* (Control 3)

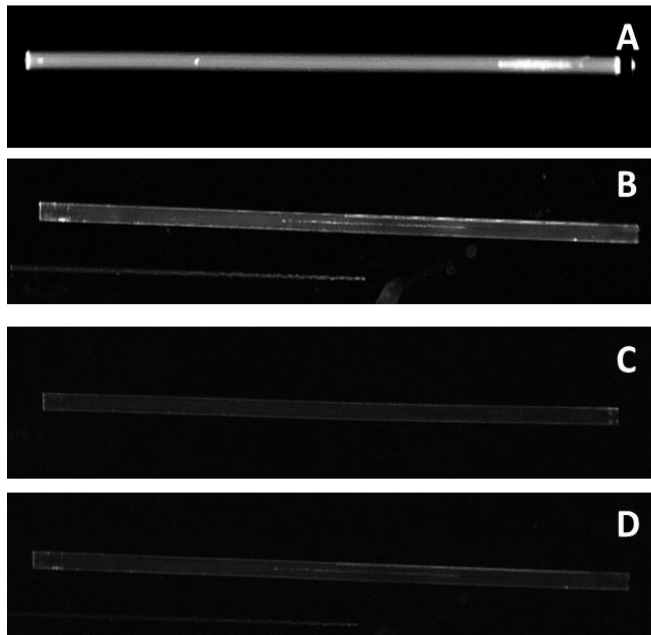


**Figure 3.52** Capillary images of crn-2 based *S. Enteritidis* detection platforms with QD signaling strategy; A) Sandwich system with crn-2, B) Unspecific binding control (Control 1) C) Specificity control with *S. aureus* (Control 2), D) Specificity control with *E. coli* (Control 3)

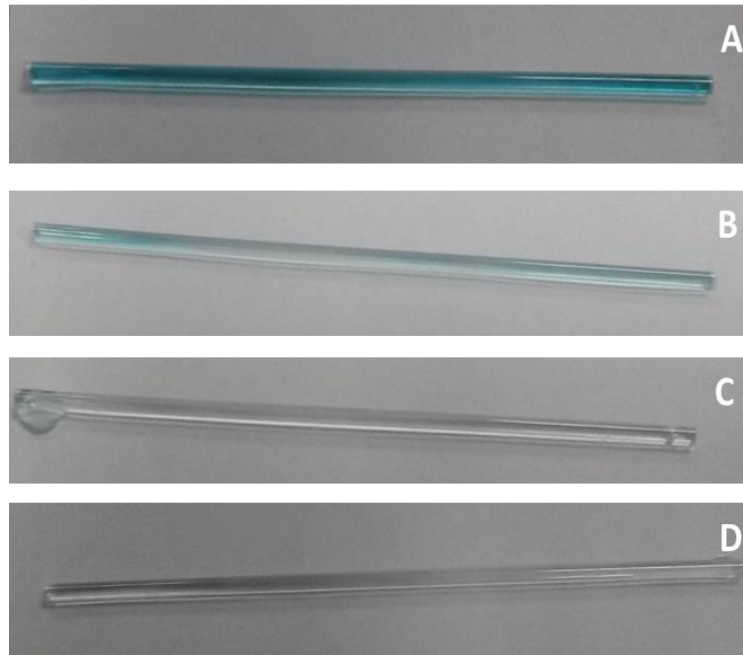


**Figure 3.53** Capillary images of crn-1 based *S. Enteritidis* detection platforms with HRP signaling strategy; A) Sandwich system with crn-1, B) Unspecific binding control (Control 1) C) Specificity control with *S. aureus* (Control 2), D) Specificity control with *E. coli* (Control 3).

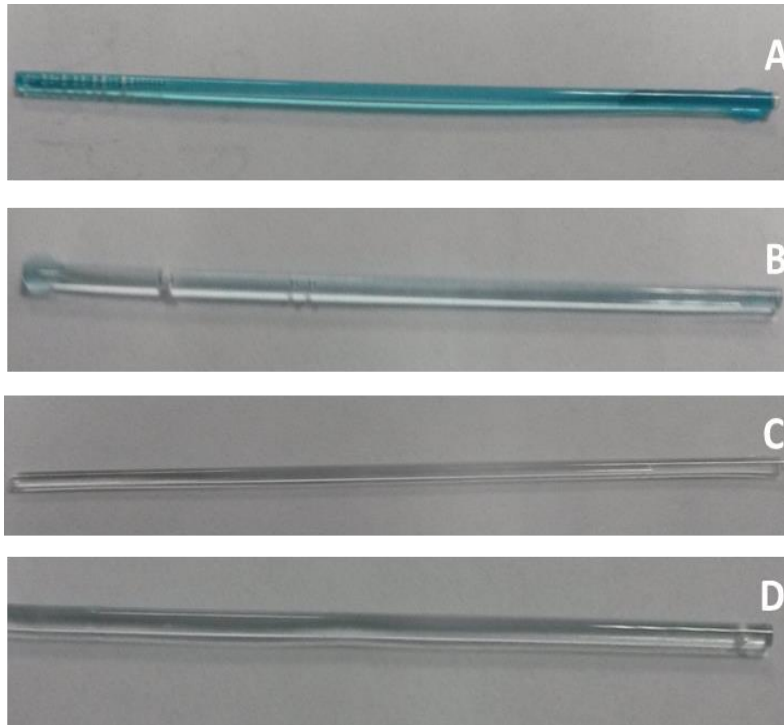


**Figure 3.54** Capillary images of crn-2 based *S. Enteritidis* detection platforms with HRP signaling strategy; A) Sandwich system with crn-2, B) Unspecific binding control (Control 1) C) Specificity control with *S. aureus* (Control 2), D) Specificity control with *E. coli* (Control 3).

After the construction of crn-1 and crn-2 based sandwich type capillary platform for *S. Enteritidis*, the detection limit of these detection platforms were evaluated. Capillaries were immobilized with capturing aptamers which were the thiol modified crn-1 and crn2 and then, responses of these platforms againsts different amount of target cells were observed with both QD and HRP signaling strategies. Sandwich platforms and control capillaries were prepared as follows.

A; Sandwich platform 1: 10  $\mu\text{M}$  of thiol-crn-1/crn-2+  $10^6$  CFU/mL of *S. Enteritidis* + 10  $\mu\text{M}$  of biotin crn-1/crn-2, strep-QD

B; Sandwich platform 2: 10  $\mu$ M of thiol-crn-1/crn-2+  $10^5$  CFU/mL of *S. Enteritidis* + 10  $\mu$ M of biotin crn1/crn-2, strep-QD

C; Sandwich platform 3: 10  $\mu$ M of thiol-crn-1/crn-2+  $10^4$  CFU/mL of *S. Enteritidis* + 10  $\mu$ M of biotin crn-1/crn-2, strep-QD

D; Sandwich platform 4: 10  $\mu$ M of thiol-crn-1/crn-2+  $10^3$  CFU/mL of *S. Enteritidis* + 10  $\mu$ M of biotin crn-1/crn-2, strep-QD

F; Sandwich platform 4: 10  $\mu$ M of thiol-crn-1/crn-2+  $10^2$  CFU/mL of *S. Enteritidis* + 10  $\mu$ M of biotin crn-1/crn-2, strep-QD

E; Control:  $10^6$  CFU/mL of *S. Enteritidis*+ 10  $\mu$ M of biotin crn-1/crn-2, strep-QD

As shown in Figure 3.56, in the platforms constructed with QD signaling strategy, there were no significant differences in signals belonging to capillaries incubated with  $10^6$ ,  $10^5$  and  $10^4$  CFU/mL of *S. Enteritidis*. The signals of capillaries with  $10^3$  CFU/mL of cell was lower than signals of those capillaries. The capillaries containing  $10^2$  CFU/mL of *S. Enteritidis* responded similarly with unspecificity binding control capillary containing  $10^6$  CFU/mL of *S. Enteritidis* in terms of their signals. Therefore, since the lowest amount of target cell that could be observed easily and discriminated from control capillary clearly was  $10^3$  CFU/mL, limit of detection (LOD) of both crn-1 and crn-2 based detection platform was  $10^3$  CFU/mL in QD signaling strategy.

For HRP signaling strategy similar capillaries were constructed which were given as follows.

A; Sandwich platform 1: 10  $\mu$ M of thiol-crn-1/crn-2+  $10^6$  CFU/mL of *S. Enteritidis* + 10  $\mu$ M of biotin crn-1/crn-2, strep-HRP, TMB

B; Sandwich platform 2: 10  $\mu$ M of thiol-crn-1/crn-2+  $10^5$  CFU/mL of *S. Enteritidis* + 10  $\mu$ M of biotin crn1/crn-2, strep-HRP, TMB

C; Sandwich platform 3: 10  $\mu$ M of thiol-cr<sub>n</sub>-1/cr<sub>n</sub>-2+ 10<sup>4</sup> CFU/mL of *S. Enteritidis* + 10  $\mu$ M of biotin cr<sub>n</sub>-1/cr<sub>n</sub>-2, strep-HRP, TMB

D; Sandwich platform 4: 10  $\mu$ M of thiol-cr<sub>n</sub>-1/cr<sub>n</sub>-2+ 10<sup>3</sup> CFU/mL of *S. Enteritidis* + 10  $\mu$ M of biotin cr<sub>n</sub>-1/cr<sub>n</sub>-2, strep-HRP, TMB

F; Sandwich platform 4: 10  $\mu$ M of thiol-cr<sub>n</sub>-1/cr<sub>n</sub>-2+ 10<sup>2</sup> CFU/mL of *S. Enteritidis* + 10  $\mu$ M of biotin cr<sub>n</sub>-1/cr<sub>n</sub>-2, strep-HRP, TMB

E; Control: 10<sup>6</sup> CFU/mL of *S. Enteritidis*+ 10  $\mu$ M of biotin cr<sub>n</sub>-1/cr<sub>n</sub>-2, strep-HRP, TMB

Similar results were obtained from the platforms constructed with HRP signaling strategy as QD signaling strategy. Figure 3.57 showed capillaries containing different amounts of target cell labelled with HRP. At lower cell amount, the reactions between HRP and TMB yielded greenish-blue color and the green color intensities decreased gradually as the amount of cells incubated in capillaries were increased from 10<sup>3</sup> to 10<sup>6</sup> CFU/mL of *S. Enteritidis*. Capillaries containing *S. Enteritidis* at 10<sup>2</sup> CFU/mL were not distinguished from that of unspecific binding control capillaries constructed without capture aptamers in terms of their color intensities. Since unspecific binding control capillaries and platforms with 10<sup>2</sup> CFU/mL of cell gave same responses upon addition of TMB, the lowest amount of cell for both cr<sub>n</sub>-1 and cr<sub>n</sub>-2 based sandwich type capillary platform was determined as 10<sup>3</sup> CFU/mL in HRP signaling strategy.

As a result, cr<sub>n</sub>-1 and cr<sub>n</sub>-2 based sandwich detection platforms were constructed with two signaling strategies and they showed high specificity for *S. Enteritidis* with the detection limits of 10<sup>3</sup> CFU/mL.

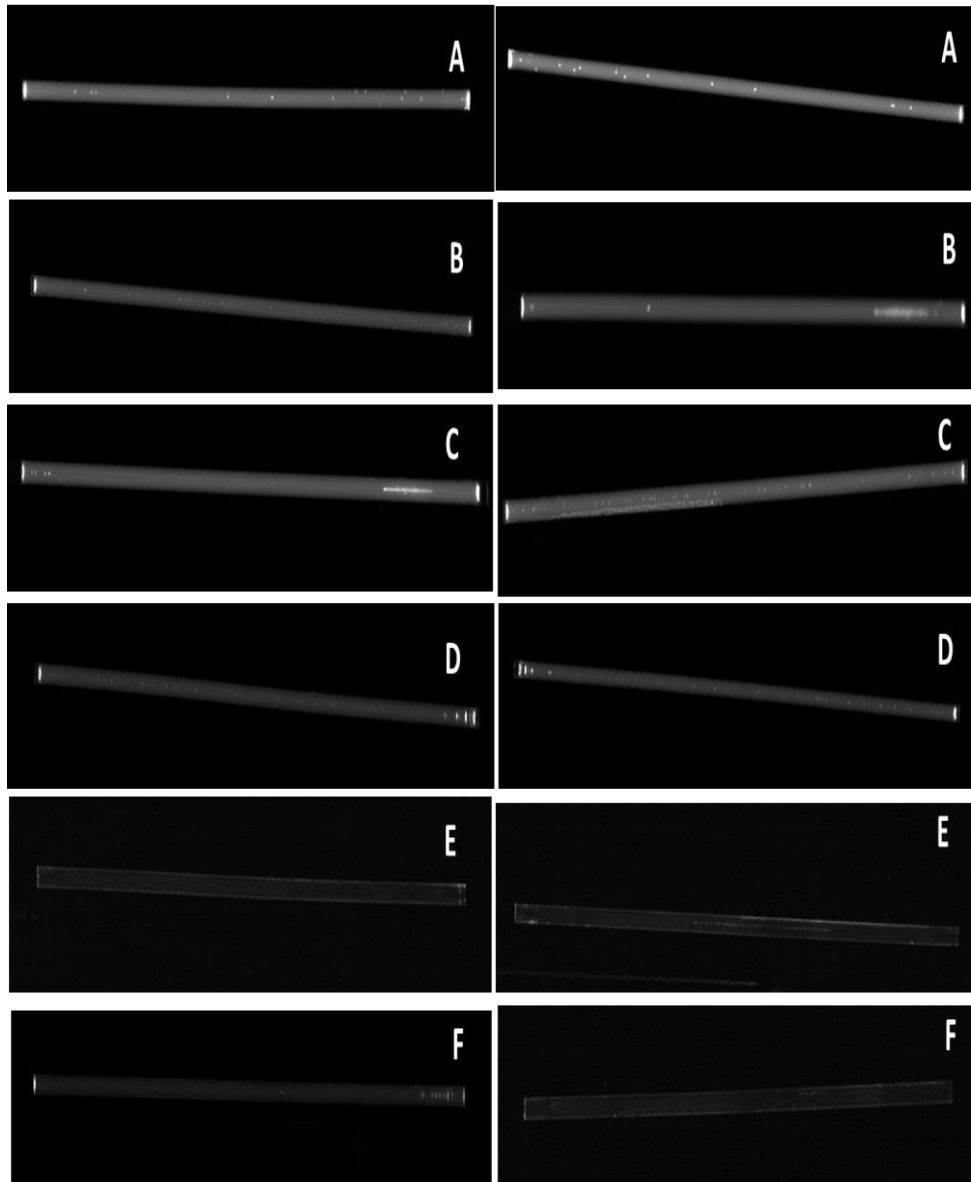


**Figure 3.55** Capillary images of crn-1 (left images) and crn-2 (right images) based *S. Enteritidis* detection platforms with QD signaling strategy for the determination of LOD; A) Sandwich system with  $10^6$  CFU/mL of cell, B) Sandwich system with  $10^5$  CFU/mL of cell, C) Sandwich system with  $10^4$  CFU/mL of cell, D) Sandwich system with  $10^3$  CFU/mL of cell, E) Sandwich system with  $10^2$  CFU/mL of cell, F) Unspecific binding control.

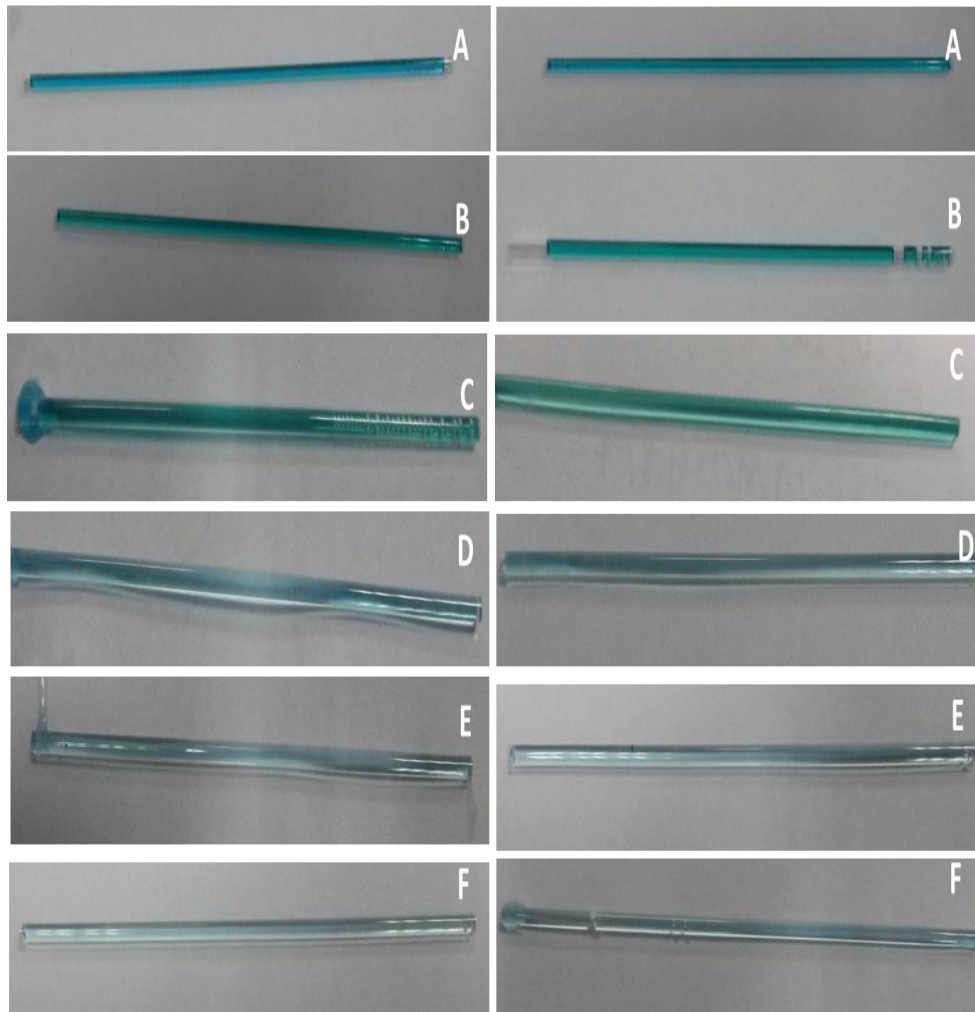


**Figure 3.56** Capillary images of crn-1 (left images) and crn-2 (right images) based *S. Enteritidis* detection platforms with HRP signaling strategy for the determination of LOD; A) Sandwich system with  $10^6$  CFU/mL of cell, B) Sandwich system with  $10^5$  CFU/mL of cell, C) Sandwich system with  $10^4$  CFU/mL of cell, D) Sandwich system with  $10^3$  CFU/mL of cell, E) Sandwich system with  $10^2$  CFU/mL of cell, F) Unspecific binding control.

### 3.2.4 Effects of Capturing Temperature of *S. Enteritidis* on the Response of Detection Platform

The response of aptamer –based detection platform was a function of the amount of cells and operating temperature. As mentioned above the detection limits of sandwich platforms constructed with crn-1 and crn-2 were both  $10^3$  CFU/mL. Therefore, experiments were performed to investigate the effect of temperature on detection efficiency of platform. As mentioned in ITC study previously, crn-1 showed binding to *S. Enteritidis* only at 4°C while crn-2 bond *S. Enteritidis* both at 4°C and 37°C. This was because the change in the temperature from 4°C to 37°C also changed the structure of crn-1 which was the basis factor affecting binding of aptamer to its target. Since crn-2 was folded into similar structure at these temperatures, binding toward *S. Enteritidis* was occurred with  $K_d$  of  $0.309 \times 10^{-6} \text{ M}^{-1}$  at 4°C and  $0.175 \times 10^{-6} \text{ M}^{-1}$  at 37°C. The results of ITC were confirmed with capillary experiments. As shown in Figure 3.58, signals were only gathered from sandwich platform of crn-1 at 4°C and those of crn-2 at 4°C and 37°C. Therefore, the use of crn-1 based sandwich platform for *S. Enteritidis* was limited to samples at 4°C while crn-2 based platform was applicable for samples at 4°C and 37°C.

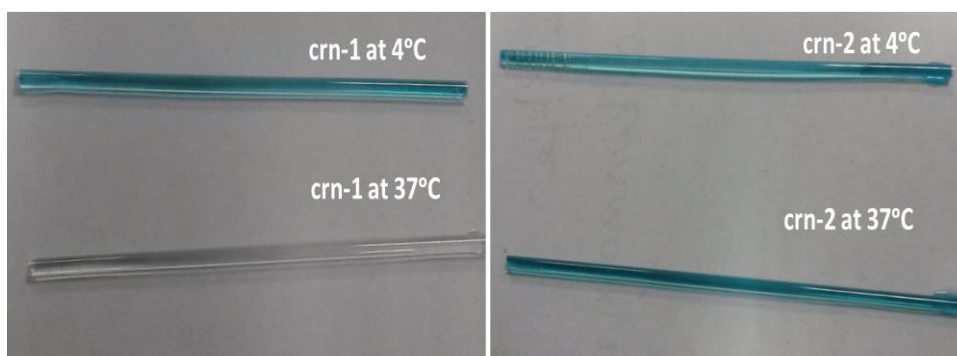


**Figure 3.57** Capillary images of detection platforms constructed with crn-1 and crn-2 for the detection of *S. Enteritidis* at 4°C and 37°C.



## CHAPTER 4

### CONCLUSION

The selection of DNA aptamers against *S. Enteritidis* via Cell-SELEX and the application of selected aptamers in the construction of aptamer-based sandwich type capillary platform for the detection of *S. Enteritidis* were aimed in this study.

For the aptamer selection process, whole bacteria were used as a target which provided many target molecules on its outer surface for aptamers to bind specifically. The use of whole cell also provided aptamers to be applicable for the detection of *S. Enteritidis* at its native state. PCR parameters were optimized for the effective amplification reaction without the production of unspecific artifacts. The annealing temperature and primer concentrations were determined as 63°C and 10 µM, respectively. Throughout SELEX rounds, amount of target cell, concentration of pools, incubation time of pool-cell complex and washing number were changed to increase stringency of selection. The selection process was controlled with fluorescence aptamer binding assay and DNA melting assay. The yields of eluted pool remained constant after round 10 till round 12. In melting analysis, three significant shifts in temperature towards higher degrees were observed due to changing parameters at selection process. The last shift was at round 11 and pools of round 11 and 12 melted at approximately same temperature. Therefore, it was stated that the enrichment of sequences ended at the round 12 of SELEX, thus, selection of aptamer for *S. Enteritidis* was ended at the 12<sup>th</sup> round. Pool at this round was sequenced for the determination of candidate aptamer sequences and three sequences most frequently present in the 12<sup>th</sup> pool were selected for further characterization of candidate aptamers.

Confocal imaging of fluorescent labelled aptamer bond to target cell, enzyme linked aptamer assay and ITC studies were firstly optimized with the use of *S. aureus* aptamer (SA-31) previously determined in the study of Cao *et al* (2009).

Based on confocal laser scanning microscopy and enzyme linked aptamer assay results, among three sequences, crn-1 and crn-2 were selected as DNA aptamers for *S. Enteritidis*. Both crn-1 and crn-2 showed highest affinity and specificity against their target *S. Enteritidis* at the concentration of 10  $\mu$ M. The binding affinities of crn-1 and crn-2 were evaluated in terms of their apparent dissociation constants found via ITC. The  $K_{ds}$  of crn-1 and crn-2 at 4°C reaction temperature were  $0.971 \times 10^{-6}$  and  $0.309 \times 10^{-6}$  M, respectively. Furthermore, ITC studied indicated that crn-2 showed binding to *S. Enteritidis* at 4°C and 37°C because of its similar structures at these two different temperatures while crn-1 bound to its target only at 4°C.

For the construction of aptamer-based sandwich type capillary platform for bacterial detection, parameters were firstly optimized with the use of *S. aureus* aptamer (SA-31). As a result, optimum parameters for efficient detection platform were found as; 10  $\mu$ M of capture aptamer, 1 hour 30 min incubation of capture aptamer, 10  $\mu$ L/sec of injection speed of washing solutions and 5% BSA as blocking agent.

With these optimum parameters two different signaling strategies were applied to detection platform. In quantum dot signaling strategy, streptavidin conjugated QDs were applied to sandwich system and biotin modified signaling aptamer bond with strep-QD. The signals were observed under UV light. In HRP signaling strategy, biotin modified signaling aptamer bond to streptavidin conjugate HRP and after the application of TMB, detection signals were visualized as blue color formations with naked eyes.

These optimum parameters and signaling strategies were, then, applied for the construction of crn-1 and crn-2 based sandwich platform for the detection of *S. Enteritidis*. The sandwich type capillary detection platforms of *S. Enteritidis* were constructed with high specificity based on crn-1 and crn-2 selected via Cell-SELEX and the detection limits of sandwich platforms for both aptamers were found as  $10^3$  CFU/mL of *S. Enteritidis* at 4°C.

The responses of detection platforms constructed separately with crn-1 and crn-2 against different sample temperatures were evaluated. Bacterial solutions were incubated at 4°C and 37°C in capillaries which were previously immobilized with

crn-1 and crn-2. Based on sandwich system results, it could be stated that the use of crn-1 based sandwich platform for *S. Enteritidis* detection was limited to the samples at 4°C while crn-2 based platform was applicable for the samples both at 4°C and 37°C.

As a conclusion, in this study two aptamers binding to *S. Enteritidis* with high affinity and specificity were selected via Cell-SELEX. Moreover, two aptamer-based sandwich type capillary platforms were constructed separately for the detection of *S. aureus* and *S. Enteritidis* in the scope of this study. The methods and protocols explained here are promising techniques to generate aptamer-based molecular probes for microbial pathogens without tedious isolation and purification of complex markers or targets.



## REFERENCES

- Ancrazio J. J. P., Helan J. P. W., Orkholder D. A. B., Ma W., Tenger D. A. S. (1999). Development and Application of Cell-Based Biosensors. *Annals of Biomedical Engineering* 27: 697–711.
- Bannikova O., Kalyna M., Barta A. (2012). Genomic SELEX to Identify RNA Targets of Plant RNA-Binding Proteins. In Stamm S., Smith C. W. J., Lührmann R. (Eds) *Alternative pre-mRNA Splicing: Theory and Protocols*, Wiley.
- Baron E. J. (2011). Conventional versus Molecular Methods for Pathogen Detection and the Role of Clinical Microbiology in Infection Control. *Journal of Clinical Microbiology* 49, 9, S43.
- Basabe-Desmonts L., Reinhoudt D. N., Crego-Calama M. (2007). Design of fluorescent materials for chemical sensing. *Chem. Soc. Rev.* 36: 993–1017.
- Bayrac A. T., Sefah K., Parekh P., Bayrac C., Gulbakan B., Oktem H.A., Tan W. (2011). In Vitro Selection of DNA Aptamers to Glioblastoma Multiforme. *ACS Chemical Neuroscience* 2 (3): 175-181.
- Berens C., Thain A., Schroeder R. (2001). A Tetracycline-Binding RNA Aptamer. *Bioorganic & Medicinal Chemistry* 9, 10, 2001: 2549-2556.
- Bromage E.S., Vadas G.G., Harvey E., Unger M.A., Kaattari S.L. (2007). Validation of an antibody-based biosensor for rapid quantification of 2,4,6-trinitrotoluene (TNT) contamination in ground water and river water. *Environ. Sci. Technol.* 41:7067–7072.
- Cao X., Li S., Chen L., Ding H., Xu H., Huang Y., Li J., Liu N., Cao W., Zhu Y., Shen B., Shao N. (2009). Combining use of a panel of ssDNA aptamers in the detection of *Staphylococcus aureus*. *Nucleic Acids Research* 37, 14: 4621–4628.

Carlson K., Flick L., Hall M. (2014). DNA adsorption onto calcium aluminate and silicate glass surfaces. *Colloids and Surfaces B: Biointerfaces* 117: 538–544.

Caruthers M. H., Beaucage S. L., Becker C., Efcavitch J. W., Fisher E. F., Galluppi G., Goldman R., Haseh P. de, Matteucci M., McBride L., Stabinsky Y. (1983). Deoxyoligonucleotide synthesis via the phosphoramidite method. *Gene. Amplif. Anal.* 3; 1–26.

Caruthers M. H. (1985). Gene synthesis machines: DNA chemistry and its uses. *Science* 230: 281–285.

Caruthers M. H., Barone A. D., Beaucage S. L., Dodds D. R., Fisher E. F., McBride L. J., Matteucci M., Stabinsky Z. and Tang J.-Y. (1987). Chemical synthesis of deoxyoligonucleotides by the phosphoramidite method. *Methods Enzymol.* 154; 287–313.

Cella L. N., Sanchez P., Zhong W., Myung N. V., Chen W., Mulchandani A. (2010). Nano Aptasensor for Protective Antigen Toxin of Anthrax. *Analytical Chemistry* 82, 5: 2042-2047.

Centers for Disease Control and Prevention, [www.cdc.gov](http://www.cdc.gov), last visited on September 2014.

Chen J., Zhang L., Paoli G. C., Shi C., Tu S. I., Shi X. (2010). A real-time PCR method for the detection of *Salmonella enterica* from food using a target sequence identified by comparative genomic analysis. *International Journal of Food Microbiology* 137: 168–174.

Chrisey L. A., O'Ferrall C. E., Spargo B. J., Dulcey C. S., Calvert J. M. (1996). Fabrication of patterned DNA surfaces. *Nucleic Acids Res.* 24, 15: 3040–3047.

Chushak Y., Stone M. O. (2009). *In silico* selection of RNA aptamers *Nucleic Acids Res.* 37, 12: e87.

Clark L. Jr, Lyons C. (1962). Electrode systems for continuous monitoring in cardiovascular surgery. *Ann N Y Acad Sci*, 102, 29– 45.

Cruz-Aguado J. A., Penner G. (2008). Determination of Ochratoxin a with a DNA Aptamer. *Journal of Agricultural and Food Chemistry* 56, 22: 10456-10461.

Davis K. A., Abrams B., Lin Y., Jayasena S. D. (1996). Use of a high affinity DNA ligand in flow cytometry. *Nucl. Acids Res.* 24, 4: 702-706.

Dong Y., Xu Y., Yong W., Chu X., Wang D. (2014). Aptamer and Its Potential Applications for Food Safety. *Critical Reviews in Food Science and Nutrition* 54:1548–1561.

Doran J.L., Collinson S.K., Kay C.M., Banser P.A., Burian J., Munro C.K., Lee S.H., Somers J.M., Todd E.C., Kay W.W. (1994). fimA and tctC based DNA diagnostics for Salmonella. *Mol. Cell. Probes* 8: 291-310.

Duan Y. F., Ning Y., Song Y., Deng L. (2014). Fluorescent aptasensor for the determination of Salmonella typhimurium based on a graphene oxide platform. *Microchim Acta* 181: 647-653.

Duff M. R., Grubbs J. Jr., Howell E. E. (2011). Isothermal Titration Calorimetry for Measuring Macromolecule-Ligand Affinity. *Journal of Visualized Experiments* 55, e2796.

Ellington A.D., Szostak J. W. (1990). In vitro selection of RNA molecules that bind specific ligands. *Nature* 346:818-822.

Eyigor A., Goncagul G., Gunaydin E., Carli K. T. (2005). Salmonella profile in chickens determined by real-time polymerase chain reaction and bacteriology from years 2000 to 2003 in Turkey. *Avian Pathology* 34, 2: 101-105.

Fanulok M. (1994). Molecular Recognition of Amino Acids by RNA-Aptamers: An L-Citrulline RNA Motif and Its Evolution into an L-Arginine Binder. *Journal of the American Chemical Society* 116:1698-1706.

Feng L., Chen Y., Ren J., Qu X. (2011). A graphene functionalized electrochemical aptasensor for selective label-free detection of cancer cells. *Biomaterials* 32, 11: 2930–2937.

Ferretti R., Mannazzu I., Cocolin, L., Comi, G., Clementi, F. (2001). Twelve-hour PCR-based method for detection of *Salmonella* spp. in food. *Appl. Environ. Microbiol.* 67: 977–978.

Geng T., Bao N., Gall O. Z., Lu C. (2009). Modulating DNA adsorption on silica beads using an electrical switch. *Chem. Commun.:* 800–802.

Guo X., Chen J., Beuchat L.R., Brackett R.E. (2000). PCR detection of *Salmonella enterica* serotype Montevideo in and on raw tomatoes using primers derived from *hilA*. *Appl. Environ. Microbiol.* 66: 5248–5252.

Guo X., Wen F., Zheng N., Luo Q., Wang H., Wang H., Li S., Wang J. (2014). Development of an ultrasensitive aptasensor for the detection of aflatoxin B1. *Biosensors and Bioelectronics* 56: 340–344.

Hahn S., Mergenthaler S., Zimmermann B., Holzgreve W. (2005). Nucleic acid based biosensors: The desires of the user. *Bioelectrochemistry* 67, 2: 151–154.

Hashsham S. A., Wick L.M., Rouillard J. M., Gulari E., Tiedje J. M. (2004). Potential of DNA microarrays for developing parallel detection tools (PDTs) for microorganisms relevant to biodefense and related research needs. *Biosensors and Bioelectronics* 20, 4: 668–683.

Hayat A., Marty J. L. (2014). Aptamer based electrochemical sensors for emerging environmental pollutants. *Frontiers in Chemistry* 2, 41: 1-9.

Huang J., Luo X., Lee I., Hu Y., Cui X. T., Yun M. (2011). Rapid Real-Time Electrochemical Detection of Proteins Using Single Conducting Polymer Nanowire-Based Microfluidic Aptasensor,” *Biosensors and Bioelectronics* 30, 1: 306-309.

Hun X., Chen H. C., Wang W. (2011). A Electrogenerated Chemiluminescence Biosensor for Ramos Cancer Cell Using DNA Encapsulated Ru(bpy)<sub>3</sub>Cl<sub>2</sub> as Signal Probe. *Biosensors and Bioelectronics* 26, 9:3887-3893.

- Ikanovic M., Rudzinski W. E., Bruno J. G., Allman A., Carrillo M.P., Dwarakanath S., Bhahdigadi S., Rao P., L.Kiel J., Andrews C. J. (2007). Fluorescence Assay Based on Aptamer-Quantum Dot Binding to *Bacillus thuringiensis* Spores. *Journal of Fluorescence* 17, 2; 193-199.
- Ikebukuro K., Kiyohara C., Sode K. (2004). Electrochemical Detection of Protein Using a Double Aptamer Sandwich. *Analytical Letters* 37, 14: 2901-2909.
- Jayasena S. D. (1999). Aptamers: An Emerging Class of Molecules That Rival Antibodies in Diagnostics. *Clinical Chemistry* 45, 9; 1628-1650.
- Jelinek R., Kolusheva S. (2004). Carbohydrate Biosensors. *Chem. Rev.* 104: 5987–6015.
- Jing M., Bowser M. T. (2011). Methods for measuring aptamer-protein equilibria: A review. *Analytica Chimica Acta* 686: 9–18.
- Ju H. (2012). Signal Amplification for Highly Sensitive Bioanalysis Based on Biosensors or Biochips. *J Biochip Tissue chip* 2:3.
- Katoh K., Standley D. M. (2013). MAFFT multiple sequence alignment software version 7: improvements in performance and usability. *Molecular Biology and Evolution* 30:772-780.
- Kavruk M., Özalp V. C., Öktem H. A. (2013). Portable Bioactive Paper-Based Sensor for Quantification of Pesticides. *Journal of Analytical Methods in Chemistry*. 8 pages.
- Keefe A. D., Pai S., Ellington A. (2010). Aptamers as therapeutics. *Nature Reviews Drug Discovery* 9: 537-550.
- Kim S., Fisher B., Eisler H. J., Bawendi M. (2003). Type-II quantum dots: CdTe/CdSe(core/shell) and CdSe/ZnTe(core/shell) heterostructures. *J. Am. Chem. Soc.* 125, 38: 11466–11467.

- Kim C. H., Lee L. P., Min J. R., Lim M. W., Jeong S.H. (2014). An indirect competitive assay-based aptasensor for detection of oxytetracycline in milk. *Biosensors and Bioelectronics* 51: 426–430.
- Korpan Y.I., Gonchar M.V., Starodub N.F., Shulga A.A., Sibirny A.A., Elskaya A.V. (1993). A Cell Biosensor Specific for Formaldehyde Based on pH-Sensitive Transistors Coupled to Methylophilic Yeast Cells with Genetically Adjusted Metabolism. *Analytical Biochemistry* 215, 2: 216–222.
- Kosuri S., Church M. (2014). Large-scale de novo DNA synthesis: technologies and applications. *Nature Methods* 11: 499–507.
- Labib M., Zamay A. S., Kolovskaya O. S., Reshetneva I. T., Zamay G. S., Kibbee R. J., Sattar A. S., Zamay T. N., Berezovski M. V. (2012). Aptamer-Based Impedimetric Sensor for Bacterial Typing. *Anal. Chem.* 84, 19: 8114–8117.
- Lakhin A.V., Tarantul V.Z., Gening L.V. (2013). Aptamers: Problems, Solutions and Prospects. *Acta Naturae* 5, 4, 19: 34-43.
- Lampel K.A., Keasler S.P., Hanes D.E. (1996). Specific detection of *Salmonella enterica* serotype Enteritidis using the polymerase chain reaction. *Epidemiol. Infect.* 116: 137-145.
- Lee K. M., Runyon M., Herrman T. J., Phillips R., Hsieh J. (2015). Review of *Salmonella* detection and identification methods: Aspects of rapid emergency response and food safety. *Food Control* 47: 264-276.
- Li X. M., Li W., Zhang S. S. (2010). Chemiluminescence DNA biosensor based on dual-amplification of thrombin and thiocyanuric acid-gold nanoparticle network. *Analyst* 135: 332–336.
- Li N., Nguyen H.H., Byrom M., Ellington A.D. (2011). Inhibition of Cell Proliferation by an Anti-EGFR Aptamer. *PLoS One* 6: e20299.

- Lipchik A. M., Killins R. L., Geahlen R. L., Parker L. L. (2012). A peptide-based biosensor assay to detect intracellular sky kinase activation and inhibition. *Biochemistry* 51: 7515-7524.
- Liu B., Huang P. J., Zhang X., Wang F., Pautler R., Ip A. C., Liu J. (2013). Parts-per-Million of Polyethylene Glycol as a Non-Interfering Blocking Agent for Homogeneous Biosensor Development. *Anal. Chem.* 85, 21: 10045–10050.
- Luppa P. B., Sokoll L. J., Chan D. W. (2001). Immunosensors—principles and applications to clinical chemistry. *Clinica Chimica Acta* 314, 1–2: 1–26.
- Mallinson E. T., Miller R. G., de Rezende C. E., Ferris K. E., deGraft-Hanson J., Joseph S. W. (2000). Improved plating media for the detection of Salmonella species with typical and atypical hydrogen sulfide production. *Journal of Veterinary Diagnostic Investigation* 12, 83-87.
- Malorny B., Hoorfar J., Bunge C., Helmuth R. (2003). Multicenter validation of the analytical accuracy of SalmonellaPCR: towards an international standard. *Appl. Environ. Microbiol.* 69: 290–296.
- Mehta J., Van Dorst B., Rouah-Martin E., Herrebou T. W., Scippo M. L., Blust R., Robbens J. (2011). In Vitro Selection and Characterization of DNA Aptamers Recognizing Chloramphenicol. *Journal of Biotechnology* 155, 4: 361-369.
- Meyer S., Maufort J. P., Nie J., Stewart R., McIntosh B. E., Conti L. R., Ahmad K. M., Soh H. T., Thomson J. A. (2013). Development of an Efficient Targeted Cell-SELEX Procedure for DNA Aptamer Reagents. *PLOS ONE* 8,8: e71798.
- Min K., Cho M., Han S.Y., Shim Y.B., Ku J., Ban C. (2008). A simple and direct electrochemical detection of interferon-gamma using its RNA and DNA aptamers. *Biosens. Bioelectron.* 23: 1819-1824.
- Molloy M. P., Herbert B. R., Slade M. B., Rabilloud T., Nouwens A. S., Williams K. L., Gooley A. A. (2000). Proteomic analysis of the Escherichia coli outer membrane. *Eur. J. Biochem.* 267; 2871–2881.

- Molloy M. P., Phadke N. D., Maddock J. R., Andrews P. C. (2001). Two-dimensional electrophoresis and peptide mass-fingerprinting of bacterial outer membrane proteins. *Electrophoresis* 22; 1686–1696.
- Molloy, P.M. (2008). Isolation of Bacterial Cell Membranes Proteins Using Carbonate Extraction. *Methods in Molecular Biology* 424; 397-401.
- Muhammad N., Dworeck T., Fioroni M., Schwaneberg U. (2011). Engineering of the E. coli Outer Membrane Protein FhuA to overcome the Hydrophobic Mismatch in Thick Polymeric Membranes. *Journal of Nanobiotechnology* 9, 8.
- Nagy A., Gemmill K. B., Delehanty J. B., Medintz I. L., Sapsford K. E. (2014). Peptide-Functionalized Quantum Dot Biosensors. *Ieee Journal Of Selected Topics In Quantum Electronics* 20, 3.
- Nivens D.E., McKnight T.E., Moser S.A., Osbourn S.J., Simpson M.L., Sayler G.S. (2004). Bioluminescent bioreporter integrated circuits: potentially small, rugged and inexpensive whole-cell biosensors for remote environmental monitoring. *Journal of Applied Microbiology* 96: 33–46.
- Ozalp V. C., Bayramoglu G., Kavruk M., Keskin B. B., Oktem H. A., Arica M. Y. (2014). Pathogen detection by core-shell type aptamer-magnetic preconcentration coupled to real-time PCR. *Analytical Biochemistry* 447: 119–125.
- Pan J. J., Charych D. (1997) Molecular Recognition and Colorimetric Detection of Cholera Toxin by Poly(diacetylene) Liposomes Incorporating Gm1 Ganglioside. *Langmuir* 13, 6: 1365–1367.
- Pathirana S. T., Barbaree J., Chin B. A., Hartell M. G., Neely W. C., Vodyanoy V. (2000). Rapid and sensitive biosensor for Salmonella. *Biosensors & Bioelectronics* 15: 135 – 141.
- Pathmanathan S. G., Cardona-Castro N., Sánchez-Jiménez M. M., Correa-Ochoa M. M., Puthuchery S. D., Thong K. L. (2003). Simple and rapid detection of Salmonella strains by direct PCR amplification of the hilA gene. *J Med Microbiol.* 52, 9:773-6.

Pierce M. M., Raman C. S., Nall B. T. (1999). Isothermal Titration Calorimetry of Protein-Protein Interactions. *METHODS* 19: 213-221.

Pietryga J., Schaller R., Werder D., Stewart M., Klimov V., Hollingsworth J. (2004). Pushing the band gap envelope: mid-infrared emitting colloidal PbSe quantum dots. *J. Am. Chem. Soc.* 126, 38: 11752–11753.

Pilehvar S., Mehta J., Dardenne F., Robbens J., Blustand R., De Wael K. (2012). Aptasensing of Chloramphenicol in the Presence of Its Analogues: Reaching the Maximum Residue Limit. *Analytical Chemistry* 84, 15: 6753-6758.

Proux K., Houdayer C., Humbert F., Cariolet R., Rose V., Eveno E., Madec F. (2000). Development of a complete ELISA using Salmonella lipopolysaccharides of various serogroups allowing to detect all infected pigs. *Vet. Res.* 31: 481-490.

Prusak-Sochaczewski E., Luong J. H. (1989). An improved ELISA method for the detection of Salmonella typhimurium. *J Appl Bacteriol.* 66, 2:127-35.

Purschke W. G., Radtke F., Kleinjung F., Klussmann S. A. (2003). DNA Spiegelmer to staphylococcal enterotoxin B. *Nucleic Acids Res* 31, 12: 3027–32.

Qu L. H., Peng X. G. (2002). Control of photoluminescence properties of CdSenanocrystals in growth. *J. Am. Chem. Soc.* 124, 9: 2049–2055.

Radi A. E. (2011). Electrochemical Aptamer-Based Biosensors: Recent Advances and Perspectives. *International Journal of Electrochemistry* 2011: 1-17.

Radom F., Jurek P. M., Mazurek P. M., Otlewski J., Jeleń F. (2013). Aptamers: Molecules of great potential. *Biotechnology Advances* 31: 1260-1274.

Rahn K., De Grandis S.A., Clarke, R.C., McEwen, S.A., Galan J.E., Ginocchio C., Curtiss IIR., Gyles C.L. (1992) .Amplification of an invA gene sequence of Salmonella typhimurium by polymerase chain reaction as a specific method of detection of Salmonella. *Mol.Cell. Probes* 6: 271–279.

Ramírez N. B., Salgado A. M., Valdman B. (2009). The Evolution and Developments of Immunosensors for Health and Environmental Monitoring:

Problems and Perspectives. *Brazilian Journal of Chemical Engineering* 26, 02: 227 – 249.

Robertson D. L, Joyce G. F. (1990). Selection in vitro of an RNA enzyme that specifically cleaves single-stranded DNA. *Nature* 344, 6265:467-8.

Rogers K. R. (2006). Recent advances in biosensor techniques for environmental monitoring. *Analytica Chimica Acta* 568, 1-2: 222-231.

Rusconi C. P., Roberts J. D., Pitoc G. A., Nimjee S. M., White R R., Quick G. Jr., Scardino E., Fay W. P., Sullenger B. A. (2004). Antidote-mediated control of an anticoagulant aptamer in vivo. *Nat. Biotechnol* 22: 1423–1428.

Schlenz M., Gronewold T., Tewes M., Famulok M., Quandt E. (2004). A Love-wave biosensor using nucleic acids as ligands. *Sens. Actuat. B* 101: 308-315.

Schütze T., Arndt P. F., Merger M., Wochner A., Vingron M., Erdmann V. A., Lehrach H., Kaps C., Glökler J. (2010). A calibrated diversity assay for nucleic acid libraries using DiStRO- a Diversity Standard of Random Oligonucleotides. *Nucleic Acids Research* 38, 4,e23.

Sefah K., Shangguan D., Xiong X., O'Donoghue M. B., Tan W. (2010). Development of DNA aptamers using Cell-SELEX. *Nature protocols* 5, 6: 1169-1185.

Sett A., Das S., Sharma P., Bora U. (2012). Aptasensors in Health, Environment and Food Safety Monitoring. *Journal of Applied Biosensor* 1: 9-19.

So H. M., Park D. W., Jeon E. K., Kim Y. H., Kim B. S., Lee C. K., Choi S. Y., Kim S. C., Chang H., Lee J. O. (2008). Detection and Titer Estimation of Escherichia Coli Using Aptamer-Functionalized Single-Walled Carbon-Na-notube Field-Effect Transistors. *Small* 4, 2: 197-201.

Song S., Wang L., Li J., Zhao J., Fan C. (2008). Aptamer-based biosensors. *Analytical Chemistry* 27, 2:108-117.

Song K. M., Lee S., Ban C. (2012). Aptamers and Their Biological Applications. *Sensors* 12: 612-631.

Song Y., Li W., Duan Y., Li Z., Deng L. (2014). Nicking enzyme-assisted biosensor for *Salmonella Enteritidis* detection based on fluorescence resonance energy transfer. *Biosensors and Bioelectronics* 55: 400-404.

Stojanovic M. N., de Prada P., Landry D. W. (2001). Aptamer-Based Folding Fluorescent Sensor for Cocaine. *J. Am. Chem. Soc.* 123: 4928-4931.

Thevenot D. R., Toth K., Durst R. A., Wilson G. S. (1999) Electrochemical Biosensors: Recommended Definitions and Classification, *Pure Appl. Chem.* 7: 2333-2348.

Thiel W. H., Bair T., Peek A. S., Liu X., Dassie J., Stockdale K. R., Behlke M. A., Miller F. J., Giangrande P. H. (2012). Rapid identification of cell-specific, internalizing RNA aptamers with bioinformatics analyses of a cell-based aptamer selection. *PLOS ONE* 7, 9, e43836.

Tian H., Hühmer A. F., Landers J. P. (2000). Evaluation of silica resins for direct and efficient extraction of DNA from complex biological matrices in a miniaturized format. *Anal Biochem.* 1, 283, 2:175-91.

Tietjen M., Fung D. Y. C. (1995). Salmonella and food safety. *Critical Reviews in Microbiology* 21: 53-83.

Tombelli S., Minunni M., Luzi E., Mascini M. (2005). Aptamer-based biosensors for the detection of HIV-1 Tat protein, *Bioelectrochemistry* 67, 2: 135–141.

Töreci K., Erdem E., Öngen B. (2013). Türkiye’de 2011 Yılı Sonuna Kadar İzolasyonu Bildirilen Salmonella Serovaryları. *Mikrobiyol Bul* 47, 3: 442-460.

Tsai H.C., Doong R. A. (2005). Simultaneous determination of pH, urea, acetylcholine and heavy metals using array-based enzymatic optical biosensor. *Biosens Bioelectron* 15, 20, 9: 1796-804.

- Tuerk C., Gold L. (1990). Systemic evolution of ligands by exponential enrichment: RNA ligands to bacteriophage T4 DNA polymerase. *Science* 249: 505-510.
- Vargas-Bernal R., Herrera-Pérez G., Rodríguez-Miranda E. (2012). Evolution and Expectations of Enzymatic Biosensors for Pesticides. In Soundararajan R. P. (Eds). *Pesticides - Advances in Chemical and Botanical Pesticides*. Intech.
- Vater A., Jarosch F., Buchner K., Klussmann S. (2003). Short bioactive Spiegelmers to migraine-associated calcitonin gene-related peptide rapidly identified by a novel approach: tailored-SELEX. *Nucleic Acids Res* 31, 21, 130.
- Wang J., Jiang Y., Zhou C., Fang X. (2005). Aptamer-Based ATP Assay Using a Luminescent Light Switching Complex. *Anal. Chem.* 77: 3542-3546.
- Wang P., Xu G., Qin L., Xu Y., Li Y., Li R. (2005). Cell-based biosensors and its application in biomedicine. *Sensors and Actuators B: Chemical* 108, 1–2: 576–584.
- Wang J., Zhou H.S. (2008). Aptamer-based Au nanoparticles-enhanced surface plasmon resonance detection of small molecules. *Anal. Chem.* 80: 7174-7178.
- Wang J., Lv R., Xu J., Xu D., Chen H. (2008). Characterizing the interaction between aptamers and human IgE by use of surface plasmon resonance. *Anal. Bioanal. Chem.* 390:1059–1065.
- Wang Y., Yuan R., Chai Y., Yuan Y., Bai L., Liao Y. (2011). A multi-amplification aptasensor for highly sensitive detection of thrombin based on high-quality hollow CoPt nanoparticles decorated graphene. *Biosens. Bioelectron* 30: 61–66.
- Wu W., Li M., Wang Y., Ouyang H., Wang L., Li C., Cao Y., Meng Q., Lu J. (2012). Aptasensors for rapid detection of *Escherichia coli* O157:H7 and *Salmonella typhimurium*. *Nanoscale Research Letters*.7:658.
- Wu W., Fang Z., Zhao S., Lu X., Yu L., Mei T., Zeng L. (2014). A simple aptamer biosensor for *Salmonella Enteritidis* based on fluorescence-switch signaling graphene oxide. *RSC Adv.* 4: 22009-22012.

- Wu S., Duan N., Shi Z., Fang C., Wang Z. (2014). Simultaneous Aptasensor for Multiplex Pathogenic Bacteria Detection Based on Multicolor Upconversion Nanoparticles Labels. *Anal. Chem.* 86, 6: 3100-3107.
- Xiao H., Edwards T. E., Ferré-D'Amaré A. R. (2008). Structural Basis for Specific, High-Affinity Tetracycline Binding by an in Vitro Evolved Aptamer and Artificial Riboswitch. *Chemistry & Biology* 15, 10: 1125-1137.
- Xiao Y. and Isaacs N. S. (2012). Enzyme-linked immunosorbent assay (ELISA) and blocking with bovine serum albumin (BSA)—not all BSAs are alike. *Journal of Immunological Methods* 384, 1-2: 148–151.
- Xu D., Xu D., Yu X., Liu Z., He W., Ma Z., (2005). Label-Free Electrochemical Detection for Aptamer-Based Array Electrodes. *Anal. Chem.* 77, 16: 5107–5113.
- Yan X., Gao X., Zhang Z. (2004). Isolation and characterization of 2'-amino-modified RNA aptamers for human TNFalpha. *Genomics Proteomics Bioinformatics* 2, 1: 32–42.
- Yan Y. R., Lei P. H., Zhang Y., Cheng W., Ding S. J. (2014.) A surface plasmon resonance biosensor for the determination of Salmonella. *Applied Mechanics and Materials* 568-570: 519-522.
- Yildirim N., Long F., He M., Shi H. C., Gu A. Z. (2014). A portable optic fiber aptasensor for sensitive, specific and rapid detection of bisphenol-A in water samples. *Environ. Sci.: Processes Impacts* 16: 1379-1386.
- Zammatteo N., Jeanmart L., Hamels S., Courtois S., Louette P., Hevesi L., Remacle J. (2000). Comparison between Different Strategies of Covalent Attachment of DNA to Glass Surfaces to Build DNA Microarrays. *Analytical Biochemistry* 280: 143–150.
- Zhang L., Wei H., Li J., Li T., Li D., Li Y., Wang E. (2010). A carbon nanotubes based ATP apta-sensing platform and its application in cellular assay. *Biosensors and Bioelectronics* 25, 8: 1897-1901.

Zhong X. H., Feng Y.Y., Knoll W., Han M. Y. (2003). Alloyed  $Zn_xCd_{1-x}S$  nanocrystals with highly narrow luminescence spectral width. *J. Am. Chem. Soc.* 125, 44: 13559–13563.

Zhong X. H., Han M. Y., Dong Z., White T. J., Knoll W. (2003). Composition-tunable  $Zn_xCd_{1-x}Se$  nanocrystals with high luminescence and stability. *J. Am. Chem. Soc.* 125, 28: 8589–8594.

Zhou J., Huang H., Xuan J., Zhang J., Zhu J. J. (2010). Quantum dots electrochemical aptasensor based on three-dimensionally ordered macroporous gold film for the detection of ATP. *Biosensors and Bioelectronics* 26, 2: 834–840.

## APPENDIX A

### BUFFERS AND SOLUTIONS

#### 1. Dulbecco's PBS, 10X, pH 7.2

- 1,33 g  $\text{CaCl}_2 \cdot 2\text{H}_2\text{O}$
- 1 g  $\text{MgCl}_2 \cdot 6\text{H}_2\text{O}$
- 2 g KCl
- 2 g  $\text{KH}_2\text{PO}_4$  (anhydrous)
- 80 g NaCl
- 11.5 g  $\text{Na}_2\text{HPO}_4$  (anhydrous)

They were dissolved in 900 mL of distilled water. The pH of solution was adjusted to pH 7.2 and then solution was completed to 1000mL with distilled water. Buffer was autoclaved at 121°C for 20 min and stored at 4 °C.

#### 2. Binding Buffer in SELEX

- 1% BSA (10g in 1000mL)
- 100 mg yeast tRNA
- 1.016 g  $\text{MgCl}_2 \cdot 6\text{H}_2\text{O}$

They were dissolved in 900 mL of sterile Dulbecco's PBS (1 X, pH 7.2) and then solution was completed to 1000mL with sterile distilled water. Buffer was filtered and stored at 4 °C.

### **3. Washing Buffer in SELEX**

- 1.016 g  $\text{MgCl}_2 \cdot 6\text{H}_2\text{O}$
- 4.5 g Glucose

They were dissolved in 900 mL of sterile Dulbecco's PBS (1 X, pH 7.2) and then solution was completed to 1000mL with sterile distilled water. Buffer was filtered and stored at 4 °C.

### **4. NaOH Solution, 200mM**

Sodium hydroxide of 4 g was dissolved in 500 mL of distilled water and then autoclaved at 121°C for 20 min and stored at 4 °C.

### **5. PBS, 1X**

- 8 g NaCl
- 0.2 g KCl
- 1.44 g  $\text{Na}_2\text{HPO}_4$
- 0.24 g  $\text{KH}_2\text{PO}_4$

They were dissolved in 900 mL of distilled water and then solution was completed to 1000mL with distilled water. Buffer was autoclaved at 121°C for 20 min and stored at 4°C.

## **6. SSC Buffer, 5X, pH 7.0**

- 11,03 g Sodium Citrate
- 21,9 g Sodium Chloride

They were dissolved in 400 mL of distilled water. The pH of solution was adjusted to pH 7.0 and then solution was completed to 500 mL with distilled water. Buffer was autoclaved at 121°C for 20 min and stored at 4 °C.

## **7. Binding Buffer in *S.aureus* Capillary Studies**

- 0.1 ug/mL tRNA
- 5 g BSA
- 0.05 % (v/v) Tween-20

They were prepared in 400 mL of sterile 1 X PBS and then solution was completed to 500 mL with sterile 1 X PBS. Buffer was filter sterilized and stored at 4 °C.

## **8. Washing Buffer in *S.aureus* Capillary Studies**

- 0.05 % (v/v) Tween-20

It was prepared in 400 mL of sterile 1 X PBS and then solution was completed to 500 mL with sterile 1 X PBS. Buffer was filter sterilized and stored at 4°C.

### **9. Tryptic Soy Agar, pH 7.3**

The dehydrated TSA of 40 g was suspended in 1L of distilled water and sterilized at 121°C for 15min. The media was cooled to 45-50°C and stored at 4 °C protected from direct light.

### **10. Tryptic Soy Broth, pH 7.3**

The dehydrated TSB of 30 g was suspended in 1L of distilled water and sterilized at 121°C for 15min. The media was cooled to 45-50°C and stored at 4 °C protected from direct light.

### **11. Sulfo-EMCS Solution**

- 1.109 mg Sulfo-EMCS

Sulfo-EMCS was prepared in 1 mL of sterile 1X PBS freshly before each experiment.

### **12. TCEP Solution, 10 mM**

- 0.00286 g TCEP

TCEP (10 mM) was prepared in 1 mL of distilled water and diluted with distilled water to prepare 1 mM of TCEP. TCEP solutions were stored at -20°C.

## CURRICULUM VITAE

### PERSONAL INFORMATION

Surname, Name: Bayraç, Ceren

Nationality: Turkish (TC)

Date and Place of Birth: 9 April 1984, Ankara

Marital Status: Married

Email: cerenbayrac@gmail.com

### EDUCATION

Degree	Institution	Year of Graduation
MS	METU Biotechnology	2009
BS	METU Biology	2007
Minor Program	METU Food Engineering	2007
High School	Gölbaşı Anadolu Lisesi, Ankara	2002

### WORK EXPERIENCE

Year	Place	Enrollment
2010-2014	METU Central Laboratory Molecular Biology and Biotechnology R&D Center	Research Scientist
2009 July	Chemistry Dept., Florida University	Visiting Scientist
2006-2007	Nisan Sağlık Kavaklıdere Tüp Bebek Merkezi	Internship

## **PUBLICATIONS**

Bayrac A. T., Sefah K., Parekh P., Bayrac C., Gulbakan B., Oktem H.A., Tan W. (2011). In Vitro Selection of DNA Aptamers to Glioblastoma Multiforme. ACS Chemical Neuroscience 2 (3): 175-181

Öktem H. A., Senyurt Ö., Eyidođan F., Bayrac C., Yilmaz R. (2012). Development of a laccase based paper biosensor for the detection of phenolic compounds. Journal of Food, Agriculture & Environment 10, 2: 1030-1034

Cansız S., Özen C., Bayraç C., Bayraç A. T., Gül F., Kavruk M., Yilmaz R., Eyidođan F., Öktem H. A. (2012). A sandwich-type DNA array platform for detection of GM targets in multiplex assay. Eur. Food Res Technol 235: 429-437